

Yao Liu

Heat transfer process between polymer and cavity wall during injection molding

Yao Liu

Heat transfer process between polymer and
cavity wall during injection molding



TECHNISCHE UNIVERSITÄT
CHEMNITZ

Universitätsverlag Chemnitz
2014

Impressum

Bibliografische Information der Deutschen Nationalbibliothek

Die Deutsche Nationalbibliothek verzeichnet diese Publikation in der Deutschen Nationalbibliografie; detaillierte bibliografische Angaben sind im Internet über <http://dnb.d-nb.de> abrufbar.

Zugl.: Chemnitz, Techn. Univ., Diss., 2014

Cover-Foto: TU Chemnitz/Wolfgang Thieme

Technische Universität Chemnitz/Universitätsbibliothek

Universitätsverlag Chemnitz

09107 Chemnitz

<http://www.tu-chemnitz.de/ub/univerlag>

Herstellung und Auslieferung

Verlagshaus Monsenstein und Vannerdat OHG

Am Hawerkamp 31

48155 Münster

<http://www.mv-verlag.de>

ISBN 978-3-944640-40-2

<http://nbn-resolving.de/urn:nbn:de:bsz:ch1-qucosa-157361>

Heat transfer process between polymer and cavity wall during injection molding

Von der Fakultät für Maschinenbau der
Technischen Universität Chemnitz

genehmigte

Dissertation

zur Erlangung des akademischen Grades

Doktoringenieur
(Dr.-Ing.)

vorgelegt

von M. Sc. Yao Liu

geboren am 17.03.1984 in Harbin, China

Tag der Einreichung: 29.09.2014

Tag der Verteidigung: 05.12.2014

1. Gutachter: Prof. Dr.-Ing. Michael Gehde

2. Gutachter: Prof. Dr.-Ing. Thomas Seul

Prüfungsvorsitzender: Prof. Dr.-Ing. Michael Groß

Bibliographic description

Liu, Yao

Heat transfer process between polymer and cavity wall during injection molding

Dissertation from Professorship of Plastic Materials, Department of Mechanical Engineering, Chemnitz University of Technology, Chemnitz, 2014

130 pages, 71 Figures, 9 Tables, 97 Literatures

Abstract

Injection molding is one of the most commonly applied processing methods for plastic components. Heat transfer coefficient (HTC), which describes the heat conducting ability of the interface between a polymer and cavity wall, significantly influences the temperature distribution of a polymer and mold during injection molding and thus affects the process and quality of plastic products. This thesis focuses on HTC under diverse processing situations. On the basis of the heat conducting principle, a theoretical model for calculating HTC was presented. Injection mold specially used for measuring and calculating HTC was designed and fabricated. Experimental injection studies under different processing conditions, especially different surface roughness, were performed for acquiring necessary temperature data. The heat quantity across the interface and HTC between a polymer and cavity wall was calculated on the basis of experimental results. The influence of surface roughness on HTC during injection molding was investigated for the first time. The factors influencing the HTC were analyzed on the basis of the factor weight during injection molding. Subsequently FEM (Finite element method) simulations were carried out with observed and preset value of HTC respectively and the relative crystallinity and part density were obtained. In the comparison between results from simulation and experiment, the result calculated with observed HTC shows better agreement with actually measured value, which can verify the reliability and precision of the injection molding simulation with observed HTC. The results of this thesis is beneficial for understanding the heat transfer process comprehensively, predicting temperature distribution, arranging cooling system, reducing cycle time and improving precision of numerical simulation.

Keywords: Injection molding, Heat transfer coefficient, Theoretical model, Design of experiment, FEM simulation, Measurement of melt temperature, Cooling rate, Frozen volume, Relative crystallinity, Part density

Acknowledgement

I would like to deliver all my sincere thankfulness to all the people who brought me up, educated me, enlightened me and supported me.

Great thanks to Prof. Dr.-Ing. Michael Gehde, Institute of Conveyors and Plastics in Chemnitz University of Technology, for providing me the opportunity to study in this famous and outstanding institute. He was extraordinarily patient with me and squeezed time for the work of my doctoral thesis. He guided me to the right way step by step and gave me numerous critical suggestions.

I would like also to show my gratitude to Prof. Dr.-Ing. Günter Mennig. I was convinced by his broad and profound knowledge in the field of mechanical engineering, especially plastic processing. He spent a lot of time in discussing with me about from general frame to every little detail of my doctoral thesis.

Many thanks to Prof. Dr.-Ing. Thomas Seul for reviewing my dissertation and constructive suggestions.

I appreciate Prof. Dr. Bingyan Jiang, Central South University of China. He provided excellent research opportunity for me to work independently during the period of my master's study and guided me walking on the research road of plastic processing. I also want to appreciate China Scholarship Council for the financial support during my study period in Germany very much.

I must also extend my thankfulness to other colleges in Institute of Conveyors and Plastics. Special thanks to Dr.-Ing. René Fuhrich, Dr.-Ing. Thomas Härtig, Dr.-Ing. Sven Friedrich and Dipl.-Ing. Eric Brückner for their kind help and encouragement. I would like also to appreciate Dipl.-Ing. Jan März, Dipl.-Ing. Reinhard Bönisch, B.Sc. Andreas Tändler, Frank Werner, Rocco Sickel, Sven Mauersberger and Sylke Roelke for their help in the experiments of my work.

Great thanks to my parents for their raising and supporting me. Special thanks to my sweet and pretty fiancée Siying Chen for her constant accompanying and understanding.

Chemnitz, September 2014

Yao Liu

Content

| | |
|---|-----------|
| 1. Introduction and research objectives | 13 |
| 2. State of art..... | 17 |
| 2.1 Injection molding | 17 |
| 2.2 Heat transfer during injection molding | 20 |
| 2.2.1 Heat transfer inside polymer | 22 |
| 2.2.2 Heat transfer inside mold | 26 |
| 2.2.3 Heat transfer between polymer and mold..... | 28 |
| 2.2.4 Influence factor of heat transfer process | 34 |
| 2.3 Temperature measurement during injection molding | 35 |
| 2.3.1 Thermocouple | 36 |
| 2.3.2 Infrared temperature sensor..... | 41 |
| 2.3.3 Comparison between diverse methods of temperature measurement | 43 |
| 3. Evaluation of HTC of the interface between polymer and cavity wall..... | 45 |
| 3.1 Principle of HTC evaluating | 45 |
| 3.2 Experimental conditions of HTC evaluating..... | 48 |
| 3.2.1 Material and equipment..... | 48 |
| 3.2.2 Cavity and temperature measurement system | 49 |
| 3.2.3 Experimental procedure | 53 |
| 3.3 Experimental results and discussion | 57 |
| 3.3.1 Influence of parameters on average value of HTC..... | 57 |
| 3.3.2 Heat across the interface between melt and cavity wall..... | 60 |
| 3.3.3 Surface roughness of plastic component | 63 |
| 3.4 Summary of Chapter | 65 |
| 4. Influence of HTC on the results of injection molding simulation | 67 |
| 4.1 Theory of injection molding simulation..... | 67 |
| 4.1.1 Properties of polymer..... | 67 |
| 4.1.2 Transport of polymer..... | 71 |

| | | |
|-----------------|--|------------|
| 4.1.3 | Numerical analysis methods | 72 |
| 4.1.4 | Characteristics of Moldflow Plastic Insight..... | 73 |
| 4.2 | Influence of HTC on simulated frozen volume percentage | 78 |
| 4.3 | Influence of HTC on simulated crystallinity | 82 |
| 4.4 | Influence of HTC on simulated part density..... | 87 |
| 4.5 | Summary of Chapter..... | 89 |
| 5. | Influence of HTC on the results of injection molding experiment | 91 |
| 5.1 | Influence of HTC on frozen layer..... | 91 |
| 5.2 | Influence of HTC on part crystallinity..... | 95 |
| 5.2.1 | Crystallinity of part under different HTC | 95 |
| 5.2.2 | Comparison with crystallinity simulation..... | 101 |
| 5.3 | Influence of HTC on part density | 104 |
| 5.3.1 | Part density under different HTC | 104 |
| 5.3.2 | Comparison with the part density simulation | 107 |
| 5.4 | Summary of Chapter..... | 109 |
| 6. | Summary | 111 |
| 6.1 | Conclusions | 111 |
| 6.2 | Future works | 112 |
| 7. | Literature | 115 |
| 8. | List of symbols and abbreviations..... | 123 |
| Appendix | | 129 |

1. Introduction and research objectives

Due to the outstanding processability and high performance-price ratio, plastic component plays a significant role in daily life of everyone. With development of new additives and addition of reinforcing materials (e.g. fibers), property of plastic has been remarkably improved and its application field has been obviously expanded. It makes the plastic displacing dominant materials used in diverse fields possible.

Since the invention of first screw-type injection molding machine in the 1940s, injection molding technology of plastics has been used extraordinarily widely in industry. Heat transfer is one of the most important segments in injection molding process [Bai06]. Because it has not only important effect on temperature distribution of the component, but also can alter temperature distribution in the mold. On the aspect of melt temperature, it can affect flow characteristics of polymer directly and crystallization process afterwards. Then the component quality, composed of mechanical behavior and dimensional precision, can be influenced by above-mentioned factors, especially miniature part or part with micro structure. On the aspect of mold temperature, it has close relationship with performance of cooling system and even the cycle time, which certainly influence the production efficiency greatly [Gof05, Liu09]. The effects of heat transfer during injection molding are shown in Fig.1.1.

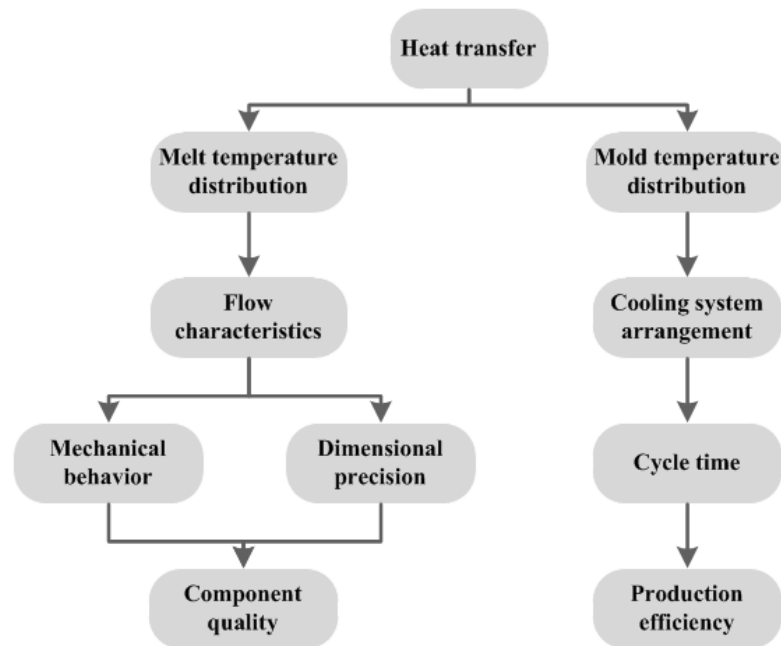


Fig.1.1 Influence of heat transfer during injection molding

Heat transfer during injection molding is generally composed of three different sections, heat transfer inside polymer, inside metal and on the interface between polymer and metal. Thermal conductivity of polymer or metal, which changes with varied temperature, is a kind of material characteristics and has been explored exhaustively. However heat transfer on the interface between polymer and metal is more unacquainted to most of users, which is quite significant as well. Heat transfer coefficient (HTC), which changes with diverse factors, e.g. processing parameters, material characteristics and surface morphology, is considered as a critical index to describe the heat transfer performance of the interface.

Computer simulation has considerably advanced owing to the outstanding promotion of computer hard- and software ever since the end of last century. Nowadays computer simulation analysis of injection molding process can be achieved with finite element method (FEM), finite volume method (FVM) or the combination of these two methods. Computer simulation is extraordinary beneficial to validating and optimizing plastic part, injection mold, resin selection, and injection molding process. Potential defects, such as weld line, air trap, and sink mark, emerging during filling, packing and cooling stage can be predicted before the first molding trial, and therefore mistake of design can be modified without overfull expense of money and time. In addition, computer simulation can accomplish the experiments which can be difficultly operated in reality. For instance, a set of experiments contains numerous variables, and each variable has several different levels. It is almost impossible to finish the whole set of experiments, but with computer simulation it can be accomplished in relatively shorter time, even at the same time. Sometimes values of parameters beyond regular range can be set, if some extreme situations are concerned, even they can cause some damage to the machines or people. Therefore it can help to analyze and thus improve the whole process, raise success rate of first molding trial, reduce cost of manufacture and shorten the development cycle. Meanwhile, computer simulation has been also used in reactive injection molding, injection-compression molding, gas-assisted injection molding and co-injection molding.

In computer simulation, heat transfer also plays an important role for obtaining precise outcome. Some simulation software, e.g. Moldflow, provide the function that users can define the real values of HTC in stages of injection, packing and part ejection and for a few senior users HTC can be set as custom curve changing with time which can represent the actual heat transfer situation on the interface more accurately.

In consideration of the importance of heat transfer during injection molding, especially the great effect of HTC on simulation precision, following objectives and assignments were

achieved and accomplished in this dissertation.

- a. Heat transfer phenomenon during injection molding was theoretically studied, especially heat transfer on the interface between polymer and metal, including diverse factors which can influence HTC and their influence degree.
- b. Through theoretical analysis, formula which can calculate real HTC was developed based on measured temperature of mold and melt. Real HTC values under different situation, e.g. different surface roughness, melt temperatures and injection rates, were obtained by means of injection molding experiment and subsequent data processing.
- c. Computer simulations were finished with real HTC obtained by above-mentioned experiments, and also with default values. Frozen volume percentage of plastic part, relative crystallinity and part density under different HTC value were simulated. And then comparison between result calculated with observed HTC value and that of preset value was accomplished.
- d. Corresponding experiments for validating and verification were carried out, and the results of them were compared with simulation results.

The significance of this dissertation is not only providing practical reference in cooling system design, but also offering reliable HTC value for injection molding simulation and then acquiring more precise simulation result.

2. State of art

2.1 Injection molding

Injection molding, defined as a cyclic and automated process for producing identical plastic articles from a mold, is the most widely used polymer processing operation. The process can produce either very small or very large parts using virtually any plastic material [Mal11]. The injection molding is itself a very complex system composed of multiple components, which are subjected to many cycles of temperatures and stresses [Kaz07]. Injection molding has several features, including direct path from resin to finished part, i.e. no or only minimal finishing of the molded part necessary, process can be fully automated and good reproducibility of production [Mic95]. So that the main advantage of this process is the capacity of repetitively and economically fabricating parts with complex geometries at high production rate [Zhe11]. It represents the most important process for manufacturing plastic parts and is suitable for mass producing components [Pöt95]. Typical injection molding can be found everywhere in daily life, e.g. automotive parts, consumer electronics wares and increasing number of construction part made from fiber reinforced plastic.

The basic molding equipment is composed of an injection molding machine, an injection mold, and a mold temperature control unit. These three components can influence the manufacture process directly and decide its success or failure. They also interact with one another through pressure, temperature, and speed [Joh94]. The injection molding machine is shown as Fig.2.1.

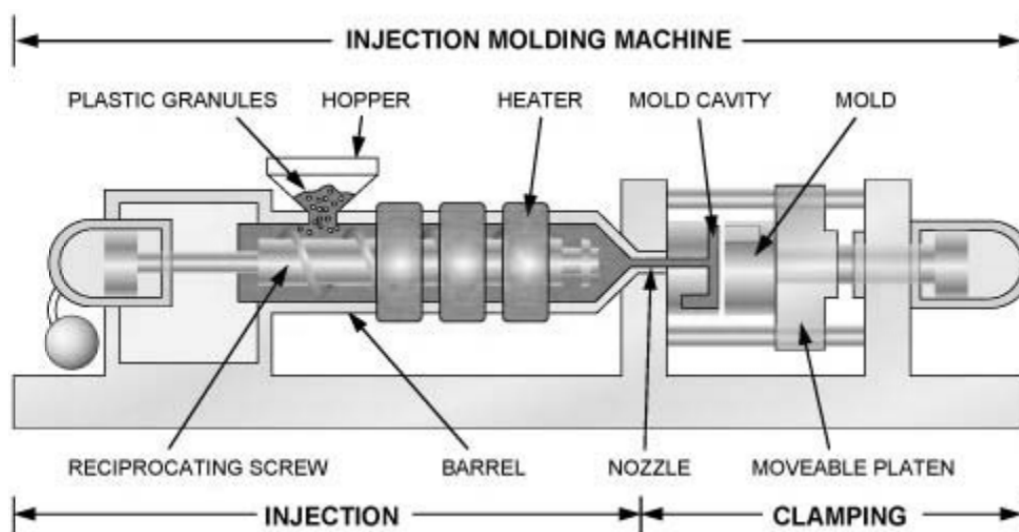


Fig.2.1 Constitution of injection molding equipment [Max10]

An injection molding machine can be defined as a machine which produces formed components in a repeated manner from polymer materials [Joh94]. The beginning of injection molding can be dated rather precisely. In 1872, J.W. Hyatt solved the problem of plasticizing and shaping a mixture of nitrocellulose and camphor with his “packing machine” (US-patent 133229) [Rub73]. An injection molding machine can be broken down into the following components: plasticizing/injection unit, clamping unit, driving unit and control unit. Plasticizing /injection unit provides energy to make the solid polymer into hot melt and then to inject melt into mold cavity. Clamping unit, driven hydraulically, mechanically or electrically, is used in opening and closing the mold during the production cycle. Driving unit provides necessary pressure of hydraulic oil or kinetic energy from electric motor. And the sequence of the injection molding cycle is manipulated by a control unit, which is integrated within the machine and operated through a touch screen nowadays.

The central element of the injection molding process is the mold, shown as Fig.2.2. Each mold contains at least one cavity, into which the plastic material is injected and which forms the final part geometry. Mold inserts are designed independently for producing more or less complex injection molding parts.

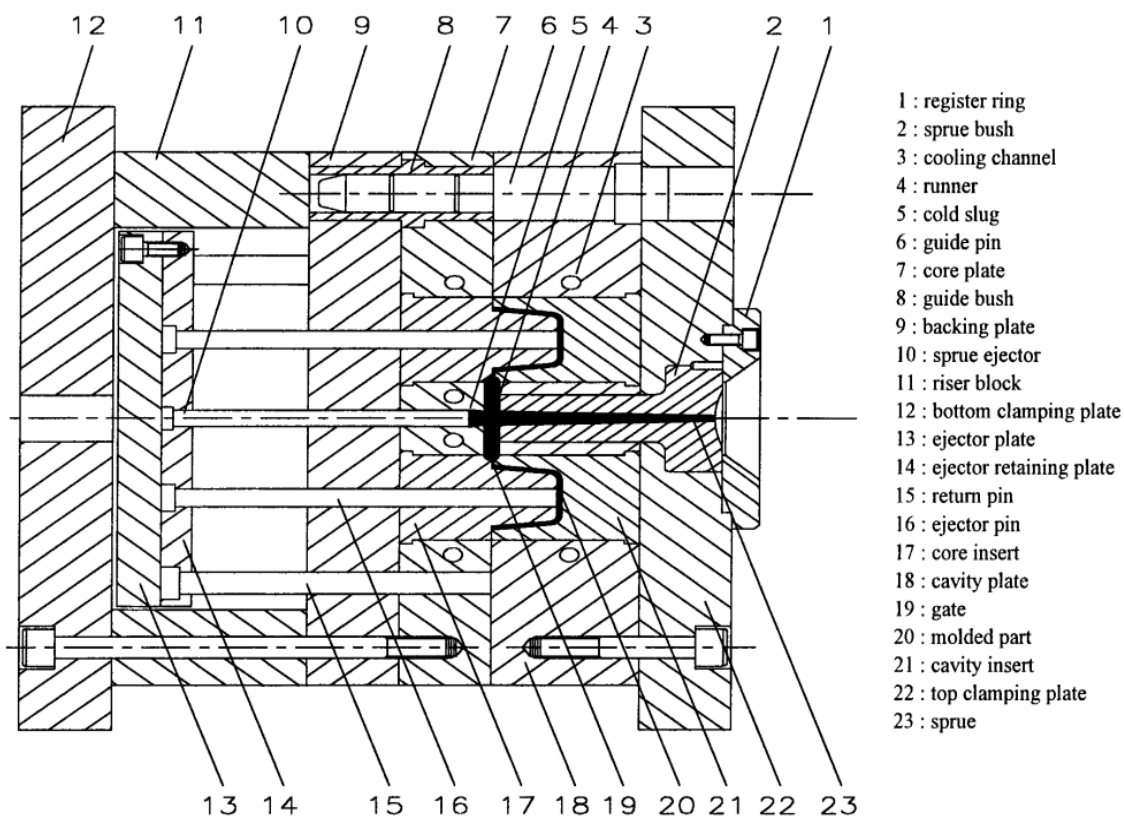


Fig.2.2 Schematic of standard injection mold [Mok01]

The injection mold is a complex system that must simultaneously meet many requirements. The primary function of the mold is to contain the polymer melt within the mold cavity so that the mold cavity can be completely filled to form a plastic component whose shape is reverse to the cavity. The second function of the mold is to transfer heat from the hot melt to the cold mold quickly and steadily, so that injection molded products can be produced efficiently and uniformly. The third function of the mold is to eject the part from the mold cavity in a repeatable manner, so that the molding component can be produced automatically [Kaz07].

Injection molding process is a consecutive process that includes a series of sequential steps, including stages of plasticizing/filling, packing, cooling and part ejection, shown as Fig.2.3 and depicted in detail subsequently.

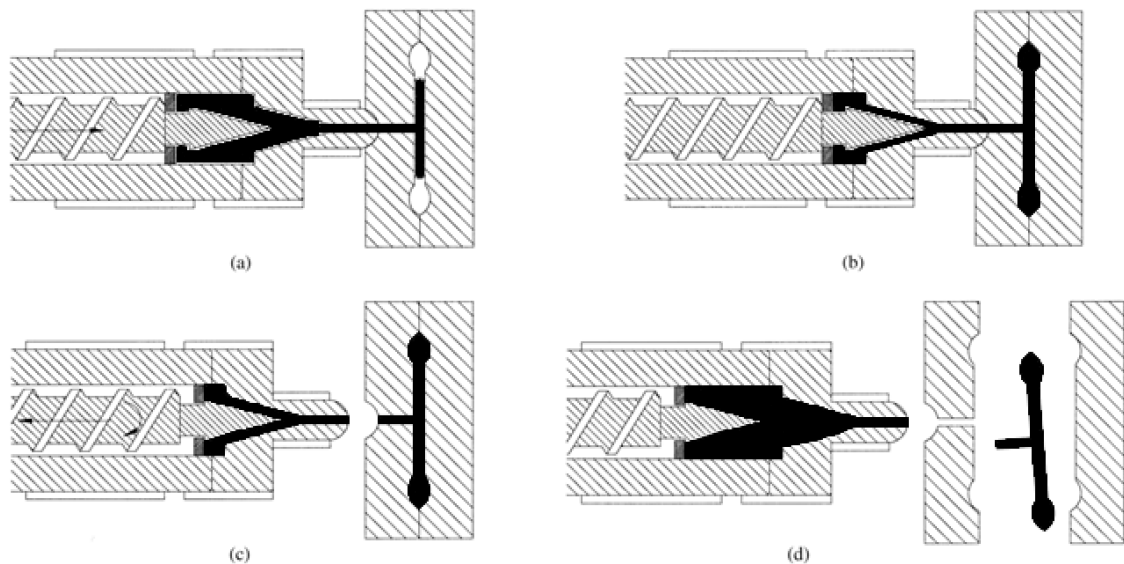


Fig.2.3 Schematic of injection molding procedure [Yan00]

(a) plasticizing/filling stage, (b) packing stage, (c) cooling stage and (d) part ejection

Plasticizing/filling stage: plastic granules are fed to the machine through the hopper, and the screw rotates and moves the granules forward to the screw barrel. The polymer is plasticized from solid granules through the combined effect of heat conduction from the heated barrel and the internal shear heating caused by rotation of the screw. And then, the clamping unit moves forward until the movable half of mold is in close contact with the static half. The screw moves forward axially without rotation and the polymer melt is forced from the barrel into the mold. The hot polymer flows into the one or more mold cavities, which form the shape of plastic component, through runner system including the sprue, the runners and the gates.

Packing stage: after the cavity is filled, the screw moves with a small displacement to maintain a holding pressure and provides additional material into the cavity against the shrinkage caused

by cooling of the component, to ensure complete filling and detailed replication as far as possible. When the polymer in the gate is solidified, melt can no longer flow into the cavity, so pressure provided by injection molding machine can be removed from this time on.

Cooling stage: after the polymer melt ceases to flow, the cavity pressure gradually decreases to zero or a very low value. Cooling stage, which begins with cavity completely filled, provides additional time for the component continued cooling down and solidifying without polymer compensation. Therefore volume contraction of component occurs at this time and gaps vacuum or filled with air may emerge on the interface between polymer and metal. Simultaneously, the screw starts rotating and moving backward, and the plasticizing stage of next cycle starts. In general, cooling stage dominates most of the cycle time because the rate of heat flow from the melt to the mold steel is limited, especially under the situation of thick-wall component injection molding.

Part ejection: when the molded part has cooled sufficiently and become stiff enough, the mold opens and the component can be ejected by ejector pin, sometimes with the help of robot. After this stage, an injection cycle has been completed, and the next cycle can start.

The whole injection molding process runs automatically and all motions of the machine are monitored and controlled by the control unit of the injection molding machine.

2.2 Heat transfer during injection molding

The polymer enters the hopper at room temperature, T_R . It is then heated in the barrel to the operating temperature T_O and is cooled down in the mold to an ejection temperature, T_E . T_E is usually much higher than T_R . For example, normally T_R is about 20-25°C, but T_E may be between 50 and 80°C. Certainly, it depends on the type of polymer. To heat the polymer from the cold granules to the temperature at which it becomes hot melt which can be injected, a certain amount of energy must be added to it. This takes place in the barrel of the molding machine. The energy is supplied mainly by the work of the screw, which transforms mechanical energy via dissipation into heat, and also with some heat supplied from the heaters surrounding the barrel. So actually, the mold is a heat exchanger, because most of the energy which has been added to the polymer in the barrel, to make it suitable for injection, must be removed before the mold can be opened to eject the plastic component, which must be stiff enough for withstanding the force of ejection [Ree02].

Although, cooling stage takes most time of the injection cycle, mentioned above, heat flow takes place not only during the cooling stage, but also during filling and packing stage, even component can bring a certain amount of heat away when it is ejected out of the cavity. Proper design of cooling system can result in two desirable outcomes. First, it can lead to an efficient cooling result. Cooling and cycle times can be reduced, so that production efficiency can be much improved. Second, it can bring a more well-distributed cooling result. The temperature of each area on the plastic component can decline at almost equal rate. So that it can avoid the defects of differential shrinkage and warpage. Thereby dimensional accuracy of the plastic component can be guaranteed.

The best method of cooling evaluation can be obtained when an integrated computer aided process simulation is performed [Mal11]. Through the analysis, the information about cooling time can be provided, moreover the prediction of shrinkage and warpage can be acquired. It is great aid for the mold designer to optimize the cooling system for achieving efficient and balanced cooling for each area of the injection molded component. But first of all, the process and theory of heat transfer behind the injection molding process should be comprehended thoroughly.

In the field of heat transfer, heat is energy in transit from a hot body to a cold one. Temperature is a property of bodies which determines the direction of the heat flow. The amount of heat flux, \vec{q} , flowing from one location to another is the product of negative local temperature gradient, $-\nabla T$, and the thermal conductivity, k . This is differential form of the Fourier's Law, and expressed as Eq.2.1.

$$\vec{q} = -k\nabla T \quad (2.1)$$

The thermal conductivity is often considered as a constant, though this is not always true. Although the thermal conductivity of a material generally varies with temperature, the variation can be small over a significant range of temperatures for some common plastics. According Eq. 2.1, the amount of heat transferred Q can be derived as Eq. 2.2.

$$Q = -ktA\nabla T \quad (2.2)$$

t is time, and A is the cross sectional area. For many simple applications, Fourier's law is used in its one-dimensional form. For example, in the x-direction, the heat transfer between two endpoints, point A and B, can be simplified as follows.

$$Q = ktA \left| \frac{dT}{dx} \right| = ktA \frac{\Delta T}{d} \quad (2.3)$$

In Eq. 2.3, ΔT and d are the temperature difference and the distance between point A and B respectively.

During injection molding, at first the heat from the plastic flows into the mold, then flows from the mold into the cooling channels. And finally the heat flows into the air or into the cooling machine with medium together. As the highest and lowest temperature in this system, the ΔT between the polymer and the cooling medium must be considered. The greater the ΔT between the plastic and the coolant, the more energy will flow from polymer to mold in a certain period of time. Therefore if ΔT is large, the temperature of component will decrease faster than if ΔT is small. When the polymer cools down, ΔT gets smaller and smaller, so that in the end the rate of heat transfer can be ignored in practice [Ree02]. It means the temperature of cooling medium should be much lower than ejection temperature, so that short cooling time can be obtained.

2.2.1 Heat transfer inside polymer

In the filling stage, hot melt flows through sprue, runners and gates, finally into the cavity. Because most injection molding parts have complicated three-dimensional configurations and the rheological response of polymer melt is generally non-Newtonian and non-isothermal, it is extremely difficult to analyze the filling process without simplifications. The generalized Hele-Shaw (GHS) flow model introduced by Hieber and Shen [Hie80] is the most common approximation that provides simplified governing equations for non-isothermal, non-Newtonian and inelastic flows in a thin cavity. The assumptions of the GHS flow model are following. (1) The thickness of the cavity is much smaller than the other dimensions. (2) The velocity component in the direction of thickness is neglected, and pressure is a function of x and y only. (3) The flow regions are considered to be fully developed Hele-Shaw flows in which inertia and gravitational forces are much smaller than viscous forces. (4) The flow kinematics is shear-dominated and the shear viscosity is taken to be both temperature and shear rate dependent [Su04]. Based on above mentioned theory, the polymer melt flowing in a thin cavity can be simplified as a two-dimensional model.

Polymer melt in the middle of thin cavity is always divided into three different regions, front region, fountain flow region and lubrication region, as shown in Fig.2.4. The front region is also called free surface region. The unsteady flow of a polymer melt with a free surface is

driven at a constant velocity with a fixed equilibrium shape. Fountain flow region is behind the front region. It is assumed to be a slip stage in the fountain flow region. The flow interface moves slower as it gets closer to the mold wall. Lubrication region is a fully developed region, and it is assumed to be a non-slip stage in this flow region [Li94].

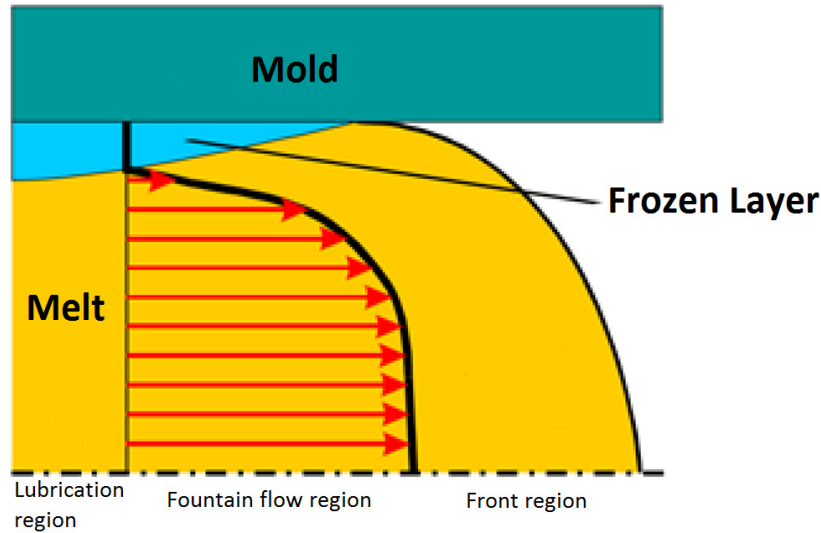


Fig.2.4 Flow pattern inside the cavity during injection [Ame07]

With flowing of hot melt into the cavity, it generates frozen wall layer close to the cavity wall. Because of the heat transfer from melt to cavity wall, temperature of hot melt decreases continually, so that polymer of frozen wall layer turn into solid phase. Under the high pressure of injection inside the cavity, the surface of hot melt still gets close to that of frozen wall layer, that means on the interface between hot melt and frozen layer there is no air gap, which makes the situation much simpler.

Thermal conductivity is the value of rate at which a material conducts the heat from hot to cold. Plastics are normally poor conductor of heat and thermal conductivities of them always change under condition of high pressure [Daw06]. Thermal conductivities of some typical polymers as example are shown in Table 2.1.

For neat polymer material, thermal conductivity varies in the range between 0.15-0.5W/(m·K). The thermal conductivity of semi-crystalline thermoplastics decreases with increasing temperature till the melting point. But at the melting point, because the crystalline part of polymer melts, which has better heat conduction ability than amorphous part, thermal conductivity value decreases more quickly. In the higher temperature region, thermal conductivity of polymer is nearly independent of temperature. On the contrary, temperature has

little influence on the thermal conductivity of amorphous thermoplastics [Mic95], which can also be derived from Table 2.1. Even for semi-crystalline thermoplastics, the variation of thermal conductivity is in a much smaller range comparing with the thermal conductivity value of metal. So when the frozen layer generates, it has almost no obvious effect on heat transfer inside the cavity.

Table 2.1 Thermal conductivity of some typical polymers [Mar07]

| Polymer | Temperature / K | Thermal conductivity / W/(m·K) |
|-------------------------------|-------------------|-----------------------------------|
| Poly(hexamethylene adipamide) | 303 (crystalline) | 0.43 |
| | 303 (amorphous) | 0.36 |
| | 423 | 0.15 |
| Polystyrene | 273 | 0.105 |
| | 373 | 0.128 |
| | 473 | 0.13 |
| Poly(vinylchloride) | 273 | 0.158 |
| | 373 | 0.165 |

The specific heat is the amount of heat per unit mass required to raise the temperature by one degree Kelvin. In general, polymer needs much more energy than metal of same weight, when they raise equal degrees of temperature. The specific heat of some typical polymers is shown as Table 2.2.

Table 2.2 Specific heat of some typical polymers [Mar07]

| Polymer | Status or temperature / K | Specific heat / J/(kg·K) |
|------------------------------|---------------------------|--------------------------|
| Poly(ethylene) | 300 | 1555 |
| | melt | 2202 |
| Poly(propylene) | 300 | 1622 |
| | melt | 2099 |
| Poly(methyl methacrylate) | 300 | 1375.5 |
| | 400 | 2076.6 |
| Poly(styrene) | 300 | 1223.0 |
| | 400 | 1932.2 |
| Poly(ethylene terephthalate) | 300 | 1172 |
| | 400 | 1820.3 |

It can be summarized from Table 2.2 that thermoplastics show the specific heat increasing with temperature, and normally the value locates in the range between 1000 and 2500 J/(kg·K), which is approximately 2-6 times of the specific heat value of carbon steel. However, for semi-crystalline thermoplastics, the phase transformation releases extra heat, when the temperature decreases. In other words, heat transferred out of polymer, but the temperature keeps the same around the crystallizing point, so that there is a discontinuity of specific heat value in this region.

According to Eq. 2.2, in a certain period of time, quantity of heat is proportional to thermal conductivity and temperature gradient, when cross-section of heat transferring is fixed. In injection molding process, with decreasing of melt temperature and slightly increasing of mold temperature, the temperature difference between them gets smaller. The value of thermal conductivity of polymer is relatively constant, as mentioned above. So the quantity of heat decreases nearly proportionally with decreasing temperature difference. At the same time, the releasing heat of polymer is equal to the heat transferring to the mold. So Eq. 2.3 can be derived as Eq. 2.4.

$$Q = ktA \frac{\Delta T}{d} = cm\Delta T' \quad (2.4)$$

c is the specific heat of polymer, m is the mass of polymer and $\Delta T'$ is temperature difference of polymer during the time t . So it can be transformed to following form.

$$\Delta T' = a \frac{\Delta T}{c} \quad (2.5)$$

a is the value of $\frac{kAt}{md}$, which can be approximately considered as a constant. So $\Delta T'$ is in direct proportion with ΔT , but in negative proportion with c . But during injection, the variety range of ΔT , between the beginning and end of process, is much larger than that of c . So ΔT plays more important role than c in the variety of $\Delta T'$, in other words $\Delta T'$ gets smaller after it reaches the peak value and converges towards zero.

The thickness of the frozen layer increases continuously during filling and packing phase. At the end the frozen layers from both sides meet in center of the cavity with the emergence of polymer shrinkage, which is due to the temperature decreasing, and no polymer can pass through any more.

2.2.2 Heat transfer inside mold

During the injection molding cycle, the mold temperature rises when the cooling channel transfers heat from the mold continuously. After the injection finishing, no more heat will be added to the mold plate, but the cooling channel continues to remove heat from the mold until the next injection starts. It is important that, once the mold is on cycle, which means thermal equilibrium has been built, the amount of heat entering the mold is the same to the amount of heat removed from the mold [Ree02].

In Eq. 2.1, \vec{q} is proportional to the thermal conductivity k , and the temperature gradient ∇T . Two implications can be obtained from this equation about the heat transfer phenomenon inside mold. Firstly, the rate of heat transferring is proportional to the thermal conductivity of metal, which means highly conductive metal as QC-10 can transfer heat faster than P20. In addition, thermal diffusivity α , is the thermal conductivity divided by density and specific heat, shown as Eq. 2.6.

$$\alpha = \frac{k}{\rho c} \quad (2.6)$$

ρ is the density of the metal. Thermal diffusivity α , describes the metallic ability of adapting environmental temperature, which means metal with higher thermal diffusivity will reach the thermal equilibrium faster when the temperature changes. So a good thermal diffuser achieves steady state and uniform temperature distribution quickly. The thermal conductivity and thermal diffusivity of P20 and QC-10 are shown as Table 2.3.

The advantage of the metal with higher thermal diffusivity is not only transferring heat and achieving thermal equilibrium more quickly than normal mold material, but also decreasing the average mold temperature and obtaining more equal cooling result, which can improve performance of the whole cooling system as shown in Fig.2.5.

Table 2.3 Thermal conductivity and thermal diffusivity of P20 and QC-10 [Ban08, Au07]

| Metal | Thermal conductivity / W/(m·K) | Thermal diffusivity / 10 ⁻⁶ m ² /s |
|-------|-----------------------------------|---|
| P20 | 29 | 8.03 |
| QC-10 | 160 | 66.5 |

It can be derived from Fig.2.5 that mold temperature experiences periodic variety and maintains higher temperature level than that of medium in cooling channel. It reaches the peak temperature after the moment of heat transferred from polymer to mold and then drops gradually. Average temperature of a cycle increases with times of continuous injection molding until final thermal equilibrium has been built. It can also be seen from Fig.2.5 that temperatures at the positions of QC10 Ch5 and P20 Ch5 represent the temperature around the cooling channel. Owing to the higher thermal conductivity value of QC-10, under the thermal equilibrium condition the temperature around cooling channel has a higher value than that of P20, and accordingly the mold temperature has a lower value than that of P20.

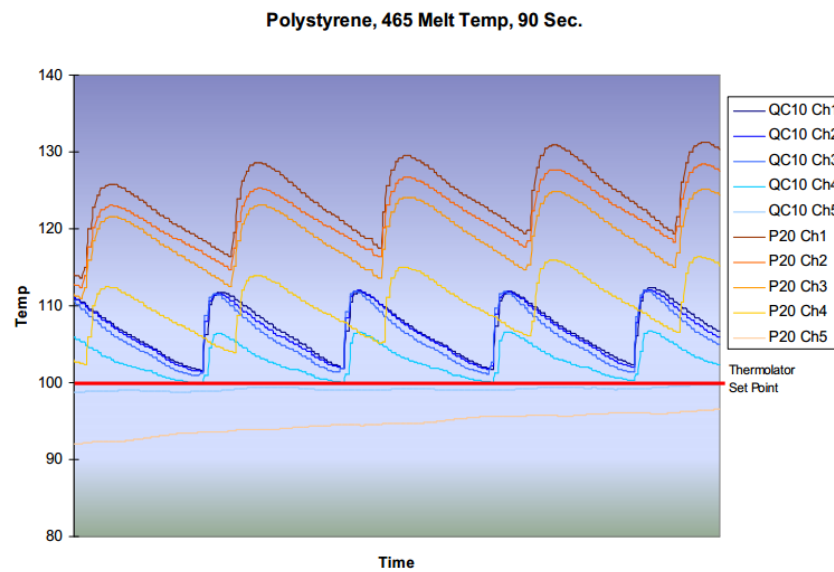


Fig.2.5 Mold temperature of four cycles, different mold material and measuring position [Ban08]

The second implication is that temperature gradient is demanded by heat transferring, which means cooling time can be reduced by increasing the temperature gradient. There are two concrete methods to improve the temperature gradient. One is moving the cooling channel to the surface of the mold cavity as close as possible, which can certainly exacerbate the inhomogeneous temperature distribution. The other one is reducing the medium temperature in the cooling channel. It can cause inhomogeneous temperature distribution and maybe also waste of energy. So design of cooling system should be considered carefully in view of the efficiency, expense, processability and product quality. Typical temperature distribution of mold is shown as Fig.2.6.

It can be seen from Fig.2.6 that isothermal curves distribute around the cooling channels as the shape of concentric circles and the heat transferring direction is scattering. But near the flat-plate component, a plastic concave lens, isothermal curves distribute perpendicularly to the

thickness direction of plastic component, and the heat transferring direction in this area is parallel to the thickness direction of component. So for the flat-plate plastic component, there is hardly any heat transfer in other directions.

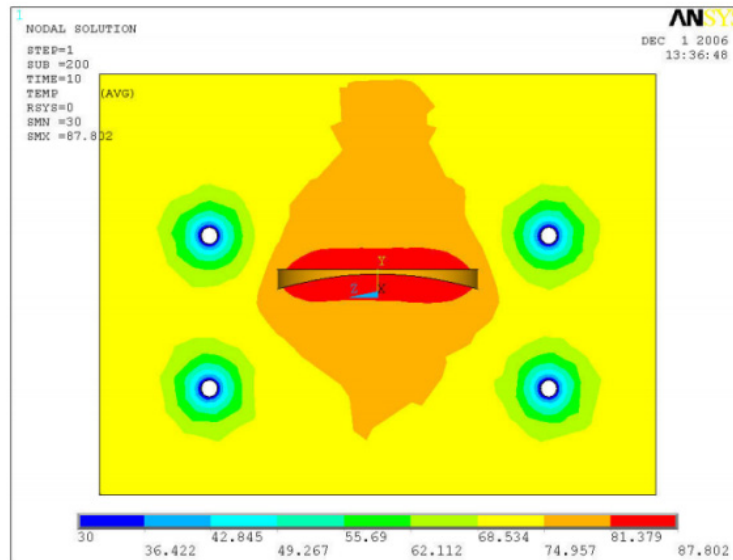


Fig.2.6 Mold temperature distribution from FEM simulation [Che07]

Heat is not only removed by cooling channel, but also in a fraction, by the plastic components, for they have always been ejected when they are still hotter than raw material before processing. Therefore, they carry a certain amount of heat, which will be radiated or conducted into the environment [Ree02]. But it takes only a very small proportion of gross amount of heat, which can be ignored in most conditions.

2.2.3 Heat transfer between polymer and mold

As above mentioned, heat transfer inside polymer and mold has been discussed thoroughly. Besides, the heat transfer between polymer and mold plays an important role in the whole process. And it can also provide activation energy for reaction injection molding and decide the reaction rate on the surface of cavity by changing ambient temperature [Nag14]. According the model of Farouq Y. [Far05], it can be described in Fig.2.7.

Walls 1 and 3 represent cavity walls on both sides. Wall 2 represents the plastic component. And RTC means the resistance of thermal contact between polymer and mold. So if the model is symmetrical, one half of the heat transfer model can be simplified as Fig.2.8, in which heat transfer system seems to be electrical system including electric resistance, voltage and current.

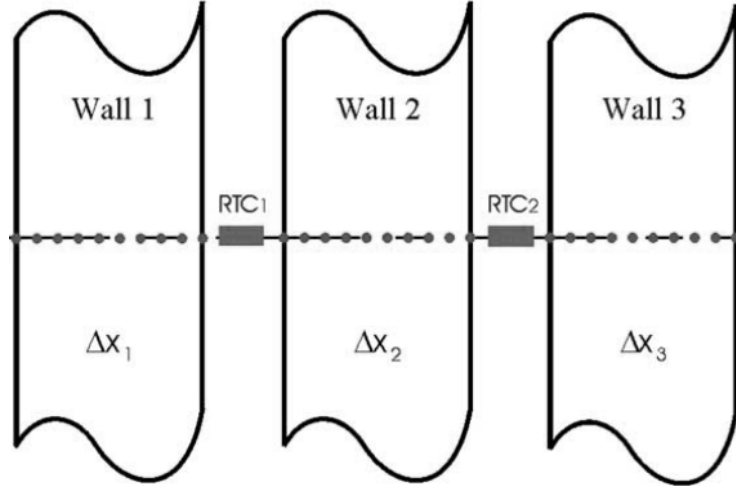


Fig.2.7 Heat transfer model during injection molding [Far05]



Fig.2.8 Simplified heat transfer model during injection molding

From Fig.2.8, it can be seen that heat transfer has been divided into three parts, the heat transfer process inside polymer, the process on the interface between polymer and melt and the process inside mold. And TR_p , TCR_l and TR_M represent the thermal resistance of polymer, thermal contact resistance of the interface between polymer and mold and thermal resistance of mold respectively. T_{poly1} , T_{poly2} , T_{mold1} and T_{mold2} represent corresponding temperatures on every nodal point with decreasing trend.

Thermal resistance, whose unit is $(m \cdot K)/W$, is reciprocal of thermal conductivity as a characteristic of material also. It describes the difficulty degree of heat passing through certain substance. When heat flows from the hotter body to the colder body, a temperature drop emerges on the interface between the two surfaces in contact. This phenomenon is the result of a thermal contact resistance effect existing between the contacting surfaces [Hol10]. Thermal contact resistance is a resistance to the flow of heat across an interface of two surfaces that are in contact, which is reciprocal of heat transfer coefficient (HTC), whose range of value is between 2000 and 200000 $W/(m^2 \cdot K)$ according to the book of Madhusudana [Mad96]. The temperature profiles of two contacting objects, without and with thermal contact resistance effect, are shown as Fig.2.9.

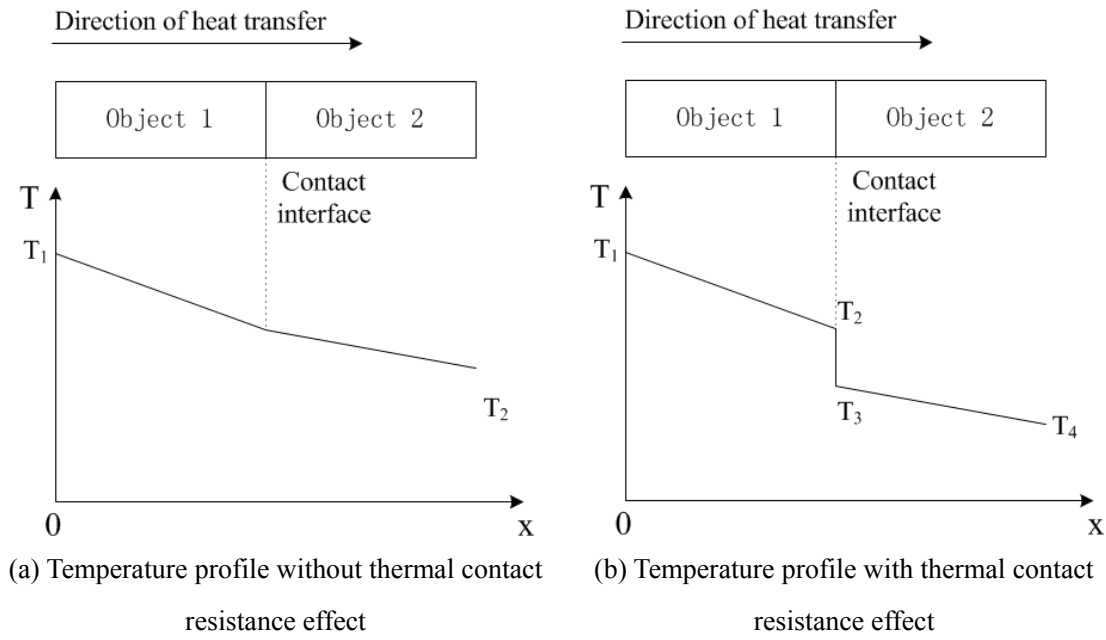


Fig.2.9 Schematic of thermal contact resistance effect

As the reciprocal of thermal contact resistance, HTC represents the heat transferring ability of the interface between polymer and metal. The relationship between amount of transferred heat and HTC, Q and h respectively, is shown as Eq. 2.7.

$$Q = htA\Delta T \quad (2.7)$$

The value of h changes considerably during injection molding process, which can affect the heat transfer process obviously. Therefore more attentions are drawn by the changing process of it. In earlier stage, according to the work of Yu [Yu90], HTC has potential significant effects on predicted cooling times. In research of Young [You07], it has been proved that there is a very strong relation between achievable filling distance and HTC values over the range 1000–10000 W/(m²K). Yu [Yu04] tried to build the model for describing flow and heat transferring process in micro- and macro injection molding. He found that the uncertainty of the local HTC in micro channels contributes greatly to the difficulty in predicting the filling length. Otmani kept similar opinion in his paper [Otm11] that, HTC should be taken into account during the whole simulation process and it is definitely a key parameter that needs to be determined to obtain accurate simulation results.

Some researchers tried to ascertain the value of HTC through the method of building mathematical model. Sridhar [Sri00] modeled the development of the thermal contact resistance during injection molding process, using an air gap conductivity model and showed

that a significant increasing of thermal contact resistance emerged. Fuller [Ful01] built an analytical thermal conduction model, using contact mechanics principles and basic material properties to predict the thermal conduction of metal/polymer joints. Masse [Mas04] calculated the mold temperature, polymer surface temperature, heat flux and residual stress based on the self-built thermal conduction model and achieved a good agreement with the result of experiments.

Some others carried out some experiments and then obtained HTC after data processing. Delaunay [Del00] fabricated equipment for measuring in an injection mold. They found a rapid increase in the thermal contact resistance when an air gap developed in the mold cavity. Bendada [Ben04] also adopted the experimental method to ascertain the value of HTC, which locates in the range between 125 and 250 W/(m²K) and varies with processing time. Schmidt [Sch98] measured HTC of the polymer–mold interface during blow molding and obtained HTC values in the range approximately 900–2500 W/(m²K) with increasing blowing pressure. Masse [Mas04] obtained the values of HTC between 1000 and 5000 W/(m²K), which varies with processing time. Parihar [Par97] tested the processing of elastomers, and obtained HTC values in the range between 384.6 and 714.3 W/(m²K). In the work of Beilharz [Bei07], HTC was ascertained as 250 W/(m²K) under room temperature, and it can reach 100000 W/(m²K) because of low hardness of the mold material. Dawson [Daw08] quantified HTC relevant to polymer processing including the effect of air gaps by means of experiment, and he found the magnitude of thermal resistance is small and consequently the uncertainties in the HTC are relatively high. Goff [Gof05] built injection mold for experiments and calculated the value of HTC based on measured temperature which varies between 200 and 1000 W/(m²K). In the work of Brunotte [Bru06], HTC from experiment is in a relatively low level and varies with different kind of polymer. For Polypropylen, HTC value is in the range of 500-600 W/(m²K), which is shown in Fig.2.10. And for Polycarbonat it is between 400 and 600 W/(m²K).

Through our own experimental work [Liu13], the average value of HTC during injection molding process has been ascertained between 18000 and 36000 W/(m²K).

Another unconventional method was employed by Nguyen-Chung [Ngu08, Ngu10] and Löser [Lös09]. Nguyen-Chung found the closest simulation result to the experimental result by altering the value of HTC, which can also stand for the different processing conditions, shown as Fig. 2.11. In the work of Nguyen-Chung, HTC value varies in the range between 0 to 30000 W/(m²K), which is not the simulated value or the value calculated from experimental result directly but can bring about a more precise simulation result with reverse engineering.

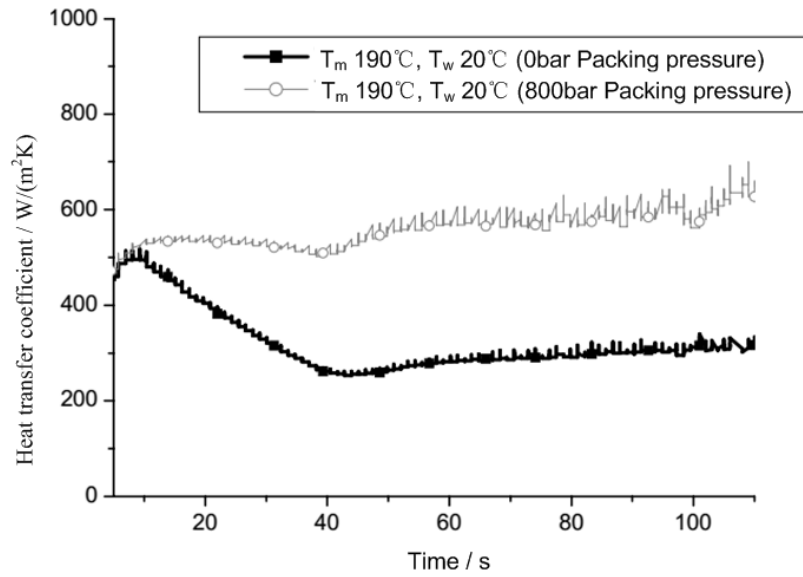


Fig.2.10 Heat transfer coefficients without and with packing pressure [Bru06]

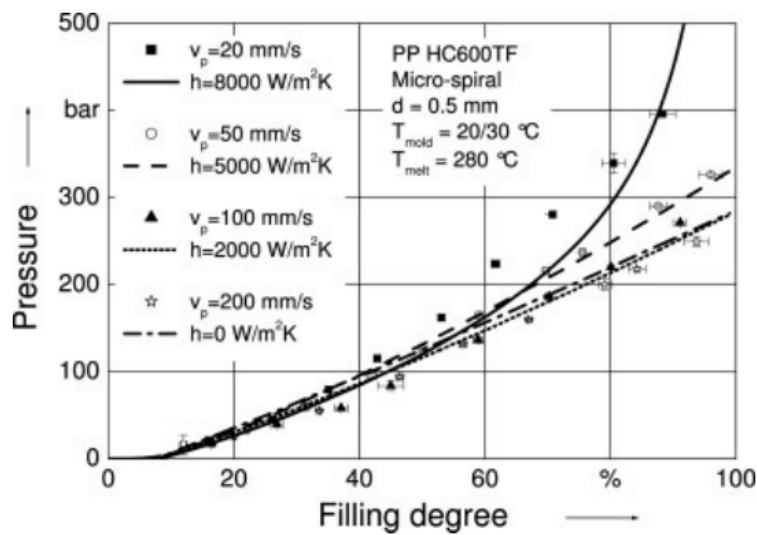


Fig.2.11 Filling degree vs. pressure under different HTC and injection rate [Ngu10]

There is a wide variation of HTC values reported in the literature, owing to difference of apparatus, material property, processing parameter and surface roughness.

Actually the variety of HTC can also be divided into several stages as the whole injection molding process, correspondingly to filling, packing, cooling and part ejection as shown in Fig.2.12.

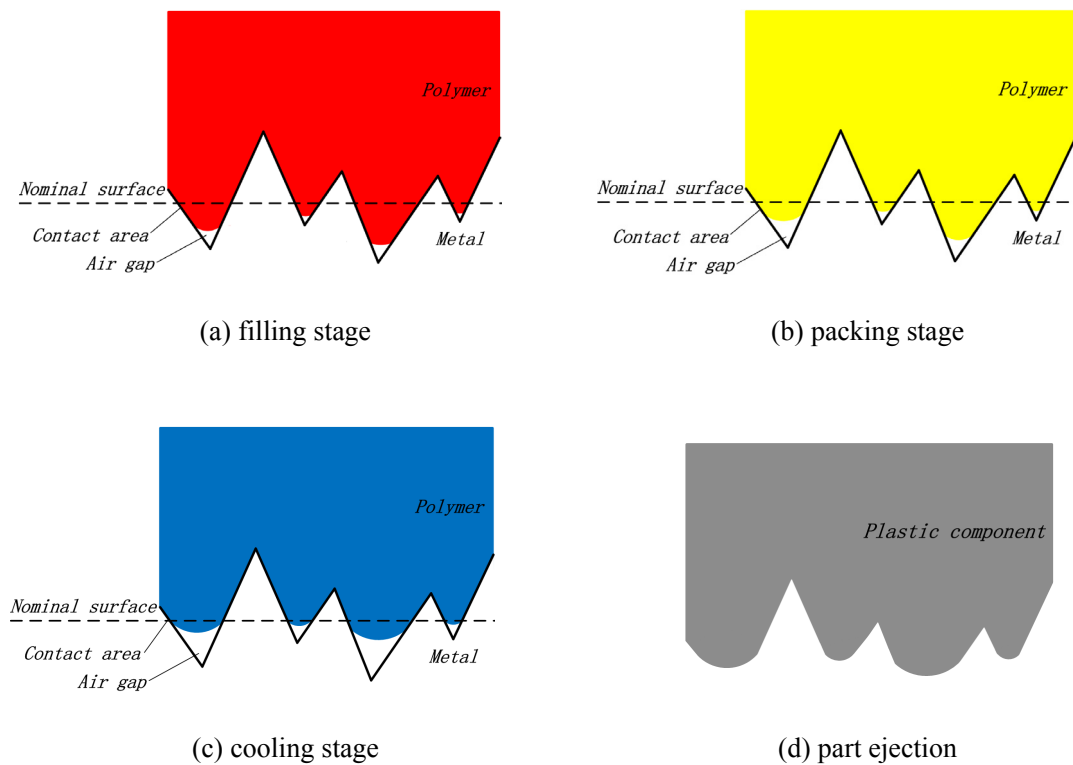


Fig.2.12 Schematic of contact situation on the interface between polymer and metal

It can be seen from Fig.2.12 that there are “peak” and “valley” obviously in microscopic scale, which is described as surface roughness in macroscopic scale normally.

- a. In filling stage, polymer melt flows into the cavity, at the same time contact between melt and cavity wall is built. Heat flow from polymer to metal starts, driven by temperature difference. Due to the high viscosity of polymer melt, there are some small air gaps on the interface.
- b. In packing stage, with melt temperature decreasing, air gaps are apt to be enlarged. But in this stage, gate of part is still open, so under high packing pressure, polymer can be pressed closely on the interface. So the value of HTC can be only changed slightly.
- c. After shrinkage of plastic during cooling, the real contact area would not still follow the surface of mold because of the shrinkage, but develop smaller regional contact. At the same time, the air gap, which has poor heat transferring ability, exists in other area. Therefore in the stage between gate frozen and ejection heat transfers by two ways, directly from polymer to metal and transferred to air gap firstly and then to metal, which causes significant reduction of heat transferring ability, HTC, lower than previous value.

- d. Finally, when the component is ejected out of the cavity, heat transferring process stops and HTC is brought to be zero.

2.2.4 Influence factor of heat transfer process

It can be seen from above, there is close relationship between HTC and contact situation of the interface. It rises with increasing contact area on the interface. When contact area is determined, that means HTC h , amount of transferred heat Q is decided by temperature difference ΔT only, as expressed in Eq. 2.7.

During injection molding, contact area on the interface depends on melt temperature, cavity pressure and morphology of cavity surface. Melt temperature has distinct influence on HTC. For one thing, melt with higher temperature has lower viscosity, and it can easily get into the little gaps on surface of cavity wall for forming larger contacting area. When melt temperature is higher, the time point of gate frozen is delayed, and pressure holding time is longer. It is advantageous for melt and cavity wall keeping contact, which increases heat transferring ability of the interface. On the other hand, higher melt temperature creates more volumetric shrinkage in cooling process and larger gap between melt and cavity wall, which makes heat transferring more difficult. Secondly, injection rate is related to cavity pressure, and high injection rate needs large pressure for pushing the melt into cavity quickly. And when the melt temperature is the same, higher pressure can press melt into little gaps on surface of cavity wall, which leads to a better contact situation. Moreover, due to shearing heat, higher injection rate can raise internal energy of melt to a certain degree, and correspondingly injection pressure can be raised, which also affects heat transferring ability of the interface. Last but not least, in an injection cycle, surface roughness has direct effect on average value of HTC. It is easier to have more contact area between melt and cavity wall when the surface is rougher, and also better for heat transferring. And when surface roughness is smaller, especially as mirror plane, it can only provide little contact area due to shrinkage caused by cooling.

Some researchers have investigated the influence of surface roughness on morphology of plastic component and even considered it as significant factor of heat transferring process already. When the dimensions of injection part are small, especially micro injection molding, mold surface roughness may play an important role in the flow of polymer melt [Kle04]. The experimental results of Yang [Yan12] revealed that increasing surface roughness led to a change of filling length of the molded micro features and the effect of surface roughness was weakened by high-pressure trapped air when melt temperature or injection rate is increased.

With the mold surface roughness increasing, the contact area between the hot melt and the cavity wall also increases. Heat transfer between the melt and the wall is enhanced. Therefore heat transfer rate is proportional to the contact surface area [The03]. In the work of others, they also found that higher roughness will enhance heat transfer while keeping the other conditions constant [Cro04, Koo05, Kan03]. The work of Otsuka [Ots11] showed that flow length increased gradually for increasing mold surface roughness because of the heat insulating effect caused by air. Smialek [Smi98] found that an increase of mold surface roughness can prevent slippage in filling stage. Griffiths [Gri06, Gri07] investigated the flow behavior of polymer melt in micro cavities with different surface roughness levels through experimental method. The results showed that mold surface roughness has an influence on the melt flow, but its effect on the slip-stick phenomena was not obvious. Zhang and Ong [Zha07, Zha08, Ong09, and Zha08] finished a systematic research focusing on effect of surface roughness in micro injection molding. The experimental results revealed that mold surface roughness does resist the cavity filling of polymer melt in micro injection molding. The increase of mold temperature will decrease surface roughness effects. But the change of melt temperature is insignificant for surface roughness effects. In addition, a three-dimensional roughness model was built which takes into consideration the roughness effects on the filling polymer flow in micro injection molding.

In general, about the value of HTC and effect of surface roughness on it, some specialists have accomplished experimental and theoretical study. But among the results of them, there are some disagreements, even being contrary or several orders of magnitude differing. Moreover although based on mathematical model built by them, it can provide only a few of results, and still not be applied in industrial field.

2.3 Temperature measurement during injection molding

Temperature measurement is widely used in scientific and industrial territory. Although it has been developed over several decades, the measurement equipment is still being improved nowadays for meeting some extreme but probable occasions. Temperature can never be measured directly, meaning that every temperature measurement involves the use of some type of calibrated sensor or transducer to convert a measurable quantity into a temperature value [Ben98]. Four temperature measurement methods, most commonly used in industry, are mercury in glass thermometer, thermocouple, platinum resistance thermometer and optical pyrometer, indicating temperature through length of mercury, voltage, resistance and radiant flux.

In the process of temperature measurement, errors cannot be avoided, shown as Fig.2.13. The actual temperature of object is T_{undist} , but after inserting temperature sensor into the whole system the temperature of object would be changed into T_{dist} . Errors can also emerge in the process of thermal coupling, signal transducing and result transcription. So the final temperature T_{rep} can never be exactly the original object temperature T_{undist} , no matter most advanced measurement apparatus is applied or not.

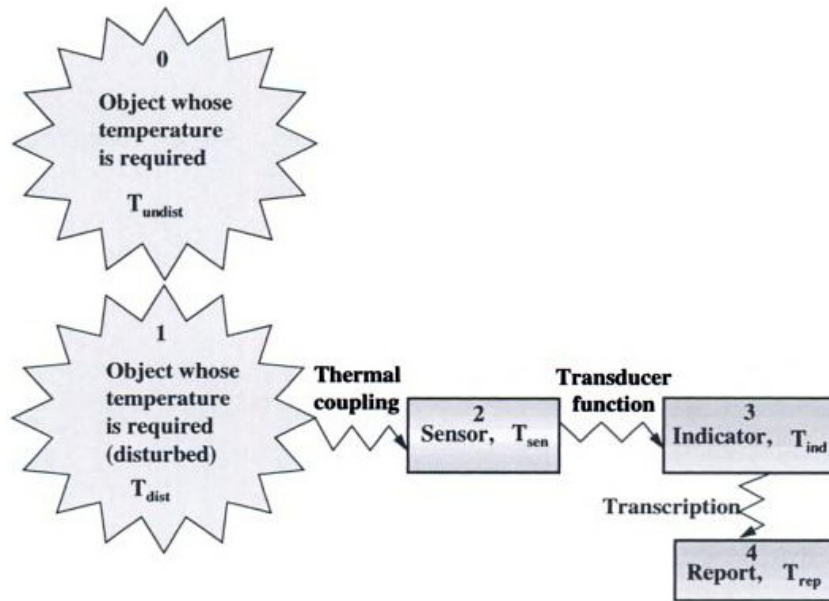


Fig.2.13 Schematic of the temperature measurement process [Ben98]

So the most effective method of temperature measurement depends on the features of object to be measured. Both of melt temperature and mold temperature are the objects to be measured during injection molding. The range of polymer temperature is normally from 20 to 300°C, and the range of mold temperature is lower than melt, especially in higher temperature zone. The variety of melt temperature is a high-dynamic changing process, which requires shorter response time and smaller heat capacity of temperature sensor. So melt temperature measurement is more difficult, which should be considered carefully. From the view of installing convenience, working durability and stability, thermocouple and infrared temperature sensor are chosen as alternative plans.

2.3.1 Thermocouple

The origin of thermocouple is from Seebeck, who found that small electric currents flow in a closed circuit that consists of two unlike conductors when a temperature difference exists between their junctions [Kin73]. In effect, a thermocouple provides a way for the conversion

from thermal energy to electrical energy. The resultant electrical energy is a function of the temperature difference and consequently can be used as a method for temperature measurement [Pol91].

Many researchers have adopted thermocouple in the temperature measurement of polymeric melt. Kamal [Kam84] used a thermocouple to determine the temperature near the centerline of the plastic component and then obtained a continuous record of melt temperature in order to validating the self-built mathematical model of heat transfer. In the work of Lucchetta [Luc12], two thermocouples were applied for obtaining high-dynamic temperature profile during injection molding, to validate the result of simulation. Temperature in the middle of cavity is extremely hard to be measured. Nicolazo [Nic10] used a tubular needle for guiding an embedded micro thermocouple inside the cavity. The temperature probe consists of a type K thermocouple with a diameter of 80 μ m, which has small heat capacity. And the measurement result shows good agreement with result of numerical calculation. The cavity, the feed system and the in situ temperature probe are represented in Fig.2.14.

Goff [Gof09] applied thermocouples which are implanted in the middle of the central plate for acquiring the temperature in middle of the cavity. The corresponding measuring apparatus and result are shown as Fig.2.15 and Fig.2.16 respectively.

Fig.2.16 displays the five temperatures measured by the first two thermocouples T_{c1} and T_{c2} located in the flux sensor one, by the first two thermocouples $T_{c1'}$ and $T_{c2'}$ in the flux sensor two and finally by the thermocouple located in the central plate T_{pc} . In stage D, the mold was heated up to 115°C, which is a temperature lower than the melting point of Polypropylene, for testing the dynamic response of thermocouples at different positions.

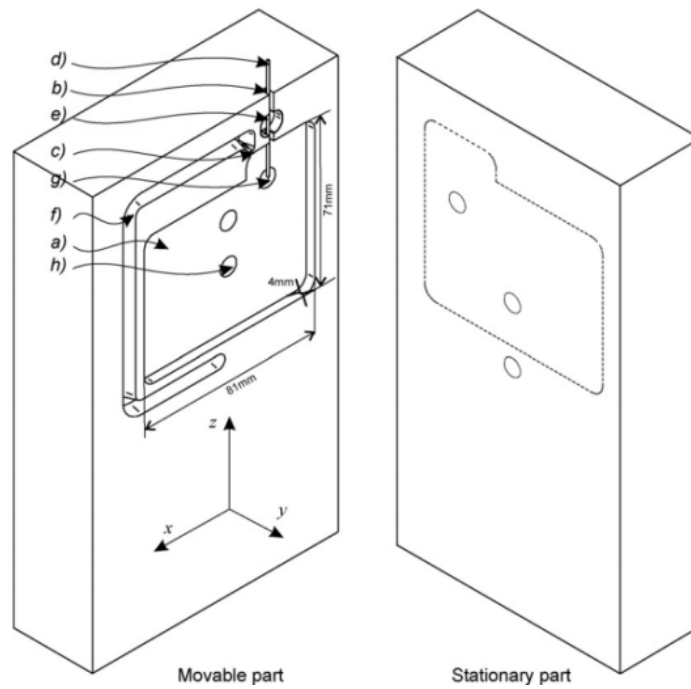


Fig.2.14 Mold cavity with temperature sensor (a)cavity (b)temperature probe-housing cavity (c)feed orifice (d)needle (e) thermoplastic elastomer block housing (f) runner (g)temperature probe (h) pressure and temperature transducer [Nic10]

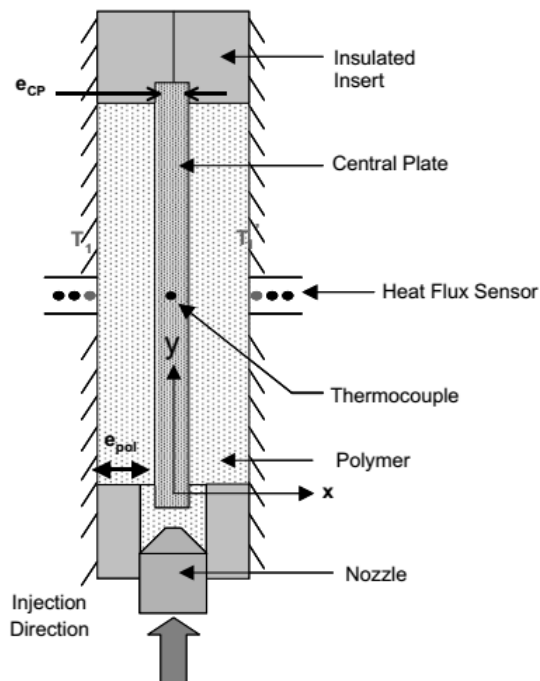


Fig.2.15 Mold cavity with a central plate which contains a thermocouple [Gof09]

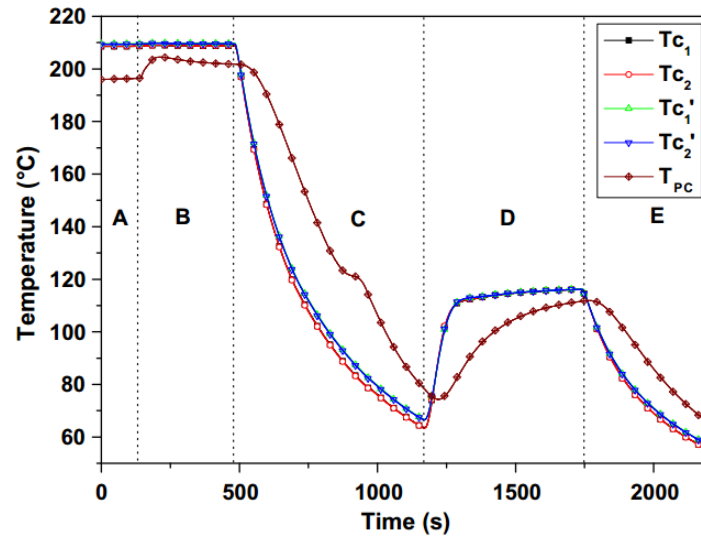


Fig.2.16 Temperature curves measured by thermocouples [Gof09] A: Injection phase; B: Packing phase; C: First cooling phase; D: Reheating phase; E: Second cooling phase.

A removable set of thermocouples (Type K, non-isolated, 0.25mm diameter) is placed in each cavity before injection of polymer in the work of Naranjo [Nar08], shown as Fig.2.17. With this system, temperature in middle of the cavity can be measured, and even the temperature after ejection can be recorded. The inconvenience is obvious that, thermocouple should be laid before every injection cycle.

Nakao [Nak03, Nak08] measured melt temperature and mold temperature with thermocouples for calculating heat flux through the interface between polymer and metal. The thermocouples were welded by YAG laser with two wires 25 microns in diameter, which were cut to a cone shape by femtosecond laser to prevent releasing trouble after injection molding. The results of temperature and heat flux are shown as Fig.2.18. And it can be seen that the peak temperature of sensor A is not as high as injection temperature 220°C. So it can be derived that, even extremely small thermocouple has a certain heat capacity, which can affects the result of temperature measurement.

In the work of others, Liu [Liu09] applied two-dimensional thermocouple mesh to measure temperature in different position in the cavity. And Chen [Che10, Che12] used commercial thermocouples, from Priamus System Technologies, Switzerland, and from Kistler Instrumente AG, Switzerland, separately, for measuring the melt temperature.

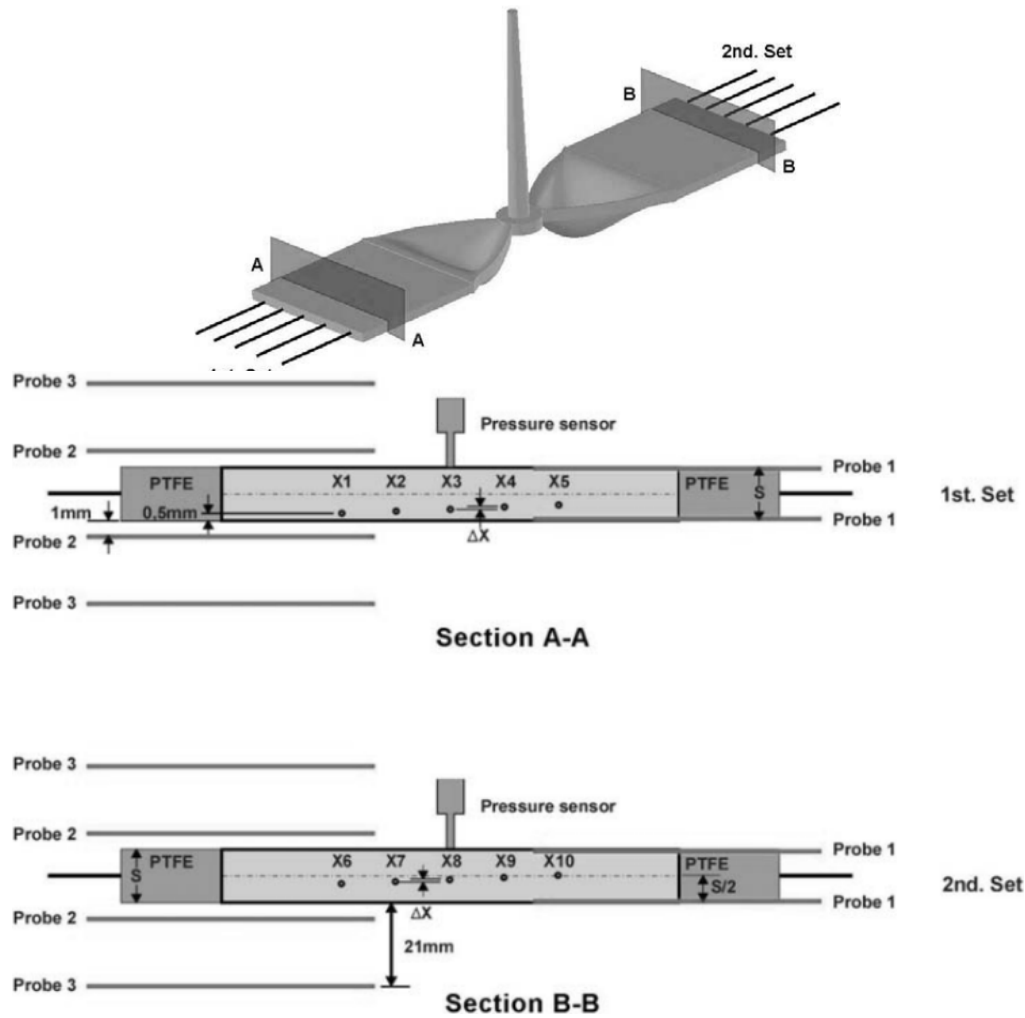


Fig.2.17 Schematic of sensor positions, measure melt temperature in various depths [Nar08]

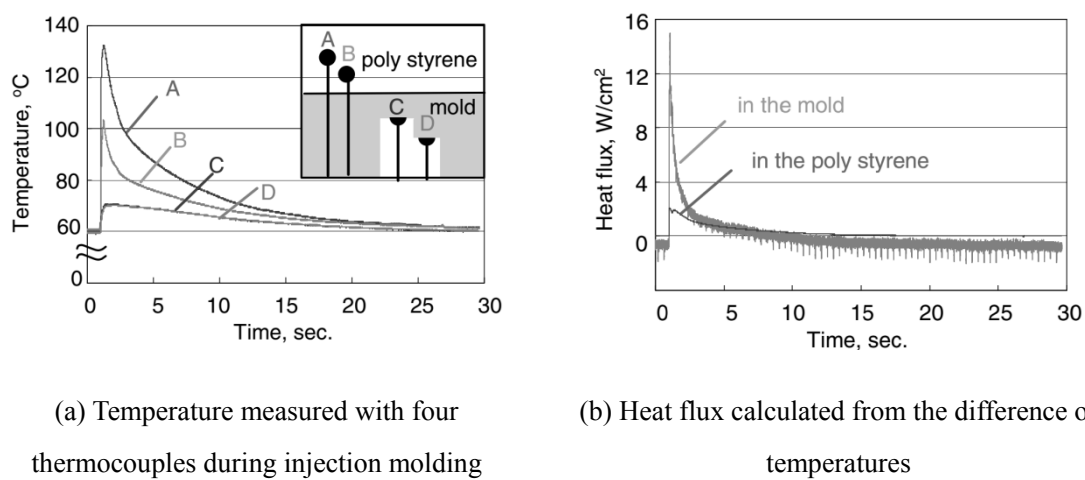


Fig.2.18 Temperature, heat flux and temperature sensor positions and measuring results [Nak08]

2.3.2 Infrared temperature sensor

Every object emits radiant energy, and the intensity of the radiation is a function of the object's temperature, which is described as Stefan–Boltzmann law and shown as Eq. 2.8.

$$M(T) = \sigma T^4 \quad (2.8)$$

$M(T)$ is the total energy radiated per unit surface area of a black body across all wavelengths per unit time, and σ is Stefan–Boltzmann constant. Not only the radiance at different temperature is not same but also the radiance at different wavelength is diverse, which can be seen from Fig. 2.19. In this figure, (b) is partially amplified picture of (a).

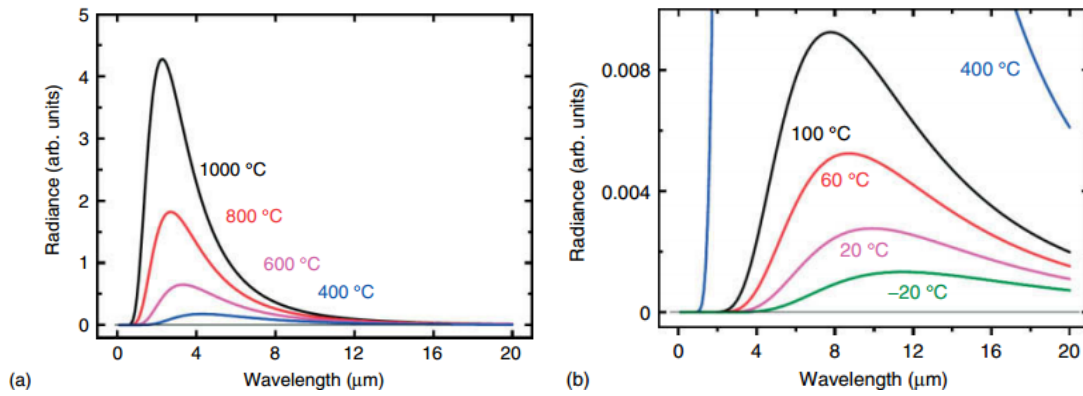


Fig.2.19 Radiance of blackbodies of temperatures between -20 and 1000°C . (b) is locally amplified drawing of (a). Radiance is given in the same arbitrary units for (a) and (b) [Bud10]

However actual object is always gray body and the emissivity distribution of it is non-linear. Therefore the radiation which is situated between from 0.4 to $20\text{ }\mu\text{m}$ belong to the visible and infrared (IR) radiation bands, captured by the IR detector can be used to measure temperature of the body. Infrared temperature measuring system is a kind of non-contact thermometer, which measure the temperature of a body based upon its emitted thermal radiation. No disturbance of the existing temperature field occurs in this non-contact method [Mic91]. And IR temperature measuring system can be divided into two kinds, IR camera and IR temperature sensor.

In the works of Schuck [Sch09] and Lin [Lin05], IR thermal image systems were set up for temperature distribution measurement. The system of Schuck was shown as Fig.2.20. Through deflecting mirror, the infrared ray was captured by IR camera, and shown on the display. After

data processing the temperature value was obtained by them.

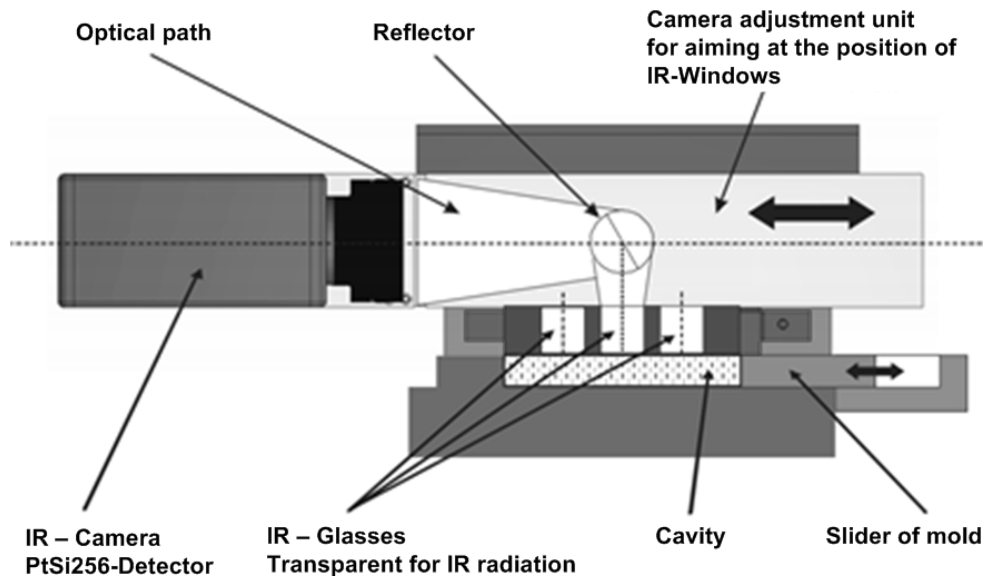


Fig.2.20 Developed mold with IR-Camera measurement system [Sch09]

Brunotte [Bru06] and Rogelj [Rog08] applied IR temperature sensors in experiments. Both of their sensors are MTS 408T, from FOS Messtechnik GMBH, Germany, which can be inserted into mold directly and whose tip can be flush with cavity wall, shown as Fig. 2.21. The radiation from polymer enters in the sensor through a sapphire window, which can withstand high temperature (up to 400°C) and high pressure (up to 250Mpa). Then the radiation was detected by IR diode, guided to corresponding signal amplifiers, and transferred to processing and displaying units. Chen [Che11] also used IR temperature sensor for measuring the surface temperature of mold, which was heated by hot melt and kept a dynamic temperature variety too.



Fig.2.21 IR temperature sensor which can be used in melt temperature measurement,

Model MTS 408T [Bru06]

Bur [Bur04] and Abeykoon [Abe12] used IR temperature sensors in melt temperature measurement in extruding process. And both of them adopted thermocouples as reference object of IR sensors. In the work of Bur, conventional thermocouple showed slower response characteristic and the temperature value was lower than that of IR sensor. Abeykoon employed thermocouple mesh, which has longer response time but can provide 2-dimensional temperature profile of cross-section instead of point temperature. Although IR sensor showed better performance in detecting thermal variations, temperature profile of same pattern and closed measurement value can be obtained by thermocouple mesh.

2.3.3 Comparison between diverse methods of temperature measurement

In the polymer temperature measurement during injection molding process, some researchers applied thermocouples and the some others chose IR temperature sensors as their measurement tools. IR camera is not quite compatible to injection mold, because of volume limitation and calibration of temperature value.

Thermocouple is widely used in industrial field, and the manufacture technology is relatively mature. But the measurement principle of thermocouple restricts the response characteristic of it. When the thermocouple touches hot polymer, heat needs to be transferred from hot polymer to the tip of thermocouple at once. Because of the heat capacity of thermocouple, it needs some time to reach the thermal equilibrium, which means the temperature of thermocouple is equal to that of the polymer it measures. During the time, energy from the melt has been conveyed to cooler area, including the tip of thermocouple. Finally, polymer temperature decreases and it is not the original temperature should be measured any more. That means thermocouple cannot meet requirement of the occasion, which contains high-dynamic variety of temperature. But with developing of material and manufacture technology, the thermocouple with miniaturized tip has been developed by some commercial sensor manufacturer. The tip of thermocouple has much smaller heat capacity, and response time can be reduced to the minimum, which can be found in work of Bader, “Cavity temperature sensors” out of the chapter “Setup and control of molds”, and the work was included in a book of Mennig already [Men13].

The advantage of IR temperature sensor fits the lack of thermocouple. The response time of it is always locates in the range of 10-20ms. It can capture high-speed changing temperature and show it immediately. But there are also some matters with it. Firstly, IR temperature sensors cannot be used in the occasion with high temperature and high pressure directly. Normally, a window made from sapphire should be set in front of the tip of IR temperature sensor. So

radiation intensity and radiation distribution at different wavelength can be influenced when radiation crosses the sapphire window. Moreover, it is difficult for IR temperature sensor, when measured object is transparent or semitransparent to infrared ray. Due to the radiation energy from each depth can be obtained by IR detector and the temperature value it shows is not the actual temperature.

Consequently, as above mentioned the most effective method of temperature measurement depends on the features of object to be measured. And circumstance and purpose of measurement should be also considered.

3. Evaluation of HTC of the interface between polymer and cavity wall

Processing conditions during injection molding, including melt temperature, mold temperature, injection pressure, and also surface roughness have great influence on heat transfer coefficient (HTC) of the interface between polymer and mold. HTC plays an important role in polymer filling, packing and cooling stage of injection molding. Evaluation of HTC is critical for comprehending heat transfer phenomenon and also improving the precision of simulation result.

Therefore, based on theory of heat transfer between polymer and mold, the principle of HTC evaluating was built firstly. Then experimental plan and corresponding apparatus was developed. A series of injection molding experiments were executed strictly according to the experimental plan subsequently. Data processing of experimental result was finished and actual value of HTC was obtained subsequently. And analysis of the relationship between HTC and processing conditions was performed finally.

3.1 Principle of HTC evaluating

The amount of transferred heat across the interface between polymer and mold can be described as Eq.2.7. And the amount of transferred heat inside the mold can also presented as Eq.2.3, because mold material is assumed to be homogeneous medium for heat transferring. Because of intricate heat transferring condition, both of the instantaneous heat amounts may not be equal. However during an injection cycle, both amounts of transferred heat are same, when it is assumed that no heat is transferred by other ways, such as thermal radiation. So through integral of time, Eq.2.7 and 2.3 can be transformed into Eq.3.1 and 3.2 as following.

$$Q_1 = \int_0^{t_0} hA\Delta T_{12}dt \quad (3.1)$$

$$Q_2 = \int_0^{t_0} \frac{kA\Delta T_{23}}{d}dt \quad (3.2)$$

where h is the heat transfer coefficient (HTC) between polymer and cavity wall, and Q_1 and Q_2 are amount of transferred heat across the interface and inside the mold respectively. t_0 is the cycle time of injection molding. ΔT_{12} and ΔT_{23} are temperature difference between surface of polymer and mold and between diverse layers inside mold respectively. Due to both amounts of transferred heat are equal, Eq.3.3 and 3.4 can be obtained.

$$h \int_0^{t_0} \Delta T_{12} dt = \frac{k}{d} \int_0^{t_0} \Delta T_{23} dt \quad (3.3)$$

$$h \left(\int_0^{t_0} T_1 dt - \int_0^{t_0} T_2 dt \right) = \frac{k}{d} \left(\int_0^{t_0} T_2 dt - \int_0^{t_0} T_3 dt \right) \quad (3.4)$$

In Eq.3.4, T_1 , T_2 and T_3 are the temperature of polymer surface, mold surface and mold in a certain depth respectively. So the average HTC in a molding cycle can be calculated by Eq.3.5.

$$h = \frac{k}{d} \left(\int_0^{t_0} T_2 dt - \int_0^{t_0} T_3 dt \right) / \left(\int_0^{t_0} T_1 dt - \int_0^{t_0} T_2 dt \right) \quad (3.5)$$

According to Eq.3.5, HTC value can be obtained only if temperature of polymer surface, mold surface and mold in a certain depth are measured. With the help of miniature temperature sensors, the purpose of temperature measurement in a quite small area can be achieved. Thermocouple and infrared (IR) temperature sensor are suitable in such situation, but both of them also have advantages and disadvantages. IR temperature sensor is a perfect choice for temperature measurement with high-dynamic variety, for it can react immediately when the temperature changes remarkably. Since the radiation energy from each depth of transparent or semi-transparent polymer can be obtained by IR detector, the value of measured temperature is always higher than it should actually be. As above mentioned, a sapphire window should be set in front of the tip of IR temperature sensor for protecting against high temperature and high pressure. The sapphire window plays a role as filter of wave length here, in other words the wave length in a certain range can go through this window. At the same time, wave length of radiation emitted from polymer with high temperature depends on the material type. Different polymer radiates energy which locates in different range of wave length. The range of wave length which can go through sapphire window must contain the range of wave length of radiation emitted from high-temperature polymer. Therefore there is a limitation on material selecting, when IR temperature sensor is employed. Thermocouple is not an expert in high-dynamic temperature measurement. Because the tip of thermocouple must be heated up by the energy transferred from polymer for showing close value to actual melt temperature, and it cannot only miss the peak of melt temperature but also lose some detailed information when melt temperature increases or decreased sharply. But during injection molding cycle, it is composed of filling, packing and cooling stages. And cooling stage possesses most time of a cycle, besides the degree of temperature variety is not as high as that in filling and packing stages. The curves of melt temperature calculated by Moldflow and Ficap are on the left side in Fig.3.1, moreover the curve measured by IR sensor is on the right side.

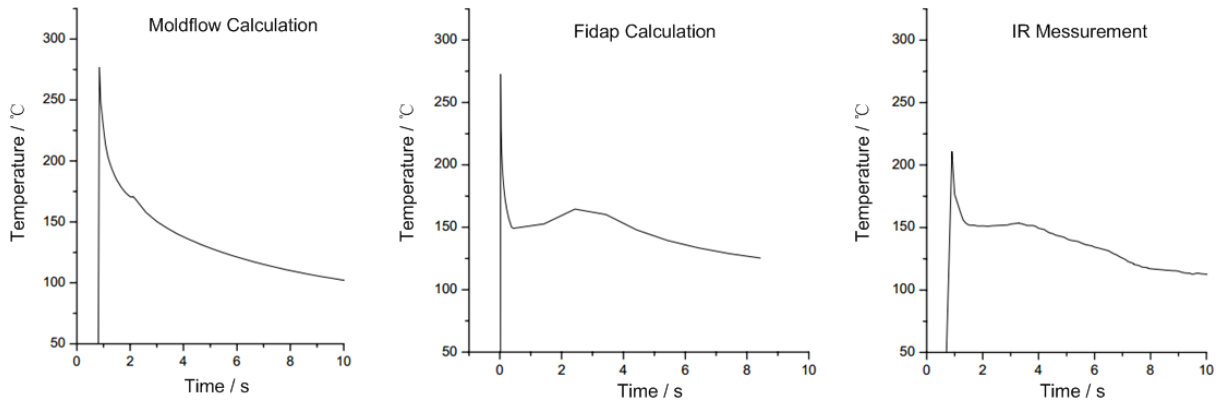


Fig.3.1 Typical polymer temperature variation during a molding cycle, from Moldflow & Fidap simulation and IR measurement [Bru06]

Therefore the average degree of temperature variety is relatively low which depends on the low degree of temperature variety in cooling stage. It can also be obtained from Eq.3.5 that, through the subtraction of temperature integrals, missing of temperature peak and losing of some detailed information in such small period it has no great influence on calculating of average HTC value of whole molding cycle. Moreover the thermocouple with miniaturized tip has much smaller heat capacity and much better response behavior, so that it can acquire more details when measuring the temperature with high-dynamic variety. Consequently, thermocouple can meet all the requirements of measurement for HTC calculating in an injection cycle here and it should be the prior option.

With the help of miniature thermocouples, melt temperature on the component surface and mold temperature in different depths can be measured, and the schematic view is shown in Fig.3.2.

Correspondingly, in Eq.3.5 T_1 , T_2 and T_3 are measured by Sensor 1, Sensor 2 and Sensor 3 respectively. Because T_1 and T_2 represent the temperature of polymer surface and mold surface, which are also related to the calculation accuracy of transferred heat across the interface, so Sensor 1 and Sensor 2 should be set as closely to the interface as possible. Finally, the h in the Eq.3.5 can be calculated from the temperature measurement results.

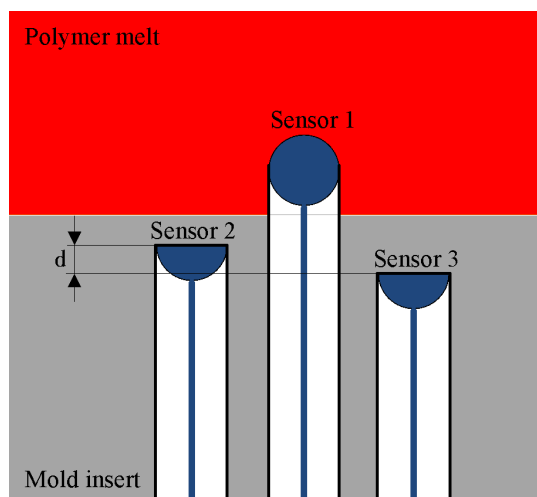


Fig.3.2 Schematic positions of miniature sensors in mold used in experiment

3.2 Experimental conditions of HTC evaluating

Based on fundamental theory above, detailed experimental plan of injection molding was worked out as follows.

3.2.1 Material and equipment

Lupolen 1800S, from Lyondell Basell Polymers, was adopted as the experimental polymer. Lupolen 1800 S is a low density polyethylene (LDPE) resin used in injection molding. It has high flowability, and good softness, toughness and dimensional stability. Lupolen1800 S is used in applications such as toys, caps & closures, engineering parts, and sports and leisure equipment [Pol14]. Lupolen 1800S belongs to semicrystalline thermoplastic. Some important material properties are shown in Table 3.1. The property of high flowability is the reason to be selected for ensuring polymer can overcome the flowing resistance in the miniature cavity, which can also be seen in Table 3.1. In view of information provided by material database of Moldflow, the recommended ranges of mold temperature and melt temperature are 20-60°C and 205-245°C respectively. And absolute maximum melt temperature is 265°C approximately.

In the injection experiment, Arburg Allrounder 320S injection molding machine was employed, whose maximum clamping force is 500kN, screw diameter is 25mm and maximum injection pressure is 250Mpa, known from the data sheet from Arburg Company. Moreover the maximum theoretical injection volume is 54cm³.

Table 3.1 Thermal conductivity of Lupolen 1800S [Pol14]

| Properties | Unit | Value |
|--|-------------------|-------|
| Density | g/cm ³ | 0.917 |
| Melt flow rate (MFR) (190°C/2.16kg) | g/10 min | 20 |
| Melting Temperature | °C | 106 |
| Vicat softening temperature | °C | 80 |
| Tensile Modulus | Mpa | 160 |
| Tensile Stress at Yield | Mpa | 8 |

Combined roughness and contour measurement system, Hommel-Etamic T8000 RC, was used for measuring the surface roughness of inserts and plastic component obtained from injection experiment.

3.2.2 Cavity and temperature measurement system

The studying object is a miniature component, which needs little injection volume, so its dimension is designed as 15mm*15mm*2mm. But comparing with the maximum theoretical injection volume, volume of miniature component is quite small, which can cause the problem of polymer ageing due to polymer remains in the screw for a long time. Therefore blind volume was added into the design of the mold cavity, which has identical thickness to studying object but much larger length and width. And the final component with partly runner system is shown as Fig.3.3.

In Fig.3.3, the studying object is on the left side and the part of blind volume is on the right side. The corresponding insert is shown in Fig. 3.4. And three thermocouples were on this side for obtaining temperature signals around the interface between polymer and mold.

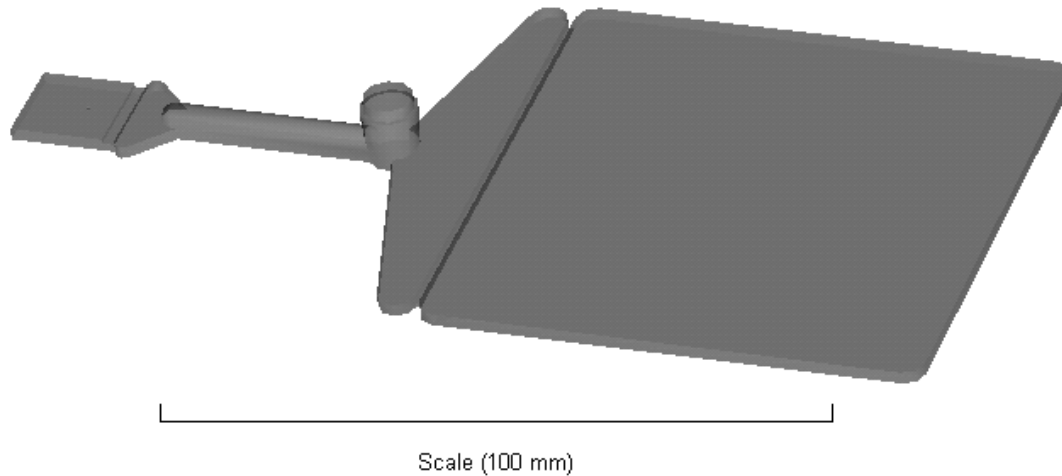


Fig.3.3 Model of component with partly runner system



Fig.3.4 The insert of studying object used in experiment

Sensor 1 and Sensor 2 should be placed as closely to the interface as possible, because T_1 and T_2 in Eq.3.5 represent the temperature of polymer surface and mold surface. But considering the machining difficulty of mold cavity, an extremely thin wall must be left between the tips of sensors and the interface. So the distances between sensor tips and the interface are shown in the final arrangement of thermocouple as Fig.3.5.

According to the operational principle of thermocouple, thermal voltage can be detected only after heat transferred onto the thermocouple. But during injection molding process, the melt temperature increase happens within a few milliseconds, and initial temperature of thermocouple is mold temperature. Thermocouple can respond to the real-time temperature after it absorbs energy, and when temperature of thermocouple is same to that of melt, it is

lower than initial temperature peak. In the aspect of sensor, on contrast to conventional thermocouples, some series have been optimized, especially on the size of sensor tip, so that when the plastic melt arrives they can react in a very short time. High dynamic temperature sensor SW142X4 and SW142X6, from sawi Mess- und Regeltechnik AG, Switzerland, were used in the experiment. They can respond to temperature variety quickly owing to the diameters of their detectors are only 1 and 0.6mm respectively. The dimensions of miniature thermocouples are shown as Fig.3.6.

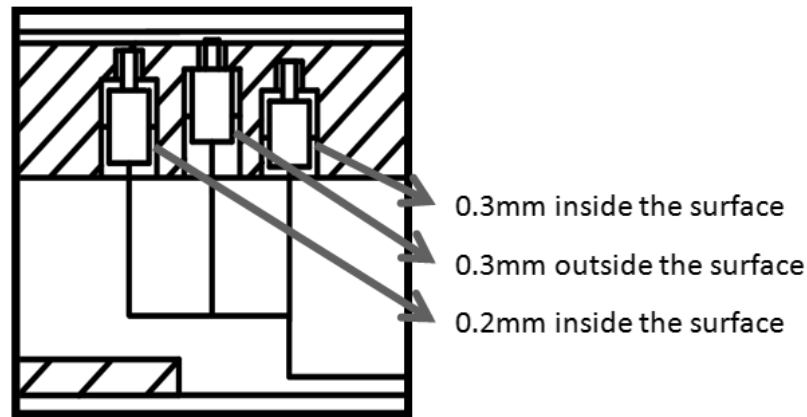
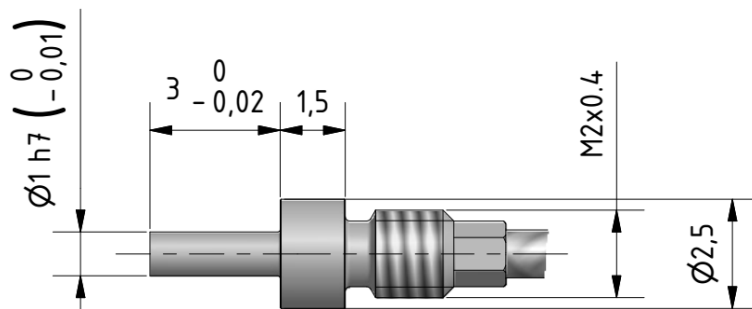
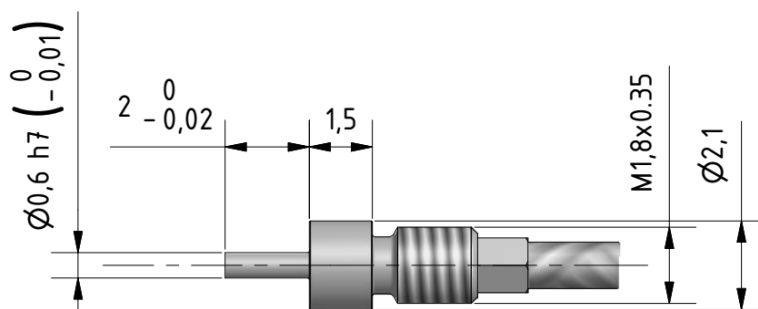


Fig.3.5 Arrangement of thermocouples in mold

SW142X6 was used as Sensor 1 for measuring polymer temperature, and two pieces of SW142X4 were used in other positions. SW142 series represent current developing situation of fast responding thermocouple. The reduction of the sensor dimensions and with it the decrease of the object mass leads to highly fast response.



(a) SW142X4



(b) SW142X6

Fig.3.6 Dimensions of miniature thermocouples used in experiment

Relevant parameters of sensors are the completely same which are shown in Table 3.2. In addition measuring points of thermocouples were electrically grounded for avoiding electromagnetic signal interference.

Table 3.2 Relevant parameters of thermocouples

| | |
|---|--|
| Thermocouple model | SW142X4/X6 |
| Thermocouple type | K |
| Standard deviations | $\pm 1.5^{\circ}\text{C}$ (-40 up to 375°C) |
| Maximum operating temperature (sensor front) | 700°C |
| Continuous operating temperature (sensor body and measuring cable) | 400°C |
| Maximum operating pressure | 200Mpa |

Signal conditioning system, from Kistler Instrumente AG, was also applied in temperature measurement. The signal measured by the thermocouple type K was inputted into 4-channel thermocouple amplifier, type 2207A, where it can be converted into voltage signal in range of $\pm 10\text{V}$. Measuring unit comes after amplifier, type 2865B00, which can digitize the amplified voltage signal. Then temperature data out of measuring unit was transferred by USB cable into computer. Finally it was evaluated by matching software, Dataflow, and temperature curves and detailed data can be shown and saved directly. The temperature curves measured by temperature measurement system are shown in Fig. 3.7.

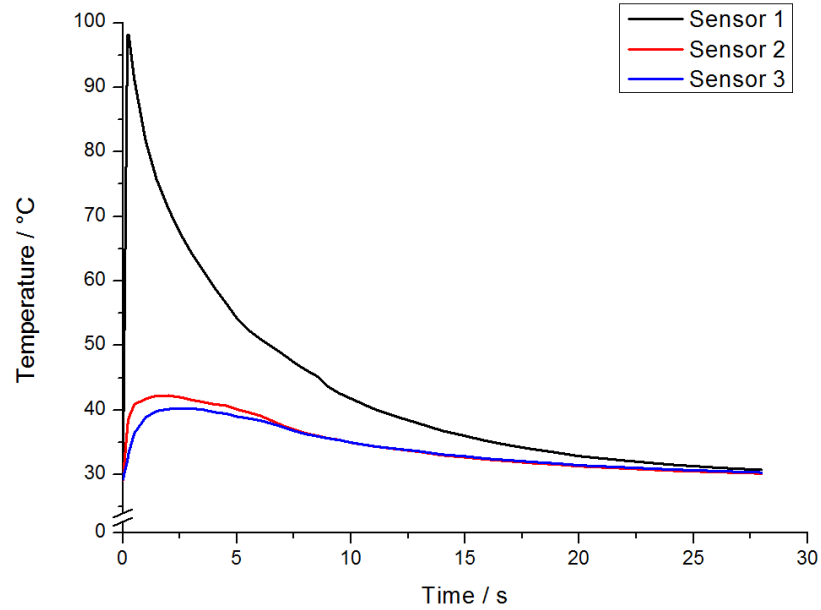


Fig.3.7 Temperature curves measured by three miniature thermocouples, melt temperature 230°C, surface roughness Ra 0.01μm, injection rate 45cm³/s. Sensor 1 is the thermocouple measuring surface temperature of melt, Sensor 2 is closer to the interface than Sensor 3 in the side of mold.

Although the peak values were not achieved, according to the principle of HTC calculation, it has little influence on accuracy of calculated HTC value.

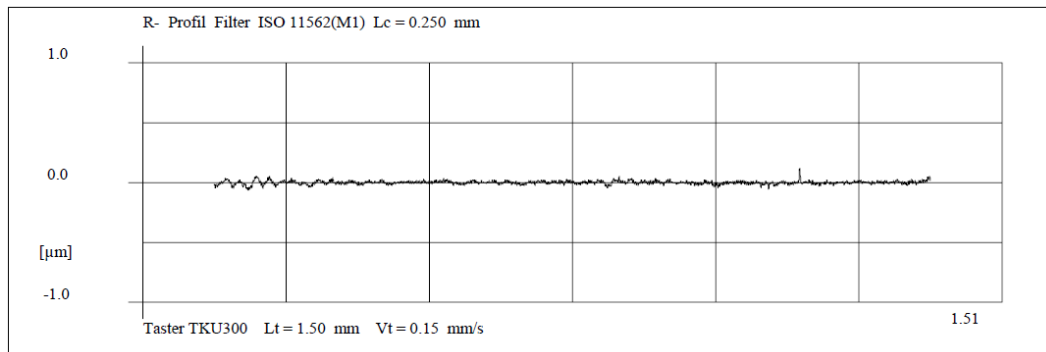
3.2.3 Experimental procedure

Based on existing literature and heat transfer theory, melt temperature, injection pressure and surface roughness of mold insert are the most important factors to HTC value. Accordingly for studying the effect trend of each parameter, three different parameter levels of each factor were determined.

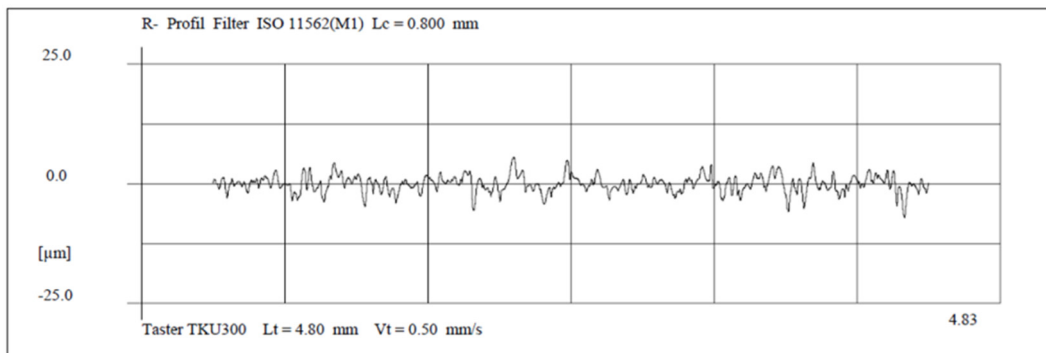
The recommended range of melt temperature of Lupolen 1800S is 205-245°C, and absolute maximum melt temperature can reach 265°C. In order to ascertain HTC values under entirely different situations, processing temperature were chosen from 200 to 260°C. Injection pressure has close and almost linear relationship with injection rate, and in Arburg Allrounder 320S injection molding machine, it is easier to control and adjust the value of injection rate. So injection rate was applied instead of injection pressure. And the range of it was chosen from 5 to 45cm³/s, which is also a relatively wide scope that can represent heat transfer process under diverse situations.

In the aspect of surface roughness, electrical discharge machining was applied for achieving different mold insert surfaces. After machining the surface roughnesses of inserts were

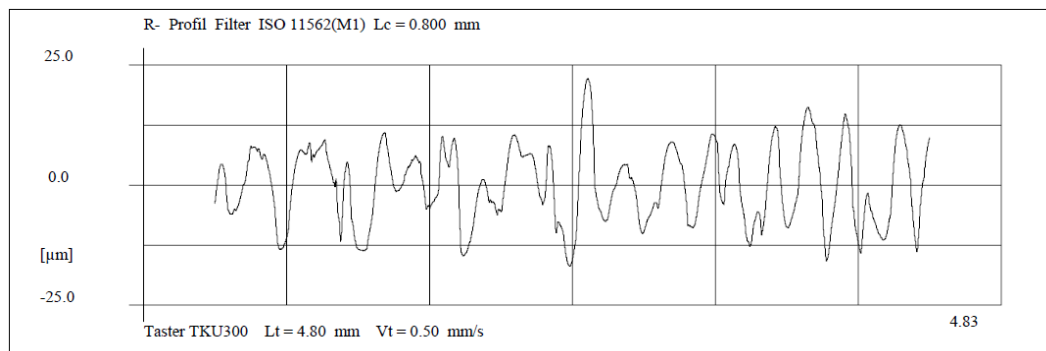
measured by Hommel-Etamic T8000 RC. The morphology of three pieces of mold inserts is shown as Fig.3.8, in which (a) has much smaller scale than (b) and (c).



(a) Insert 1



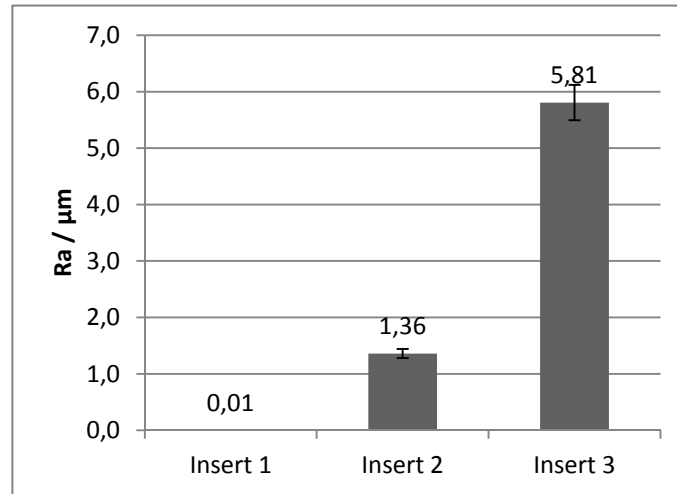
(b) Insert 2



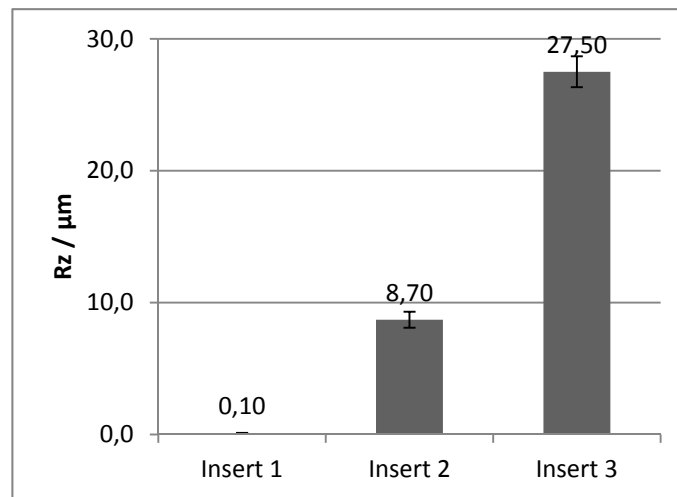
(c) Insert 3

Fig.3.8 Surface morphology of mold inserts

It can be derived from Fig.3.8 that there are great differences among the surfaces of the three mold inserts in microscopic scale. Four times of measurement were accomplished at the different positions of each insert. Positions of each insert are the same to the positions of others. Then average values and corresponding standard deviations of Ra and Rz were calculated and shown as Fig.3.9.



(a) Ra of mold inserts



(b) Rz of mold inserts

Fig.3.9 Measuring results of insert surface roughness

The average values of Ra are 0.01, 1.36 and 5.81 μm respectively. In following text, they are regarded as the code names of three inserts.

So parameter levels of melt temperature, injection rate and surface roughness of cavity are determined and shown in Table 3.3. Experiments with combinations of different parameter levels were carried out, in another word, all of 27 combinations of different parameter levels were adopted.

Table 3.3 Parameter levels of melt temperature, injection rate and surface roughness

| Parameter level | Melt temperature / °C | Injection rate / cm ³ /s | Surface roughness / μm |
|-----------------|--------------------------|--|---------------------------|
| 1 | 200 | 5 | 0.01 |
| 2 | 230 | 25 | 1.36 |
| 3 | 260 | 45 | 5.81 |

Because temperature integral is adopted for calculating in data processing, thermal history has great effect on mold temperature. That means, with experimental time increasing, mold temperature rises slightly, and integral amplifies the effect of rising. So for obtaining reliable result, testing under same surface roughness was carried out on the same day. In the side of experiment sequence, melt temperature and injection rate are from low to high, for making it has same order under same melt temperature and injection rate among 9 combinations of parameters in each day. Testing under same combination of melt temperature and injection rate but different surface roughness was carried out at same time on different day. That means the situation under same combination of melt temperature and injection but different surface roughness has same thermal history, which makes the temperature integral of it comparable with that of the same situation but other surface roughness. The experimental schedule is shown in Appendix A.

It can be seen from Appendix A, after altering melt temperature, it took 1 hour to achieve relatively steady thermal situation, i.e. thermal equilibrium through uninterrupted injection. Then twenty times of temperature measurement were accomplished for ensuring measuring accuracy, and it took approximately 20 minutes. If melt temperature is not changed, only after altering injection rate, it took 10 minutes to achieve thermal equilibrium, because temperature field of polymer and mold were just changed slightly due to shearing heat.

After temperature measurement, according to Eq.3.5, temperature data was processed with the help of Matlab, for acquiring the amount of heat across the interface and average HTC in one injection cycle.

Meanwhile, surface roughness of plastic component was measured and compared with that of mold insert for figuring out the reason of HTC variation.

3.3 Experimental results and discussion

Through long-time injection experiment according to the plan rigorously, a series of experimental data have been obtained, and also plastic component, shown as Fig.3.10. The mold temperature was maintained at 25°C all the time.

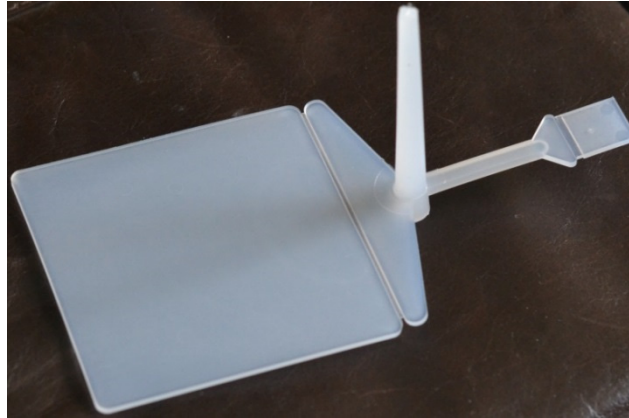


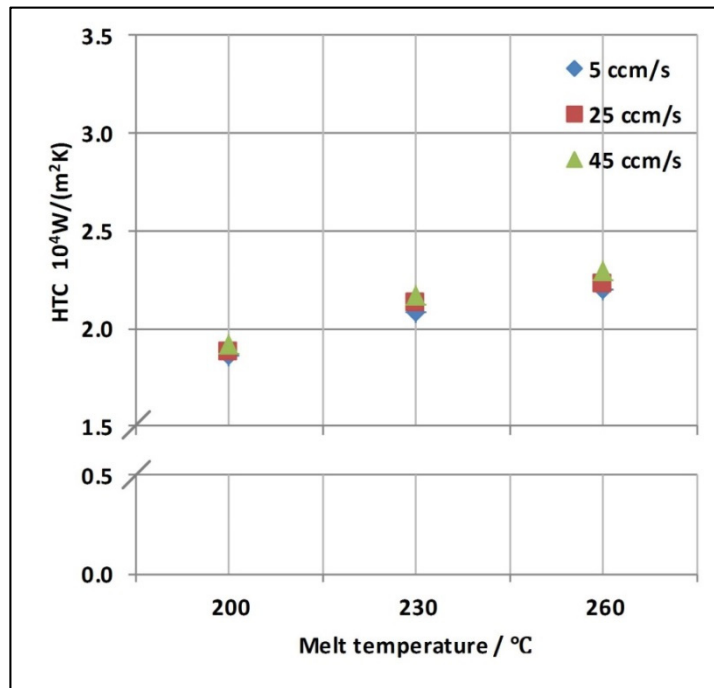
Fig.3.10 Component produced in injection molding experiment

3.3.1 Influence of parameters on average value of HTC

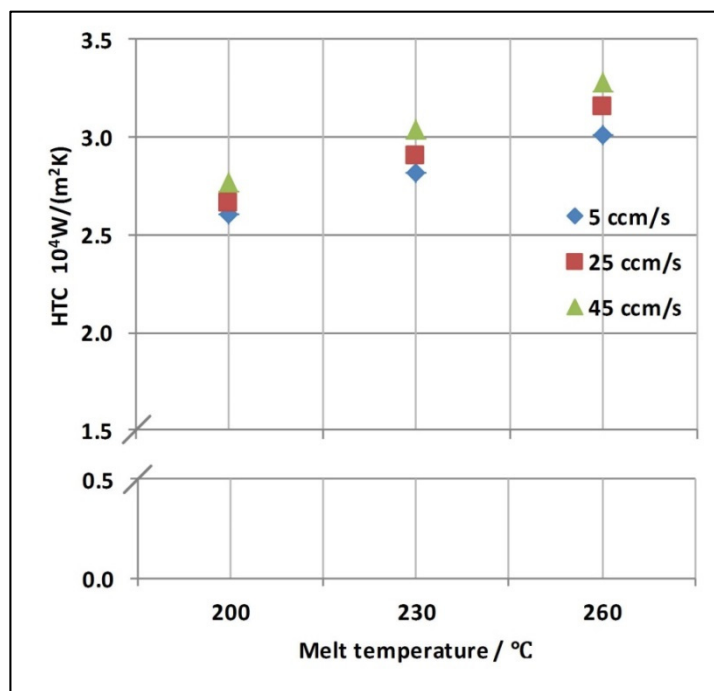
Acquired temperature data was processed and average value of HTC was calculated based on Eq.3.5. When surface roughness is constant, at 0.01, 1.36 and 5.81 μm respectively, the changing regulation of HTC under different melt temperature and injection rate is shown as Fig.3.11.

From the Fig. 3.11 it can be obtained that, HTC increases with rising melt temperature and injection rate, especially with melt temperature. The reason is due to melt with higher temperature has lower viscosity, and can easily enter the microscopic aperture gaps of cavity wall, which raises the contacting area between melt and cavity wall and lead to higher HTC.

The effect of injection rate on HTC is quite small, and can be neglected under certain conditions, for example the condition when R_a is 0.01 μm , melt temperature is 200°C and when R_a is 5.81 μm , melt temperature is 260°C. The cause of this phenomenon is when injection rate is higher, injection molding machine provides higher pressure for accelerating polymer, and shear heat rises at the same time. So heat caused by shearing action increases and melt temperature can be raised correspondingly. Therefore the contacting condition can be improved slightly due to temperature alteration.



(a) Surface roughness Ra 0.01 μm



(b) Surface roughness Ra 1.36 μm

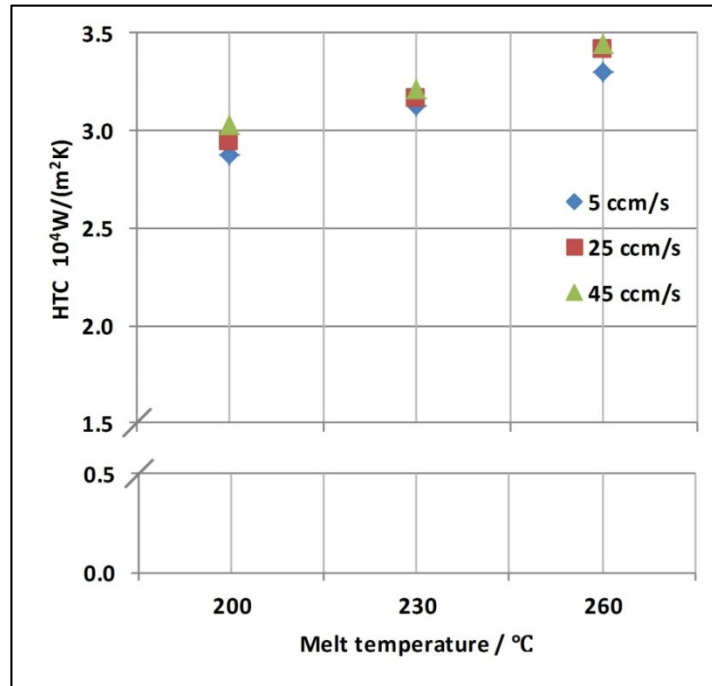
(c) Surface roughness R_a 5.81 μm

Fig.3.11 Average value of HTC at constant surface roughness, under different injection rate and melt temperature

Because injection rate has little effect on HTC, the values were compared when injection rate situation is 25 cm³/s, as shown in Fig.3.12.

From Fig.3.12, it can be derived that surface roughness of cavity wall has significant effect on average HTC value. When it increases, HTC is heightened. The reason of that is cavity surface has microscopic aperture gaps, even for polished surface. Under injection pressure, melt can adapt better to the surface of cavity wall. But when comparing injection time with the whole injection cycle, its time is extraordinarily short. Air or vacuum gap emerges on the interface, due to shrinkage of melt, which reduces the heat transfer ability sharply. But when there are more obvious and deep aperture gaps on wall surface, normally melt can get into them more deeply and during cooling stage the solid polymer would even keep contacting with metal in some area, so heat transfer ability can be promoted.

From the Fig.3.12, it can be also seen that when the surface roughness increased from 0.01 to 1.36 μm , it has more distinct effect comparing with from 1.36 to 5.81 μm , even its numerical difference is much smaller than that between 1.36 and 5.81 μm . It can indicate the influence of surface roughness on HTC increasing decreases progressively, and unceasingly increasing surface roughness would have no more great effect on HTC value.

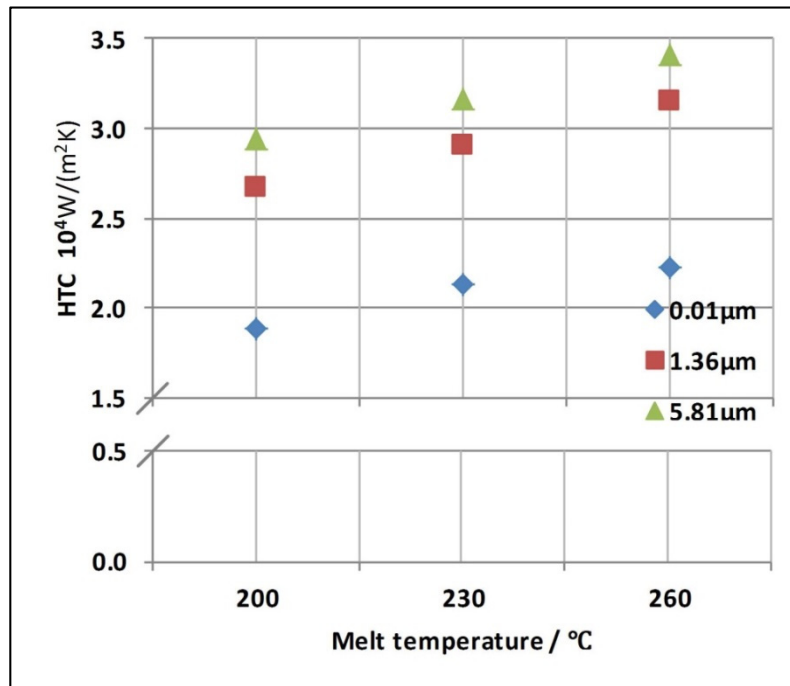
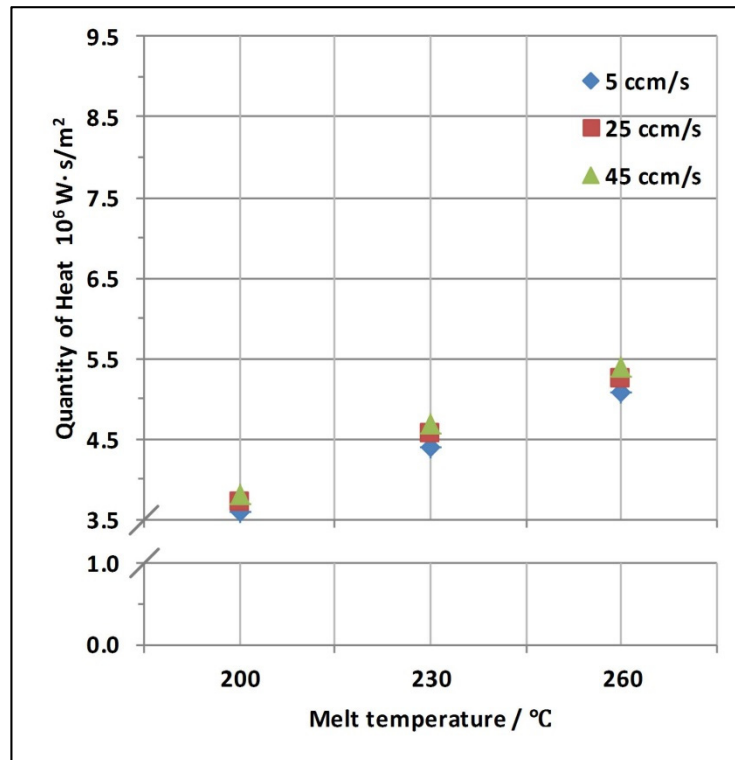
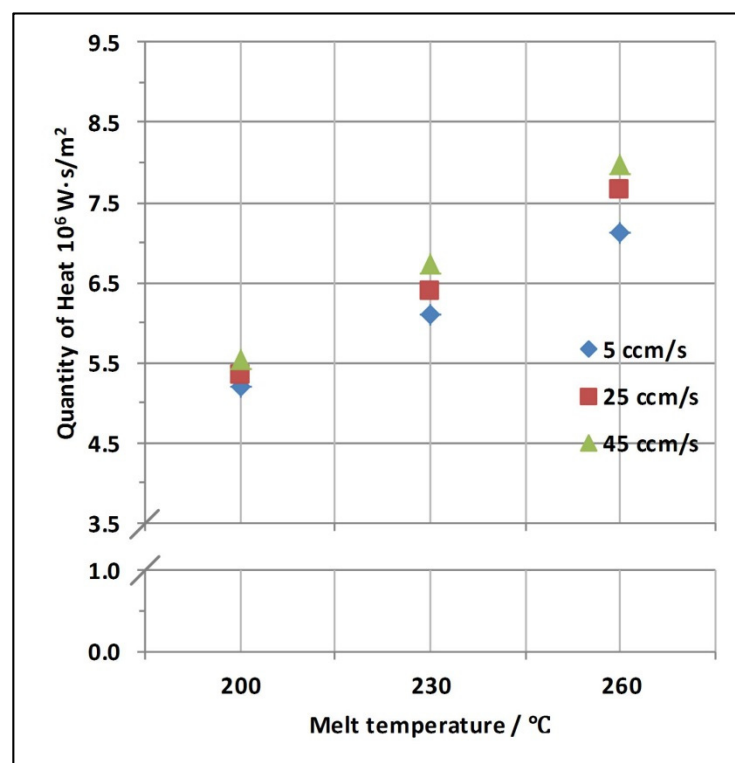


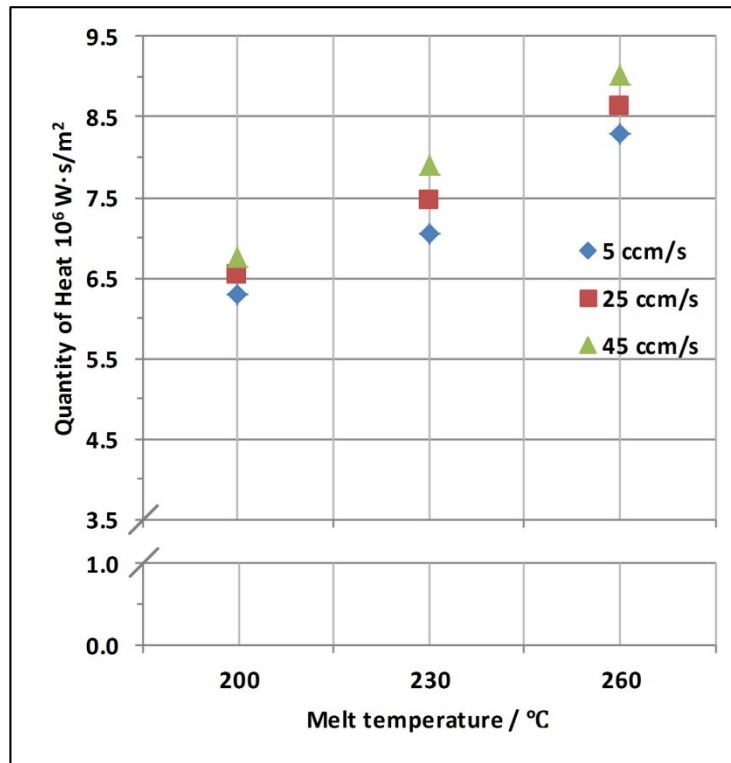
Fig.3.12 Average value of HTC, injection rate $25\text{cm}^3/\text{s}$, under different surface roughness and melt temperature

3.3.2 Heat across the interface between melt and cavity wall

The quantity of heat across the interface between melt and cavity wall can be calculated by Eq.3.2 based on temperature data from Sensor 2 and Sensor 3. And the value of it is total amount in one injection cycle. The variation tendency of it under different melt temperatures and injection rates when surface roughness is $0.01\mu\text{m}$ is shown as Fig.3.13.

From the view of theoretical analysis, the primary factors, which can decide quantity of heat across the interface, are temperature difference between melt and cavity wall and heat transfer ability of the interface, i.e. HTC. It can be seen from Fig.3.13 that, with increasing melt temperature, temperature difference increases greatly and nearly proportional, which has a direct effect on quantity of heat across the interface. Meanwhile, melt with higher temperature has lower viscosity. So it can improve the contacting situation between melt and cavity wall, which means a higher value of HTC and has also a direct effect on quantity of heat across the interface. The heat rises slightly with increasing injection rate, which can be derived from Fig.3.13, due to the HTC changing mentioned above.

(a) Surface roughness R_a $0.01 \mu\text{m}$ (b) Surface roughness R_a $1.36 \mu\text{m}$



(c) Surface roughness Ra 5.81μm

Fig.3.13 Quantity of heat across the interface at constant surface roughness, under different injection rate and melt temperature

With the same method, quantity of heat across the interface under different melt temperature and surface roughness, when injection rate is 25cm³/s, is shown in Fig.3.14.

From Fig.3.14 we can derive that, surface roughness has obvious effect on quantity of heat across the interface. The increasing value of roughness can raise the heat and the quantity of heat has the same variety trend as that of Fig.3.12, and the reason is the same too. If there are more apparent aperture gaps on the wall surface, contacting situation can be improved and heat transfer ability of the interface is better. When roughness changed from 0.01 to 1.36μm, it increases obviously, but less when from 1.36 to 5.81μm. The difference is not as large as that of in Fig.3.12.

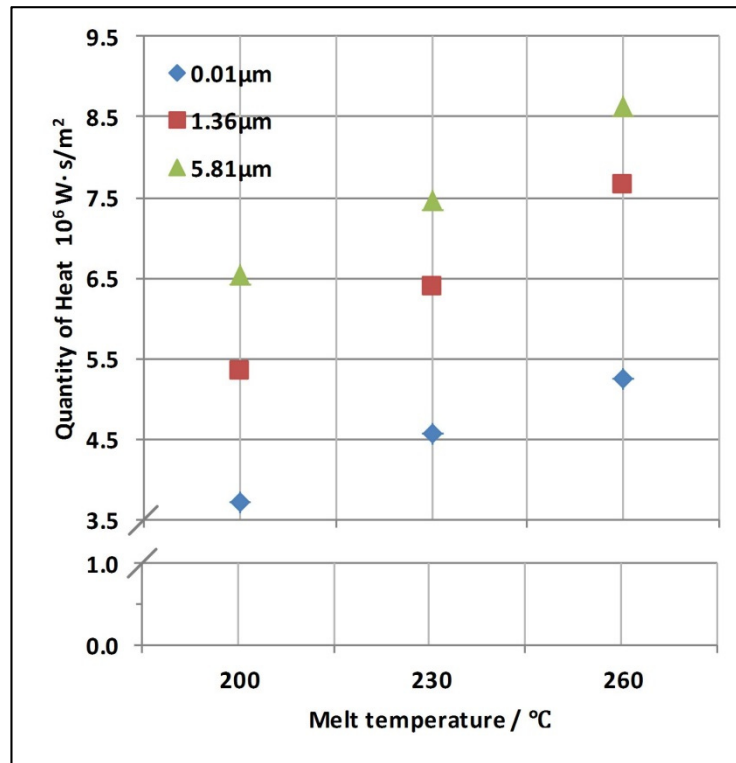
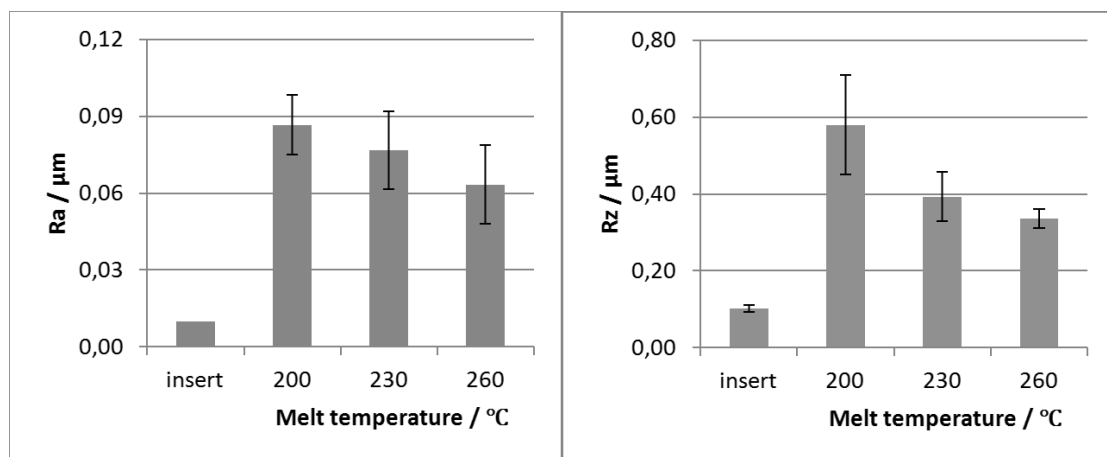


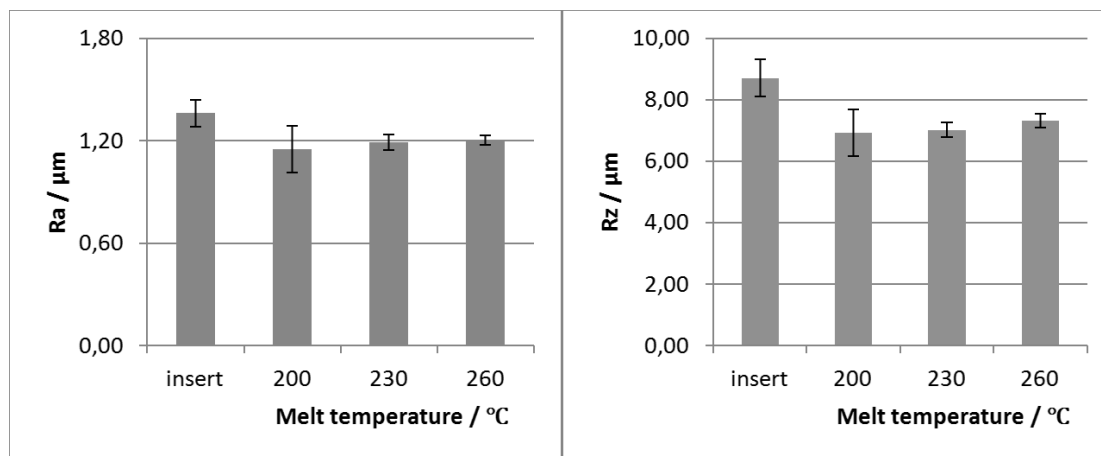
Fig.3.14 Quantity of heat across the interface, injection rate $25\text{cm}^3/\text{s}$, under different surface roughness and melt temperature

3.3.3 Surface roughness of plastic component

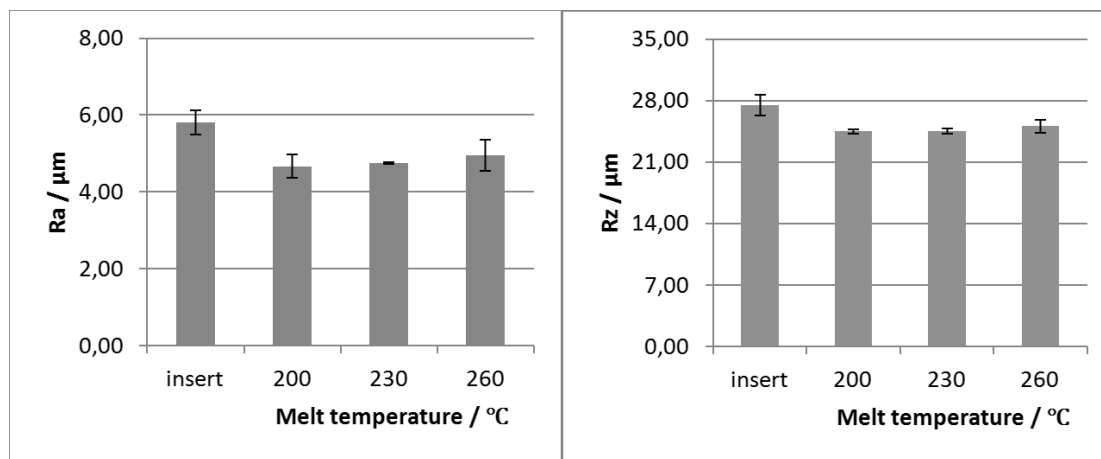
The surface roughness of the plastic components were measured by Hommel-Etamic T8000 RC and compared with those of the inserts to identify the cause of variation. The Ra and Rz values of the mold insert and plastic component are shown in Fig. 3.15.



(a) Comparison when Ra of insert is $0.01\mu\text{m}$



(b) Comparison when Ra of insert is 1.36 μm



(c) Comparison when Ra of insert is 5.81 μm

Fig.3.15 Comparison of surface roughness between insert and plastic component

Fig. 3.15(a) shows that the surface roughness of the plastic component is higher than that of the cavity wall when surface of the cavity wall is highly smooth. The surface roughness of the plastic component decreases with increasing melt temperature.

Yoshii [Yos93] also achieved the same result in his work on an optical disc with a highly smooth surface. Given the surface tension and viscosity of the polymer, the melt cannot easily enter the aperture on the wall surface, which has a size that is small enough for obstructing the polymer. The disparity of crystallization in different directions on the surface of semi-crystalline plastic causes the low replication level of the component surface. The increasing melt temperature can lead to a slower cooling rate and more uniform temperature distribution, which can reduce the disparity of crystallization. So with increasing melt temperature the replication level can be raised. This increase can also expand the contacting area between the polymer and cavity wall, thus increasing the HTC value, shown in Fig. 3.12.

On the contrary, when the surface of the cavity wall is rougher, the surface roughness of the plastic component is lower than that of the cavity wall. The surface roughness of the plastic component then increases with increasing melt temperature shown in Figs. 3.15 (b) and (c).

For these mold inserts, the aperture on the wall surface can contain the polymer melt, but air or vacuum gaps still exist because of the shrinkage of the hot melt during the cooling stage. The height of the protruding part on the component surface is always less than the depth of the aperture on the insert surface; thus, the surface roughness of the plastic component is always lower than insert. The viscosity of the polymer decreases and flowing time increases with increasing melt temperature; thus, a deep aperture position can be observed on the wall surface.

Although the cause of variation of component surface roughness is different from each other, the replication level of the component surface and contacting situation can be enhanced by increasing the melt temperature. At the same time contact situation is also improved by higher replication level and can lead to the enhancement of HTC value.

3.4 Summary of Chapter

In this chapter, it was presented a mathematical model of heat conduction across the interface. A corresponding injection experiment was conceived and performed by using the mathematical model. After processing the temperature data, the average HTC value in an injection cycle and the heat quantity across the interface between the polymer and cavity wall were obtained under different melt temperatures, the injection rates, and the surface roughness. Subsequently, the surface roughness of the plastic component was measured and compared with that of the mold insert. Finally, the effects of surface roughness and processing parameters on HTC variation between the polymer and cavity wall in the injection molding were obtained.

HTC increases with the increasing contacting area between the melt and cavity wall. Thus, HTC can be increased when the replication level of the component surface is high. Melt temperature has a significant role in HTC determination. A melt with a higher temperature has lower viscosity and longer freezing time, thus providing higher replication levels and better contacting situations. When surface roughness increases, the mean volume of the gap on the surface of the cavity wall also increases and a valid contacting area rises. This phenomenon has a similar importance as the melt temperature. Furthermore, the injection rate only has a slight influence on HTC.

By the quantitative research of HTC and the heat quantity across the interface, heat transfer process in an injection molding cycle can be comprehended deeply. The results of this study are beneficial in the prediction of the temperature field and in the design of cooling systems. Furthermore, it can also offer reliable HTC value for injection molding simulation in next step and then acquire more precise simulation result.

4. Influence of HTC on the results of injection molding simulation

After the evaluation of HTC value during injection molding, the value was introduced into corresponding simulation for representing various processing conditions. And then injection molding simulation was carried out. Finally the result from these simulations was obtained and compared with the result calculated with preset HTC value, which is default in the software and normally used by users.

4.1 Theory of injection molding simulation

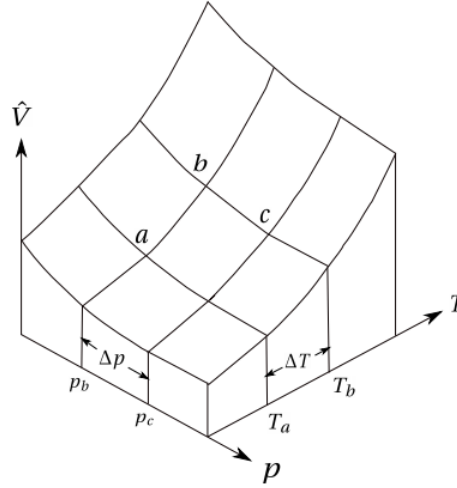
In order to simulate the process of injection molding, it is necessary to comprehend the basic equations that can represent the physical process happened during injection molding.

4.1.1 Properties of polymer

For simulation, some properties of the material need to be figured out. These material properties vary during the process. For flow analysis, which includes filling, packing, and cooling analysis, the following fundamental material properties are required: specific heat capacity, thermal conductivity, viscosity, transition temperature, pVT data [Ken13].

Thermal transition

A phase change or a thermal transition occurs with polymer when it goes through a significant change in material behavior. The phase change occurs as a result of a decreasing or increasing in material temperature. The transition temperatures as well as flow behavior are significantly affected by the pressure; the one applies to the material. Higher pressures can reduce the free volume between the molecules which restricts their movement. Therefore it requires higher temperatures for increasing the free volume to allow molecular movement, which can be clearly described by pressure-volume-temperature (pVT) diagram of amorphous polymer [Oss06], shown in Fig. 4.1. Although thermoplastic and thermoset have different kinds of thermal transition during injection molding, they cannot be considered liquid when above melting temperatures and solid when below those temperatures easily. In reality, they exhibit both viscous resistance to deformation and elasticity, called viscoelastic [Dea13]. And a polymer can be either a liquid or a solid at any temperature, which depends on the time scale or deforming speeds of its molecules. The most commonly applied method for measuring and demonstrating viscoelastic characteristic is the stress relaxation test and the time-temperature superposition principle.

Fig. 4.1 pVT diagram of polymer [Ken13]

In the stress relaxation test, a polymer specimen is deformed by a fixed amount of stress and the stress needed to hold, simultaneously deformation amount is recorded over time. The time-temperature equivalence seen in stress relaxation test results can be used to reduce data at various temperatures to one general master curve for a reference temperature, T_{ref} . For generating a master curve at the reference temperature, the curves obtained by stress relaxation must be shifted horizontally, maintaining the reference curve stationary. The amount that each curve was shifted can be plotted with respect to the temperature difference taken from the reference temperature. The amounts by which the curves were shifted are represented by Eq. 4.1 [Oss06].

$$\log(T) - \log(T_{ref}) = \log\left(\frac{T}{T_{ref}}\right) = \log(a_T) \quad (4.1)$$

In general, the horizontal shift ratio, $\log(a_T)$, between the relaxation responses at different temperatures to the reference temperature can be calculated using the Williams-Landel-Ferry (WLF) equation [Wil55]. The WLF equation is given by Eq. 4.2.

$$\log(a_T) = \frac{C_1(T - T_{ref})}{C_2 + T - T_{ref}} \quad (4.2)$$

where C_1 and C_2 are material dependent constants.

Density

The density or its reciprocal, the specific volume, is a commonly applied property for polymeric materials. The specific volume is often plotted as a function of pressure and temperature in a pVT diagram. When carrying out polymer flowing calculations, the temperature dependence of the specific volume must be processed analytically. At constant pressure, the density of polymers can be evaluated by Eq. 4.3 [Oss06].

$$\rho(T) = \rho_0 \frac{1}{1 + \alpha_t(T - T_{ref})} \quad (4.3)$$

where ρ_0 is the density at reference temperature, T_0 , and α_t is the linear coefficient of thermal expansion.

A widely applied density or specific volume model is the Tait equation. It is often used to represent the pVT -behavior of polymers and it is represented as Eq. 4.4 [Oss06].

$$v(T, p) = v_0(T) \left[1 - C \ln \left(1 + \frac{p}{B(T)} \right) \right] + v_t(T, p) \quad (4.4)$$

where $C=0.0894$. This equation of state is capable of describing both the liquid and solid regions by changing the constants in $v_0(T)$, $B(T)$ and $v_t(T, p)$, which are defined as Eq. 4.5,

$$v_0(T) = \begin{cases} b_{1,l} + b_{2,l}\bar{T}, & T > T_t(p) \\ b_{1,s} + b_{2,s}\bar{T}, & T < T_t(p) \end{cases}$$

$$B(T) = \begin{cases} b_{3,l}e^{-b_{4,l}\bar{T}}, & T > T_t(p) \\ b_{3,s}e^{-b_{4,s}\bar{T}}, & T < T_t(p) \end{cases}$$

and

$$v_t(T, p) = \begin{cases} 0, & T > T_t(p) \\ b_7 e^{b_8 \bar{T} - b_9 p}, & T < T_t(p) \end{cases} \quad (4.5)$$

where $\bar{T} = T - b_5$ and the transition temperature is assumed to be a linear function of pressure, i.e.,

$$T_{trans} = b_5 + b_6 p \quad (4.6)$$

The constants from b_1 to b_9 for the Tait equation are definitized and can be found out in existent literature.

Crystallization

Semi-crystalline thermoplastic polymers show more order than amorphous thermoplastics. Actually during cooling both amorphous and crystalline regions exist in the polymer, and the crystalline regions can be removed and restored with repeated heating and cooling process, which can prove that there is no chemical change to the polymer. Without external forces, semi-crystalline polymer will form amorphous and crystalline regions randomly, when cooling from the melt to solid state and the polymer properties are determined by the amount and orientation of the crystalline phase in the material [Ken13]. According to Hoffman-Lauritzen Growth theory, there are three basic regimes for crystal nucleation, as shown in Fig. 4.2.

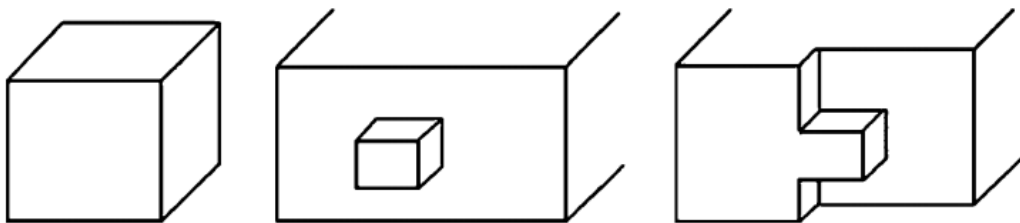


Fig. 4.2 Illustration of three basic regimes of crystal nucleation. From left to right are primary nucleation in the bulk polymer phase, secondary nucleation on the smooth growth front and tertiary nucleation at the terrae of the growth front [Hu13]

The first regime is supposed to generate a cubic crystallite with six square interfaces from the amorphous bulk polymer phase, which is called primary nucleation. Primary nucleation generates the largest new interface, so the highest free energy barrier is demanded and its initiation rate is the lowest. The second regime is supposed to generate four additional square faces of the new lateral interfaces, which is called secondary nucleation. The free energy barrier for secondary nucleation will be lower and after the incubation period for the initiation of crystal nucleation crystal growth appears to be a self-acceleration process. The third regime is supposed to generate only two additional square faces at the top and down interfaces, which is called tertiary nucleation. Tertiary nucleation has the lowest free energy barrier and thus is the fastest which is also difficult to be observed [Hu13].

4.1.2 Transport of polymer

The field of polymer transport is the basis of polymer processing. Conservation of mass, momentum and energy must be satisfied at the same time when solving flow and heat transfer problems in simulation of injection molding. Momentum and energy balances, in combination with material properties through constitutive relations, sometimes result in the problem of highly non-linear governing equations [Oss06].

Some fluid properties depend on both position and time. When analyzing fluid motion, it is necessary to take derivatives, with respect to time, of these properties. For any scalar function of position and time, $f = f(x_1, x_2, x_3, t)$, it can be presented as Eq. 4.7 [Ken13].

$$\frac{Df}{Dt} = \vec{v} \cdot \nabla f + \frac{\partial f}{\partial t} \quad (4.7)$$

where \vec{v} is velocity vector. $\frac{Df}{Dt}$ is called as the material derivative of f , which takes into account both the fluidic motion and the changing value of the fluid particle with time.

The conservation equations of mass, momentum, and energy used in the software can be expressed as Eqs. 4.8-10.

$$\frac{\partial \rho}{\partial t} + \nabla \cdot (\rho \vec{v}) = 0 \quad (4.8)$$

$$\rho \frac{D\vec{v}}{Dt} = -\nabla p + \nabla \cdot \underline{\underline{\tau}} + \rho g \quad (4.9)$$

$$\rho c_p \frac{DT}{Dt} = \beta T \frac{Dp}{Dt} + \nabla \cdot (k \nabla T) + \eta \dot{\gamma} \quad (4.10)$$

where $\underline{\underline{\tau}}$, c_p and β express stress tensor, specific heat and expansivity respectively.

In addition, boundary conditions are quite specific to injection molding, which should be applied to conservation equations. Fig. 4.3 shows the boundary conditions which should be considered for simulation [Ken13].

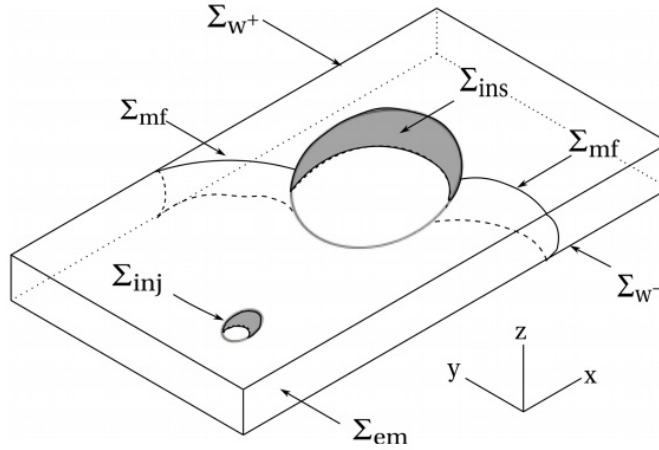


Fig. 4.3 Boundary conditions for simulation [Ken13]

Σ_{inj} is the surface through which melt enters the cavity; Σ_{em} is the edge of the mold; Σ_{W+} is the top surface of the mold; Σ_{W-} is the bottom surface of the mold; Σ_{ins} is the surface defining any insert in the mold and Σ_{mf} is the surface defining the melt front. Depending on the number of cavities and the geometry of the mold cavity, the number of Σ_{mf} may be any.

A simple mold cavity is illustrated in Fig. 4.3 for discussing the required boundary conditions. Σ_{inj} , Σ_{em} , Σ_{W+} , Σ_{W-} , Σ_{ins} and Σ_{mf} are surfaces on which boundary conditions need to be defined.

4.1.3 Numerical analysis methods

The finite element method (FEM) is a general and most popular method for solving engineering problems. It was first developed in 1956 to numerically analyze stress problem for design of aircraft structures [Tur56]. Since then it has been applied to solve more general problems in solid mechanics, fluid flow, heat transfer and other engineering problems. Moreover due to its versatility, FEM is being used to solve multiple-field coupled problems with complex geometry where the solutions are always highly nonlinear [Oss06]. The elementary idea is shown in Fig. 4.4.

In Fig. 4.4, the exact solution is the dotted line and the solid line segments are the approximation, that means the points defining the line segments $\tilde{u}(x_i)$ are approximations of the exact solution at the points $x_i, i \in \{1, \dots, 6\}$. Finite element solution of the problem will provide the approximate values of the exact solution at points which can be called nodes. The quality of the approximate values of $\tilde{u}(x_i), i \in \{1, \dots, 6\}$ depends on the mathematical model, including boundary conditions. It makes sense to have sufficient elements to cover the solution domain for obtaining more precise approximate solutions, which is usually called mesh density.

Within equal area or volume, a finer mesh means there is more elements and a higher mesh density can improve the accuracy of approximated solution.

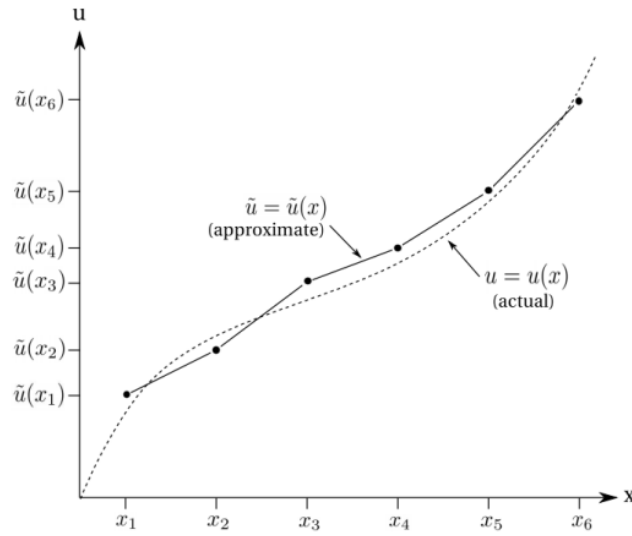


Fig. 4.4 Approximation of a simple curve by FEM [Ken13]

In Fig. 4.4, linear segments are used and a linear variation is assumed, which is called linear interpolation. Linear interpolation is the simplest, and it is also possible to employ higher order interpolation for achieving a more precise solution. Alternatively smaller linear elements and higher element density can also achieve precise solution. On the other hand, both of above mentioned methods consume more calculating time [Ken13].

The finite volume method (FVM) is another numerical method, which is also widely applied in computational fluid mechanics with faster calculating speed. But sometimes it has the difficulty when solving multiple-field coupled problems. Chang[Cha01] and Zhou[Zho06] used this method to do three-dimensional simulation of molding filling independently.

4.1.4 Characteristics of Moldflow Plastic Insight

In Moldflow Plastic Insight, from Autodesk Inc., U.S., there are two types of elements, which are 2.5D elements, which includes midplane and dual domain, and 3D elements. Normally, with 3D elements more precise solutions can be achieved, but on account of injection molding cavities being frequently thin-walled, 2.5D element approximation can also give acceptable results consuming less calculating and hardware device.

There is a high temperature gradient in the thickness direction for a thin wall component; however the pressure gradient throughout the molding is relatively low, which has been found

by Hieber and Shen [Hie80]. They introduced the idea that the temperature in the thickness may be best evaluated by finite differences and the pressure in the midplane of the molding by finite elements. Temperature during molding varies from cavity center to the area near cavity wall. Particularly there is a high gradient across the area near cavity wall. Although the temperature gradient is less in the direction of polymer flowing, it varies significantly and the temperature distribution should be solved in 3D. On the other hand there is relatively little pressure variation across the area near cavity wall. Therefore the pressure should be solved in 2D at nodes on an imaginary midplane inside the actual 3D plastic component. The combination of 3D-temperature-field and 2D-pressure-field is the origin of so-called “2.5D” elements in Moldflow [Ken13].

In order to describe the 2.5D approximation, a Cartesian coordinate system is introduced. The axes are adjusted so that at any point in the cavity the X - Y plane is parallel with the midplane of the component and Z - axis is the thickness direction. The coordinates systems of midplane and generation of midplane elements are shown in Fig. 4.5 and 4.6 respectively.

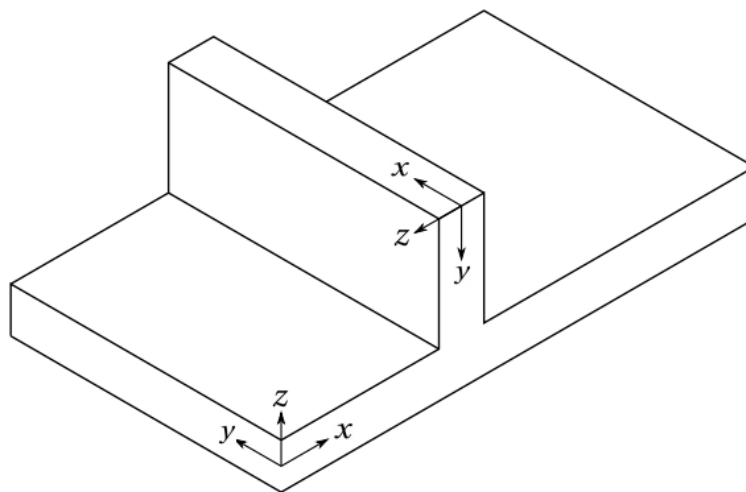


Fig. 4.5 Thin-walled cavity with coordinates systems of midplane [Ken13]

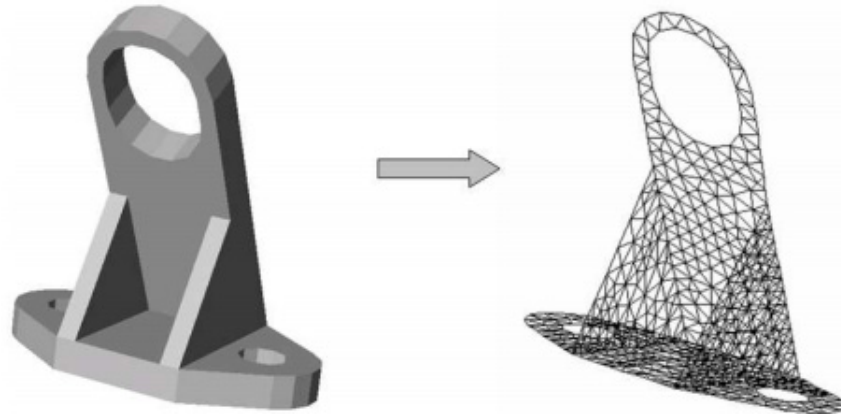


Fig. 4.6 Generation of midplane elements [Ken13]

Instead of determining the midplane from a 3D geometry, another method was used to convert the 3D geometry to an equivalent 2.5D geometry, which is called Dual Domain method and shown in Fig. 4.7.

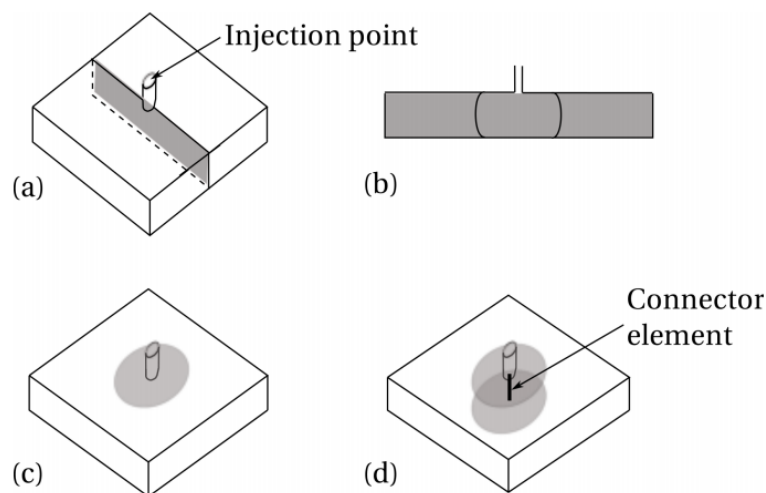


Fig. 4.7 Dual domain flow analysis; (a) depicts injection into the center of a rectangular plate; (b) shows the flow in the cross-section of the plate; (c) shows the flow front advancement on the surface mesh, and (d) shows the use of a connector element to ensure physical agreement with the true flow shown in (b)[Ken13]

The dual domain elements are composed of two opposite mesh surfaces. Each element on one of the mesh surfaces must match one element on another mesh surface and the relationship between them is one-to-one mapping, shown in Fig. 4.8 and h is the thickness of component.

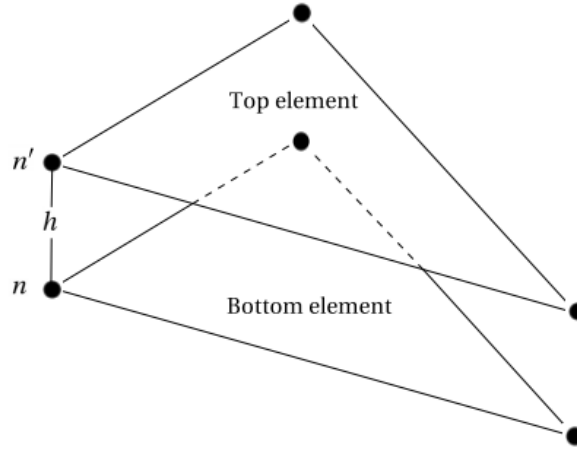


Fig. 4.8 Structural elements matched for Dual Domain analysis [Ken13]

Sometimes the real plastic components are more complicated than simple plates. It requires performing a 3D analysis, which needs more time and hardware for calculating but can avoid the 2.5D approximation assumptions and is the ultimate method of simulation in theory.

In Moldflow, a modified model, called Cross-WLF equation, is used to describe the temperature, shear rate, and pressure dependency of the viscosity, given by Eq. 4.11.

$$\eta = \frac{\eta_0}{1 + \left(\frac{\eta_0 \dot{\gamma}}{\tau^*}\right)^{1-n}} \quad (4.11)$$

where η is the melt viscosity, η_0 is the zero shear viscosity or the “Newtonian limit” in which the viscosity approaches a constant at very low shear rates, $\dot{\gamma}$ is the shear rate, τ^* is the critical stress level at the transition to shear thinning, determined by curve fitting and n is the power law index in the high shear rate regime, also determined by curve fitting. The zero shear viscosity is given by Eq. 4.12.

$$\eta_0 = D_1 \exp \left[-\frac{A_1(T-T_g)}{A_2 + (T-T_g)} \right] \quad (4.12)$$

where T_g is the glass transition temperature, determined by curve fitting, $A_2 = A_3 + D_3 p$, p is the pressure and D_1 , A_1 , A_3 and D_3 are data-fitted coefficients. The glass transition temperature is given by Eq. 4.13.

$$T_g = D_2 + D_3 p \quad (4.13)$$

where D_2 is a data-fitted coefficient.

In injection molding simulation the temperature point of thermal transition has been interpreted by introducing a no-flow temperature, which is quite necessary for defining the status of polymer. In Moldflow, the no-flow temperature is achieved by setting an extremely high value of polymer viscosity and ceases to flow when its temperature is lower than the no-flow temperature [Ken13], or it follows the Cross-WLF equation.

In Moldflow it is assumed that the growth rate follows the Hoffman-Lauritzen theory [Lau60]. The expression to describe the nucleation and growth during crystallization process in Moldflow is shown in Eq. 4.14.

$$G(T) = G_0 \exp \left[-\frac{U^*}{R_g(T-T_\infty)} \right] \exp \left[-\frac{fK_g}{T(T_m^0-T)} \right] \quad (4.14)$$

where $T_\infty = T_g - 30$, $f = \frac{(T+T_m^0)}{2T}$, G_0 and K_g are material grade-specific constants which can be determined under quiescent conditions, U^* is the activation energy of motion, R_g is the gas constant, and T_m^0 is the material grade-specific equilibrium melting temperature which is assumed to depend on pressure only. A linear function is chosen to describe the pressure dependence as Eq. 4.15.

$$T_m^0 = T_{eq} + b_6 P \quad (4.15)$$

Where T_{eq} is the equilibrium melting temperature, b_6 is a grade-specific constant of the pVT model of the material, and P is the pressure. Nucleus generation, N , is expressed as the sum of the number of activated nuclei in the quiescent condition, N_0 , and the number of activated nuclei induced by the flow, N_f , as Eq. 4.16.

$$N = N_0 + N_f \quad (4.16)$$

The number of activated nuclei in the quiescent condition is assumed to be a unique function of the supercooling temperature, $\Delta T = T_m^0 - T$, and is described by Eq. 4.17.

$$\ln N_0 = a_N \Delta T + b_N \quad (4.17)$$

where a_N and b_N are material grade-specific constants.

4.2 Influence of HTC on simulated frozen volume percentage

Injection molding simulations was conducted by using the software Moldflow Plastics Insight 2013. Both studying object and blind volume were taken into account, which were shown as right and left in Fig. 4.9 respectively.

The total number of elements is 989299 and most of them locate on studying object on the right side in Fig. 4.9. The volumes of sprue, studying object and other parts are 1.5499cm^3 , 0.4482cm^3 and 15.8845cm^3 respectively.

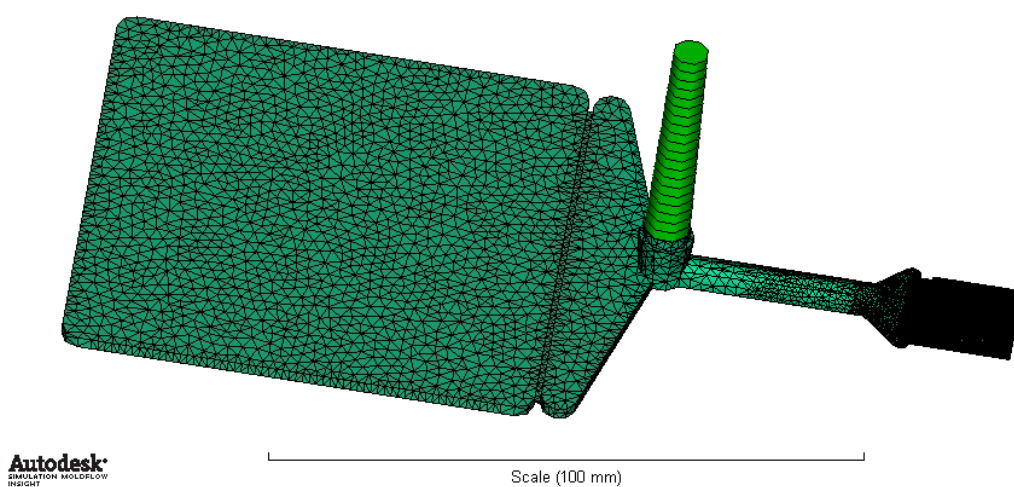


Fig. 4.9 Model of the component with runner system built in Moldflow.

The constants required in Cross-WLF equation can be found in Moldflow database, which are shown as following: $n = 0.3773$, $\tau^* = 2.35 \times 10^4 \text{ Pa}$, $D_1 = 1.09 \times 10^{16} \text{ Pa}\cdot\text{s}$, $D_2 = 233.15 \text{ K}$, $D_3 = 0 \text{ K/Pa}$, $A_1 = 37.252$, $A_2 = 51.6 \text{ K}$. And the constants used in $p\text{-}v\text{-}T$ model can be also found in Moldflow, which are shown as following: $b_5 = 403.15 \text{ K}$, $b_6 = 1.535 \times 10^{-7} \text{ K/Pa}$; for liquid phase $b_{1l} = 0.0012$, $b_{2l} = 6.721 \times 10^{-7}$, $b_{3l} = 1.6438 \times 10^8$ and $b_{4l} = 0.005$; for solid phase $b_{1s} = 0.0011 \text{ m}^3/\text{kg}$, $b_{2s} = 5.869 \times 10^{-7} \text{ m}^3/\text{kg}\cdot\text{K}$, $b_{3s} = 2.8784 \times 10^8 \text{ Pa}$, $b_{4s} = 0.0015 \text{ K}^{-1}$, $b_7 = 7.777 \times 10^{-5} \text{ m}^3/\text{kg}$, $b_8 = 0.0505 \text{ K}^{-1}$, and $b_9 = 1.136 \times 10^{-8} \text{ Pa}^{-1}$.

The frozen volume percentage of the whole polymer injected into cavity can be calculated by observed HTC value in last chapter and preset HTC value in the software which is $5000 \text{ W}/(\text{m}^2\cdot\text{K})$ in the filling stage, $2500 \text{ W}/(\text{m}^2\cdot\text{K})$ in the packing stage and $1250 \text{ W}/(\text{m}^2\cdot\text{K})$ in the cooling stage. The simulated frozen percentage in filling stage is shown as Fig. 4.10, in which the injection rate is maintained at $15 \text{ cm}^3/\text{s}$ and the surface roughness of cavity wall is $1.36\mu\text{m}$.

It can be derived from Fig. 4.10 that frozen percentage increases with time except the first injection moment. The time of polymer needs to be frozen also increases with increasing melt temperature for polymer with higher temperature contains more internal energy which needs more time to be frozen. It is also obvious that the frozen percentage calculated by observed HTC is larger than the result calculated by preset HTC most of the time. The difference between two results emerges at the time point of approximately 0.3s and enlarges continually. After a certain time, it decreases but consistently exists. The reason of that is at the first moment hot melt run into the runner and cavity under high injection pressure, in the meantime heat transfers from the polymer side to the cavity side but the polymer temperature is still higher than the frozen point of material. Thus the frozen percentage maintains as a relatively low value at the beginning.

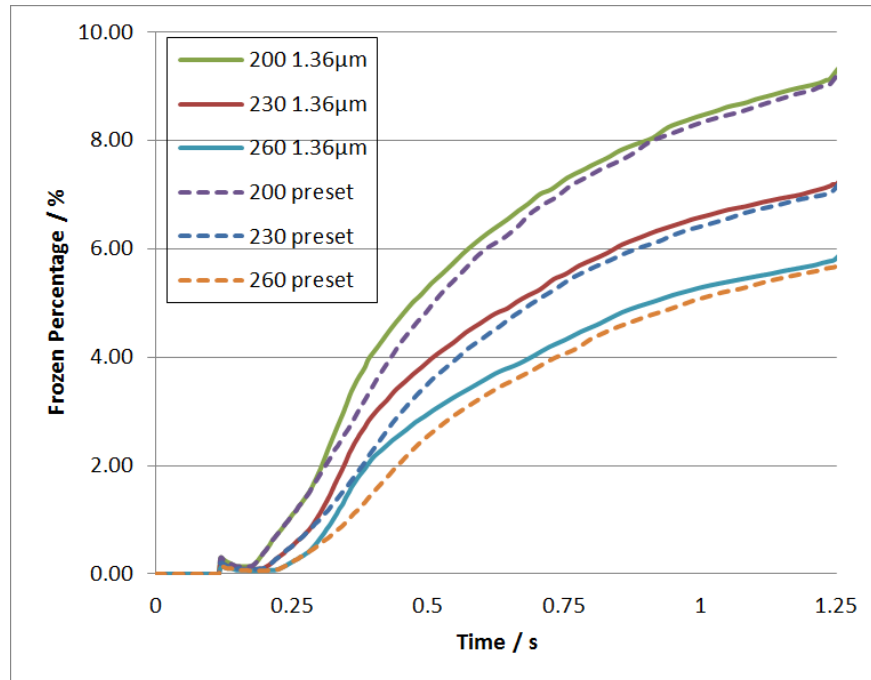


Fig. 4.10 Simulated frozen percentage vs. time in filling stage, injection rate $15 \text{ cm}^3/\text{s}$, under different melt temperature, calculated with the HTC value which is preset in Moldflow and with the observed HTC value when surface roughness $1.36\mu\text{m}$ respectively.

According to the filling analysis, shown as Fig. 4.11, although the melt run into both cavities at the same time, for the volume of studying object is much smaller than blind volume, when the studying object is full-filled with hot polymer, only a little part of blind volume is filled. Moreover the frozen percentage presented in Fig. 4.10 is the frozen ratio of the whole plastic component which also includes the blind volume. Therefore in the initial stage frozen percentage can reflect the cooling situation of studying object. Heat transfer condition with

higher HTC can cool down the melt more quickly and frozen percentage calculated by observed HTC, which is higher than preset value, increases more rapidly.

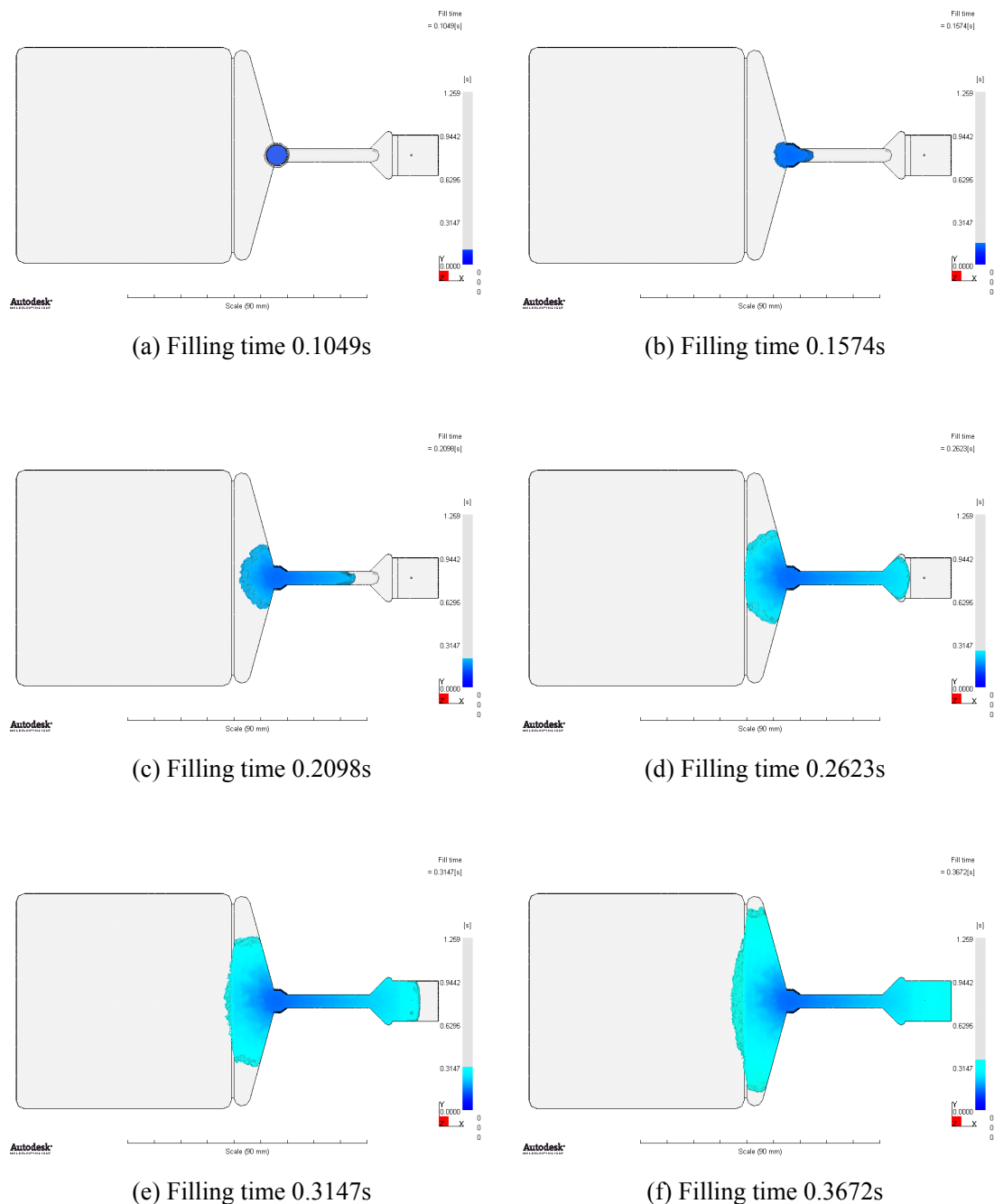


Fig. 4.11 Positions of melt front during filling process from simulation result by Moldflow

As time goes on, most of the studying object is frozen and temperature of most blind volume is still over the frozen point. Thus the difference between the result calculated by observed HTC and the result calculated by preset HTC diminishes gradually and almost vanishes finally, which can be seen from the end of filling stage in Fig. 4.10 and also from packing and cooling stage in Fig. 4.12.

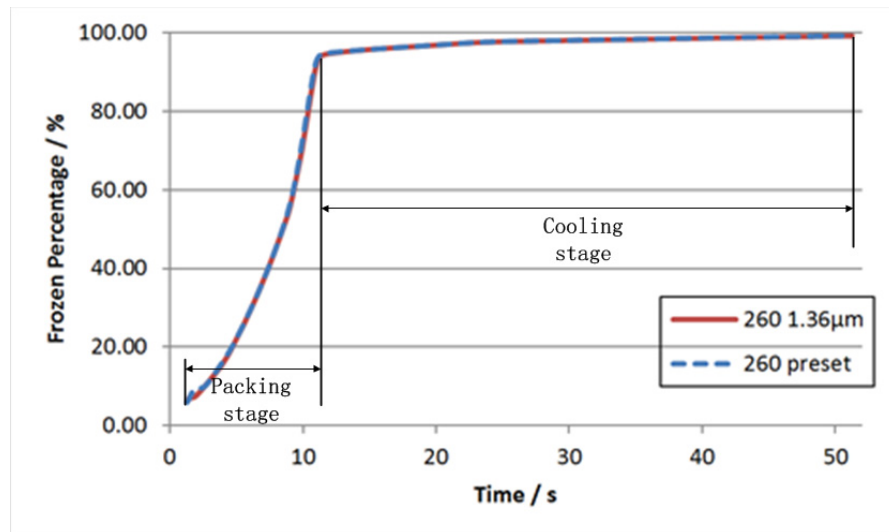
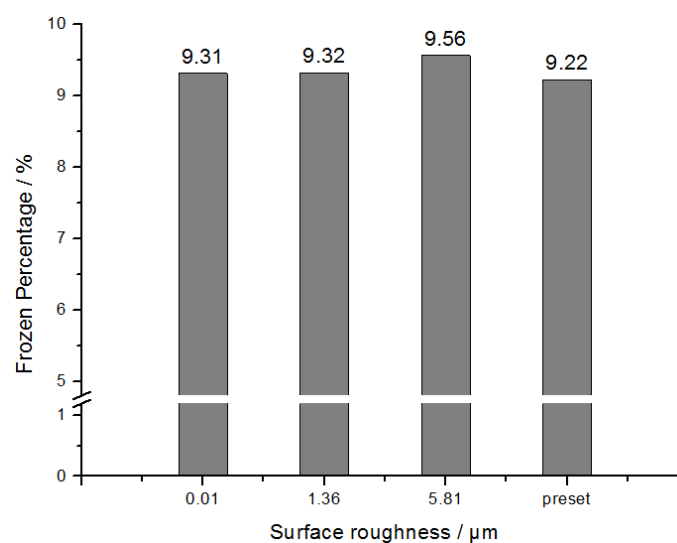


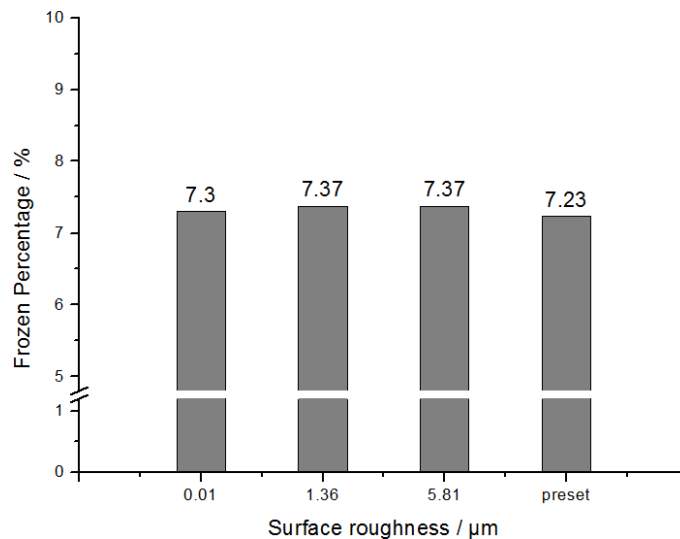
Fig. 4.12 Simulated frozen percentage vs. time in packing and cooling stage, melt temperature 260°C, injection rate 15 cm³/s, calculated with the HTC value which is preset in Moldflow and with the observed HTC value when surface roughness 1.36μm respectively.

So based on the result of frozen percentage, it can be concluded that the calculation by observed HTC value indicates a higher cooling rate of polymer, but only in the region of studying object for observed value of HTC was applied in this region which is much larger than preset value of HTC used in blind volume.

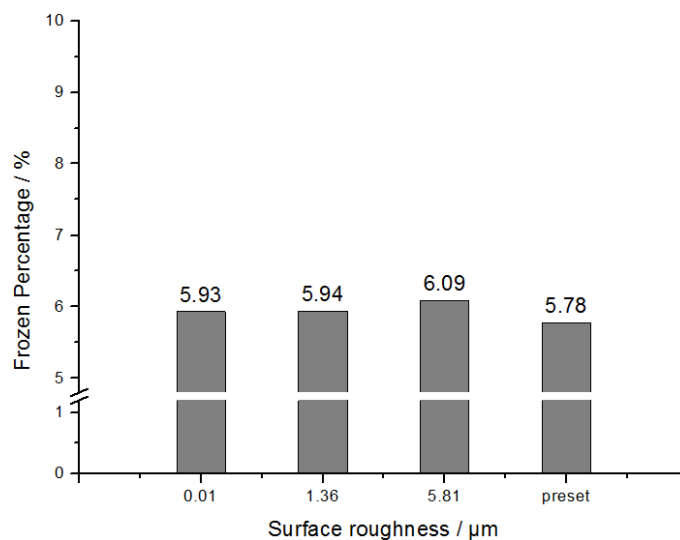
With different HTC value, frozen percentage in the end of filling stage under various surface situations was calculated and shown in Fig. 4.13, in which the bar on the right side is calculated by preset HTC value in software.



(a) Melt temperature 200°C



(b) Melt temperature 230°C



(c) Melt temperature 260°C

Fig. 4.13 Simulated frozen percentage in the end of filling stage, under different melt temperature, calculated with HTC of preset value and observed value under different surface roughness

It can be seen from 4.13, with increasing value of surface roughness, the value of frozen volume in the end of filling stage raises and the frozen percentage calculated by preset HTC is always lower than the value calculated by observed HTC. It is more important that observed HTC provides result variety which depends on different surface situation, but with preset HTC the cooling result keeps the same despite surface roughness variation.

4.3 Influence of HTC on simulated crystallinity

In Moldflow Plastics Insight 2013, final relative crystallinity result indicates the ratio of crystallized volume to the total crystallizable volume, at a single time instant, after the ejected

part has cooled to the ambient temperature. Relevant parameter for describing crystallization morphology of the polymer used in injection molding is not in material database of the version 2013, but was provided by Moldflow research group. Values of relative crystallinity can range from 0 to 1. A value of 0 corresponds to no crystallinity, i.e. in amorphous phase. A value of 1 corresponds to attainment of ultimate crystallinity for the material. For Lupolen 1800S used in this work, the ultimate crystallinity is considered and set as 0.6 according to several present literatures [Sma99, And04, Sum06, Gol08, Kle09]. Thus, the relationship between crystallinity α and relative crystallinity α_R can be described by following.

$$\alpha_R = \frac{\alpha}{0.6} \times 100\% \quad (4.18)$$

The distribution of relative crystallinity of studying object after cooling is shown in Fig. 4.14.

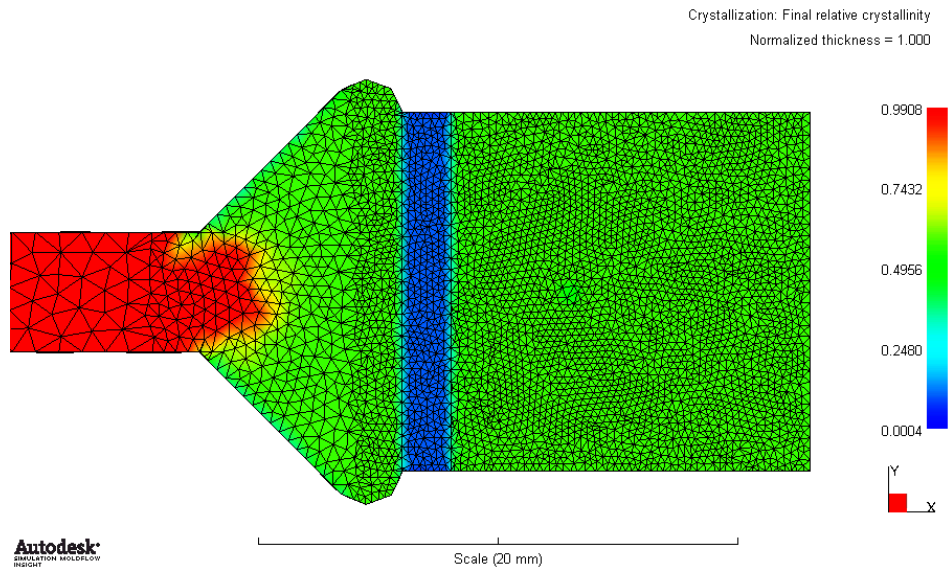
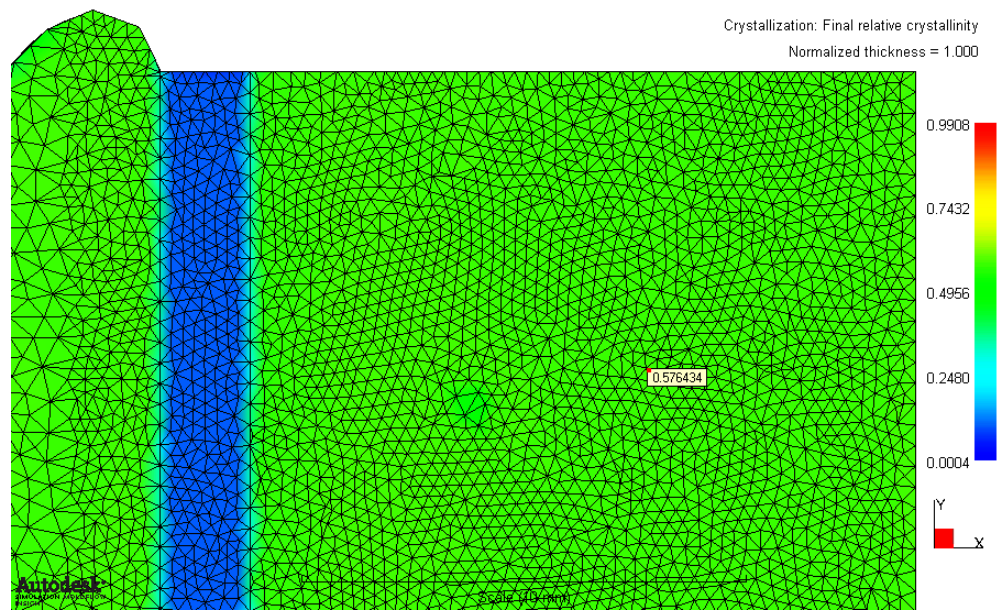


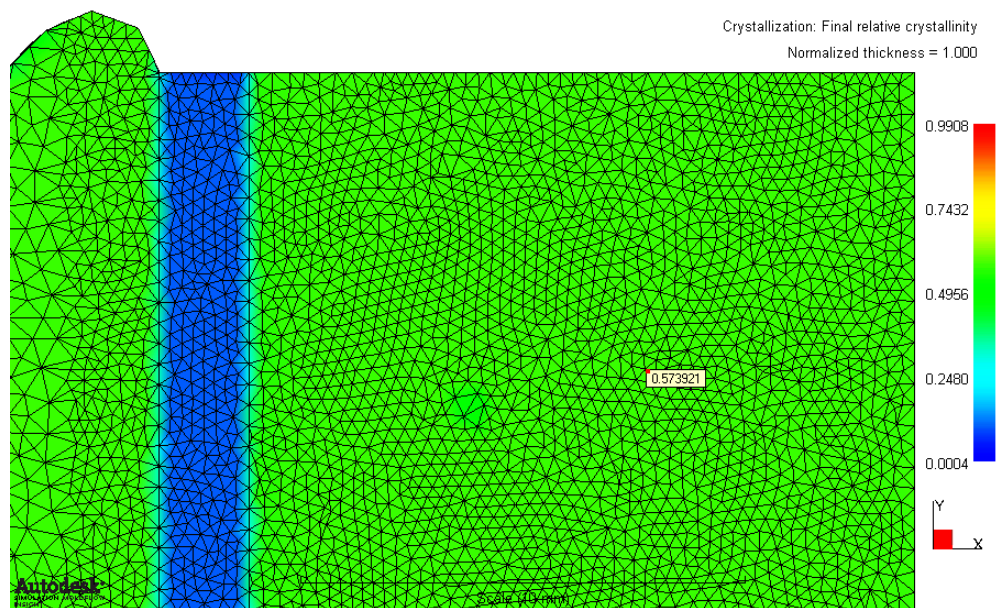
Fig. 4.14 Simulated final relative crystallinity of studying object with runner system, melt temperature 230°C, surface roughness 1.36 μ m

And it can be seen from Fig. 4.14 that due to slow cooling rate inside runner, it shows high value of crystallinity in this area, where is red in the figure. To the contrary, the thickness of gate is thinner than that of plastic part, so polymer temperature of gate drops more quickly than that of part. Furthermore it shows low value of crystallinity at the gate locations, where is blue in the figure.

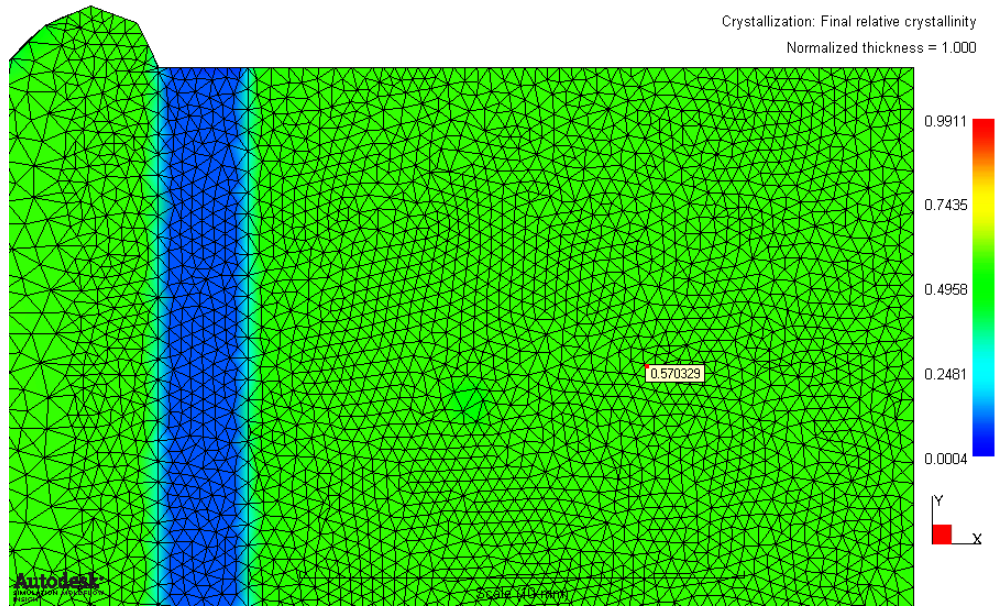
The value of relative crystallinity on the same node of each condition was selected for comparison, as shown in Fig.4.15.



(a) Surface roughness $Ra\ 0.01\mu m$



(b) Surface roughness $Ra\ 1.36\mu m$



(c) Surface roughness R_a $5.81\mu\text{m}$

Fig. 4.15 Simulated final relative crystallinity distribution of studying object, under different surface roughness, melt temperature 230°C

The calculation of final relative crystallinities under different melt temperature and calculated with preset HTC value were also carried out and the identical node was selected.

The simulated relative crystallinity under different surface roughness when melt temperature is constant on the level of 230°C is shown as Fig.4.16, in which bars of preset represent the crystallinity result calculated by utilizing the default value of HTC in software, and bars of observed HTC represent the result calculated by utilizing the value obtained in last chapter.

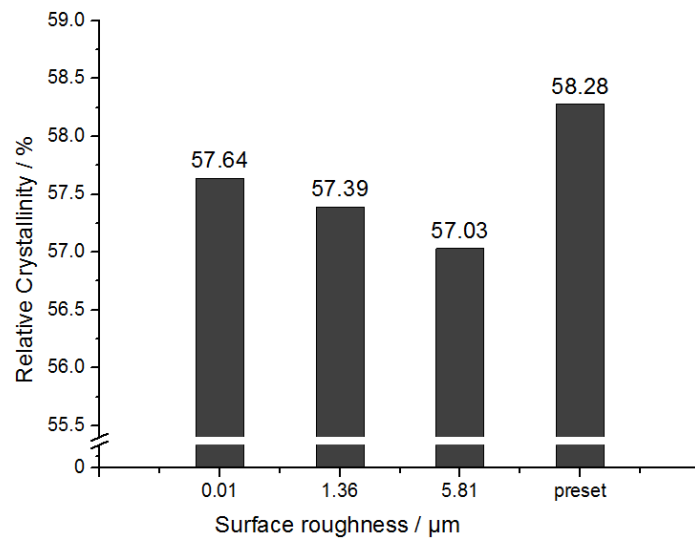


Fig. 4.16 Simulated relative crystallinity calculated with HTC of preset value and observed value under different surface roughness, melt temperature 230°C .

It can be seen from Fig. 4.16 that the relative crystallinity calculated with observed HTC is always lower than that calculated by preset HTC value. The relative crystallinity calculated by observed HTC decreases with increasing surface roughness of cavity wall, which is due to higher value of surface roughness means better contact situation for heat transferring between polymer and cavity wall, which leads to a faster cooling rate and a lower relative crystallinity. It can also be seen from Fig. 4.16 that the relative crystallinity calculated by preset HTC maintains on the same level all the time, for no parameter in software can represent the variation of surface roughness when other processing parameters are constant. Thus from this point of view observed HTC value can represent diverse surface roughness for acquiring a more precise cooling and crystallizing result in the simulation.

The simulated relative crystallinity under different melt temperature when surface roughness is constant on the level of $1.36\mu\text{m}$ is shown as Fig. 4.17.

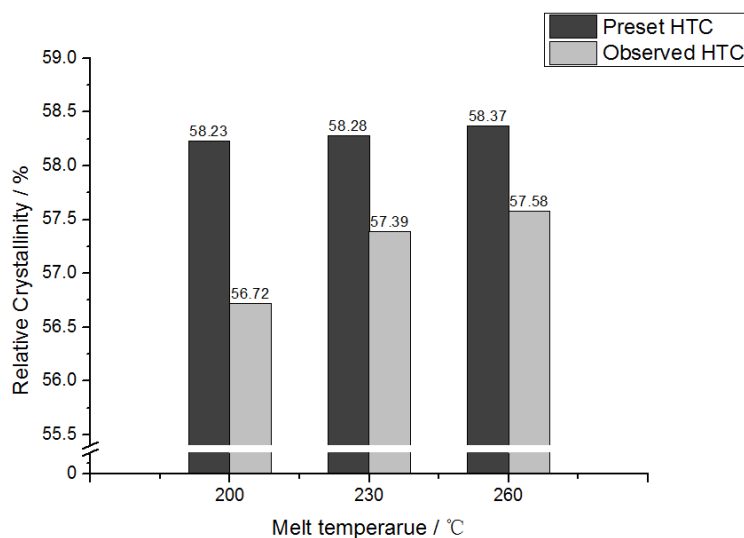


Fig. 4.17 Simulated relative crystallinity calculated with HTC of preset value and observed value, under different melt temperature, surface roughness $1.36\mu\text{m}$.

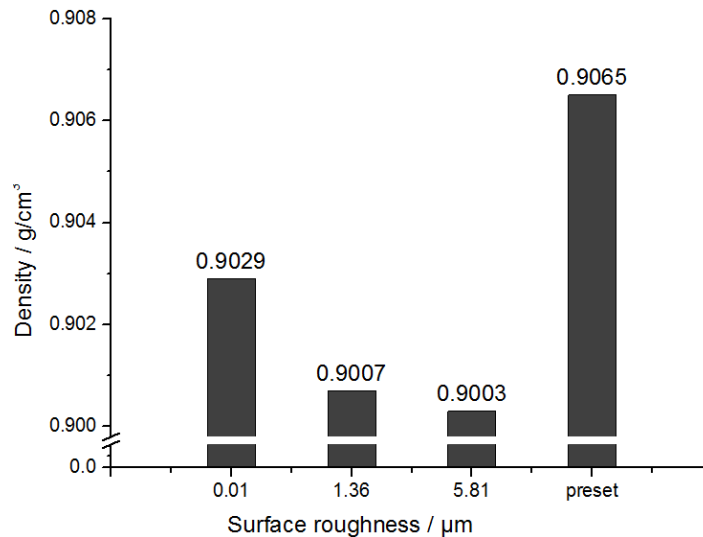
It can be obtained from Fig. 4.17 that both relative crystallinities increase with rising melt temperature but the relative crystallinity calculated with observed HTC shows more obviously increasing trend. The reason is due to the observed HTC achieves a faster cooling rate which leads to a lower relative crystallinity. And observed HTC value under different melt temperature, which presents the contact situation on the interface, is not identical with each other and can describe the cooling and crystallizing process more precisely.

4.4 Influence of HTC on simulated part density

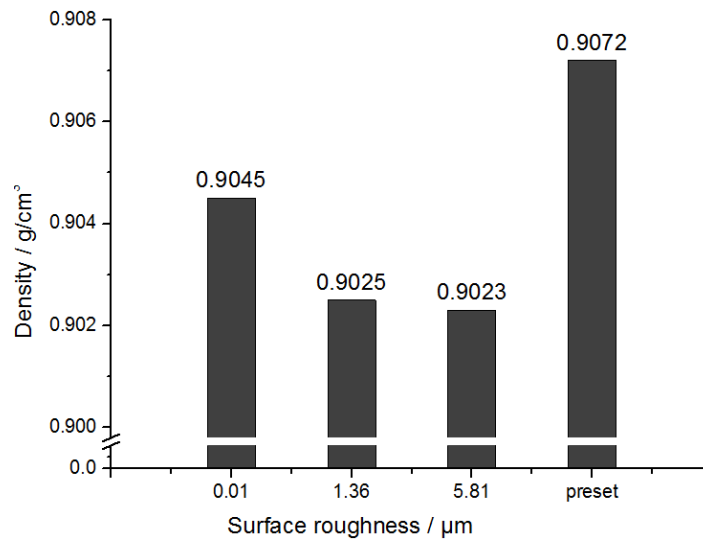
With the Moldflow Insight 2013, calculation of studying object mass was accomplished. According to its volume is 0.4482cm^3 , the density of studying object calculated with observed and preset HTC value was obtained afterward, which is shown in Fig. 4.18.

The part density is influenced by several factors during injection molding. When the melt temperature is higher, the shrinkage of polymer is more obvious in cooling stage, thus the part density is lower. On the contrary higher melt temperature can delay frozen time point of gate in packing stage and make the packing time longer which is beneficial for reducing the shrinkage of polymer. Packing pressure affects the part density too. Higher packing pressure can reduce polymer shrinkage in packing stage and increase the part density. Due to the higher cooling rate crystallinity increases, that can make the part more compact. So part density is raised afterwards.

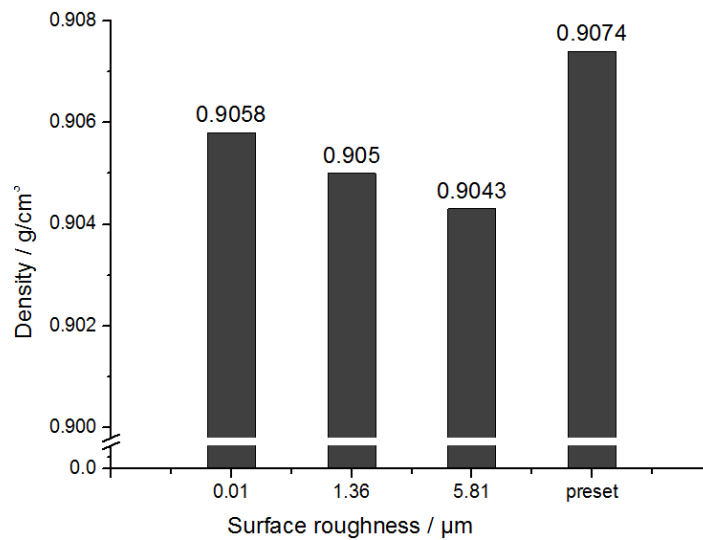
It can be seen from Fig. 4.18 that the density calculated with preset HTC does not change with different condition of surface roughness and is always higher than that calculated with observed HTC. And the density decreases with increasing surface roughness although the difference is very little.



(a) Melt temperature 200°C



(b) Melt temperature 230°C



(c) Melt temperature 260°C

Fig. 4.18 Density of studying object calculated with HTC of preset value and observed value under different surface roughness and certain melt temperature.

The reason of this phenomenon is when observed HTC is higher than preset HTC, which can lead to a higher cooling rate and lower degree of crystallinity. Therefore the density calculated with observed HTC is always lower than the other. Moreover the melt temperature and packing pressure were kept on the same level during cooling stage, so the density shows decreasing trend with increasing surface roughness because of the factor of crystallinity.

When the surface roughness is constant, the density changing with melt temperature calculated with preset and observed HTC is shown in Fig. 4.19.

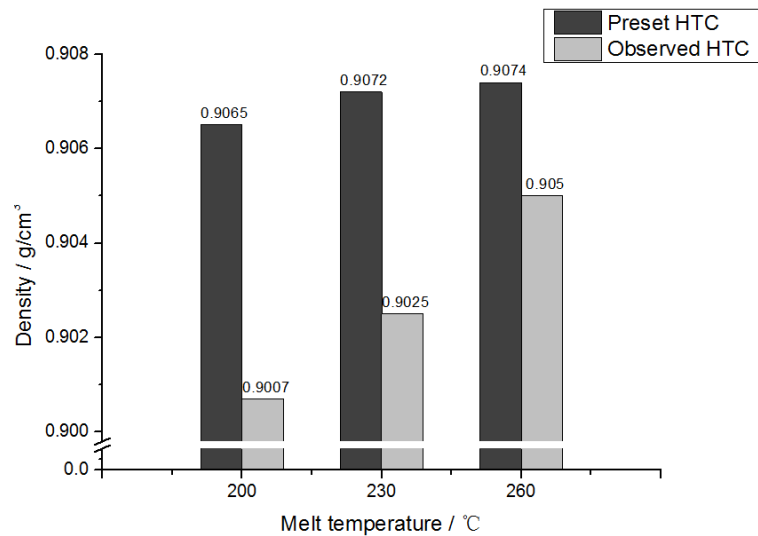


Fig. 4.19 Density of studying object calculated with HTC of preset value and observed value, under different melt temperature, surface roughness 1.36 μ m.

In Fig. 4.19 the density of studying object shows growing tendency with increasing melt temperature. The density calculated with observed HTC shows stronger increase than that calculated with preset HTC. Only the packing pressure was kept on the same level during cooling stage. Because the factor of crystallinity takes the dominant place against the factor of polymer shrinkage, the density of higher melt temperature is bigger than others. Comparing with density calculated with preset HTC, the density calculated with observed HTC can not only reflect the influence of melt temperature on density but also express the influence of HTC on density. Accordingly it shows more obvious increase with rising melt temperature.

4.5 Summary of Chapter

In this chapter, it was presented the theory of injection molding simulation, including the expression of polymer properties and polymer transport, the numerical analysis methods and the element types in Moldflow Insight 2013. Subsequently, injection molding simulation with preset and observed HTC were carried out and according simulation results were obtained. The frozen volume percentage, crystallinity and part density calculated with preset and observed HTC under different melt temperature and surface roughness were shown and compared with each other afterwards.

The frozen percentage calculated with observed HTC is larger than that calculated with preset HTC in filling stage. The difference emerges after injecting approximately 0.3s and enlarges continually. After a certain time, it decreases and vanishes before the beginning of packing stage. The value of frozen volume in the end of filling stage increases with increasing value of surface roughness and the value calculated with preset HTC is always lower than that calculated with observed HTC. The relative crystallinity calculated with observed HTC is always lower than that calculated with preset HTC value and it decreases with increasing surface roughness of cavity wall. Meanwhile the relative crystallinity increases with rising melt temperature but the relative crystallinity calculated with observed HTC shows more obviously increasing trend. The density calculated with preset HTC is always higher than that calculated with observed HTC and the density calculated with observed HTC decreases with increasing surface roughness although the difference is very little. On the other hand, the density rises with increasing melt temperature and the density calculated with observed HTC shows stronger growth trend than that calculated with preset HTC.

After the injection molding simulation, it is obtained that it is quite distinguishing between the results calculated with preset and observed HTC value. With observed HTC value, the result can display more details in the field of frozen volume, crystallinity and part density. It is more important that under different surface roughness the result calculated with preset HTC is identical as expected but a number of observed HTC which is based on actual situation can provide more diverse and precise simulation results.

5. Influence of HTC on the results of injection molding experiment

The injection molding simulation using observed and preset HTC value was carried out in last chapter already. It shows that the simulation using observed HTC value provides quite different result comparing with the simulation using preset HTC in the field of frozen volume, crystallinity and part density and it can also represent various surface situation of cavity wall that cannot be expressed by preset HTC. However there are still some questions needs to be answered that, between the results calculated with preset HTC and observed HTC, which one is closer to the actual result, how the accurate degree of simulation result is, how it can improve the final if introducing the observed HTC into simulation.

Therefore, in this chapter the experiments for observing frozen layer and measuring crystallinity and density of plastic part were achieved. The experimental results were compared with the simulation results for verifying creditability and precision of simulation using the observed HTC.

5.1 Influence of HTC on frozen layer

In vision field of microscope, wall layer, shearing layer and core layer on cross-section of plastic component can be observed apparently [Ngu11]. Due to fast cooling rate on plastic component surface, the wall layer, which is frozen layer during injection, has an extremely low degree of crystallization and different refraction capability. The thickness of wall layer locates in the range between 5 and 50 μm .

Frozen layer with dimensional value under different surface roughness and melt temperature was observed. The location of the thin slice for observing is in the range between gray lines, which is the middle part of the component. The thin slice was cut by a microtome along the direction of black lines, and the thickness of slice is 15 μm , as shown in Fig.5.1.

The microscopic photographs are shown in Fig.5.2, which are taken by polarization microscope OLYMPUS BX51.

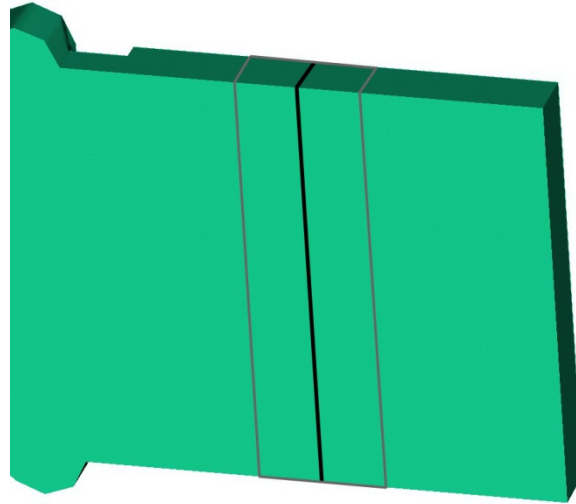
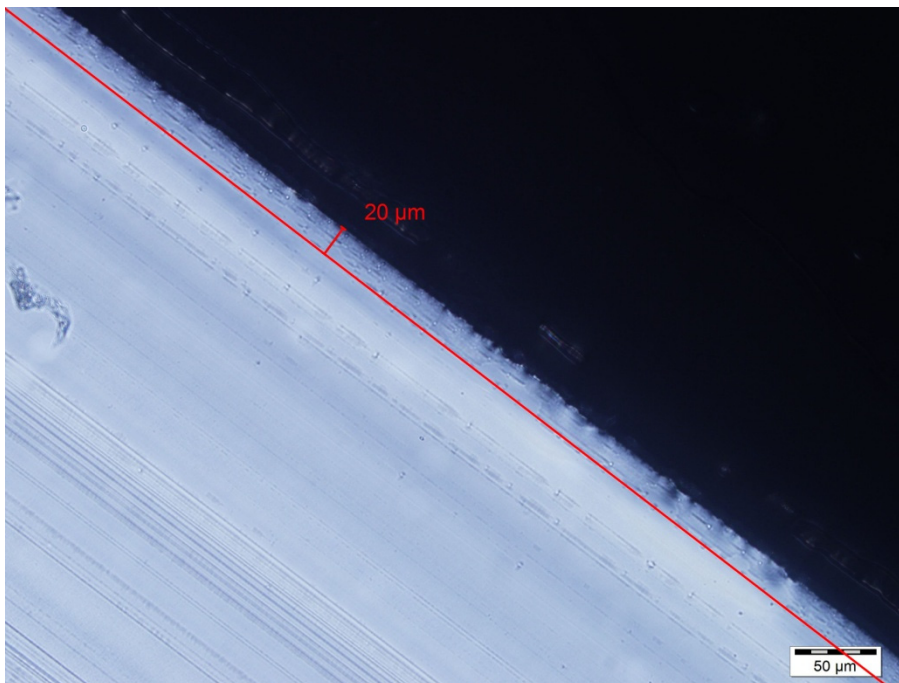
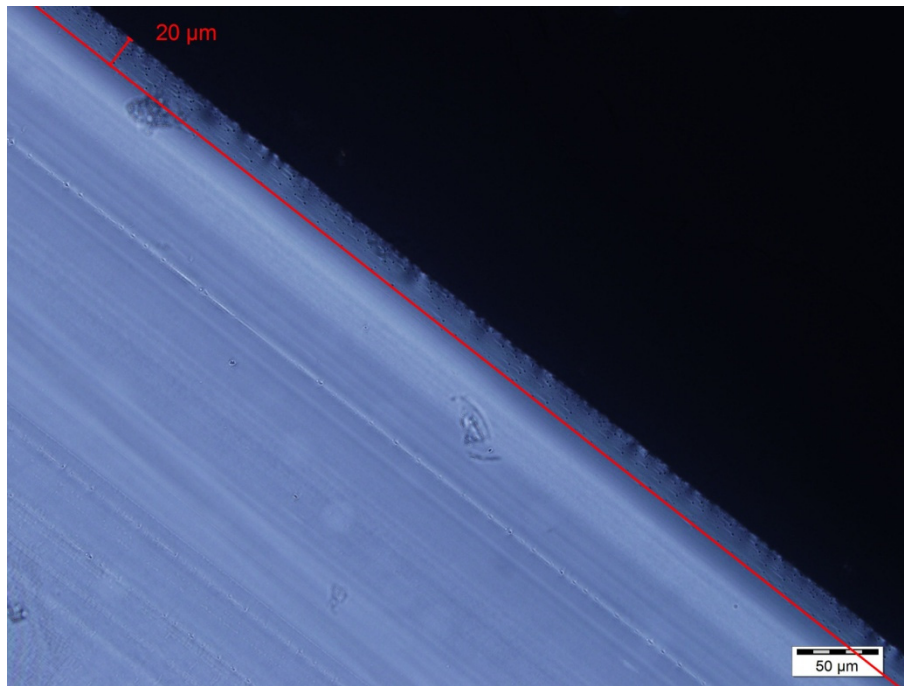


Fig. 5.1 Schematic of thin slice position used in frozen layer observation, which is in the range between gray lines and along the direction of black lines

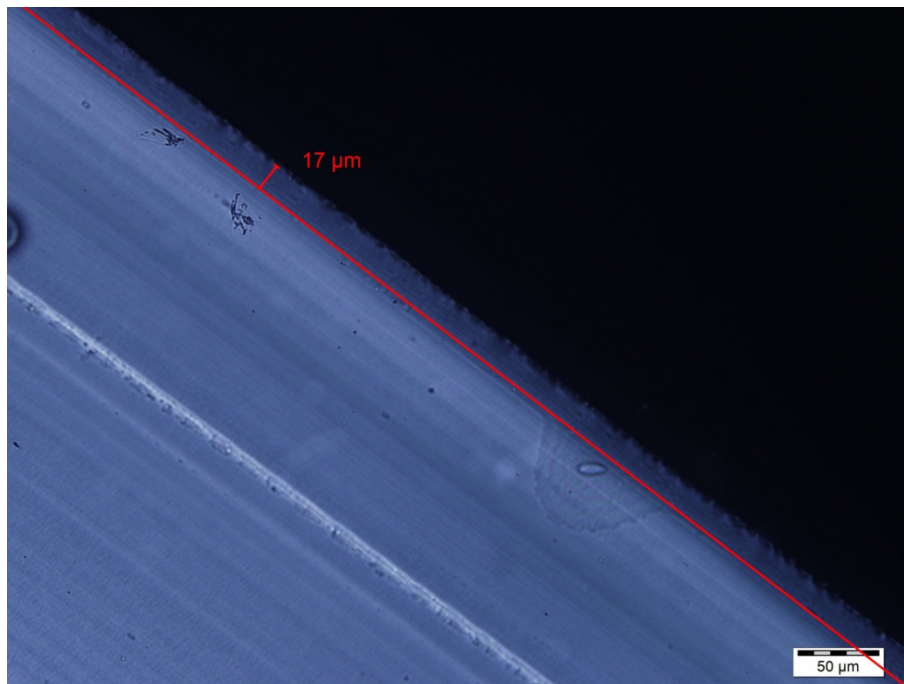
It can be seen from Fig.5.2 that under surface roughness is $0.01\mu\text{m}$, the thickness of wall layers are 20 , 20 and $17\mu\text{m}$, which corresponding to melt temperature 200 , 230 and 260°C respectively. Under melt temperature 200°C , the thickness of wall layers are 20 , 21 and $27\mu\text{m}$, which corresponding to surface roughness 0.01 , 1.36 and $5.81\mu\text{m}$ respectively.



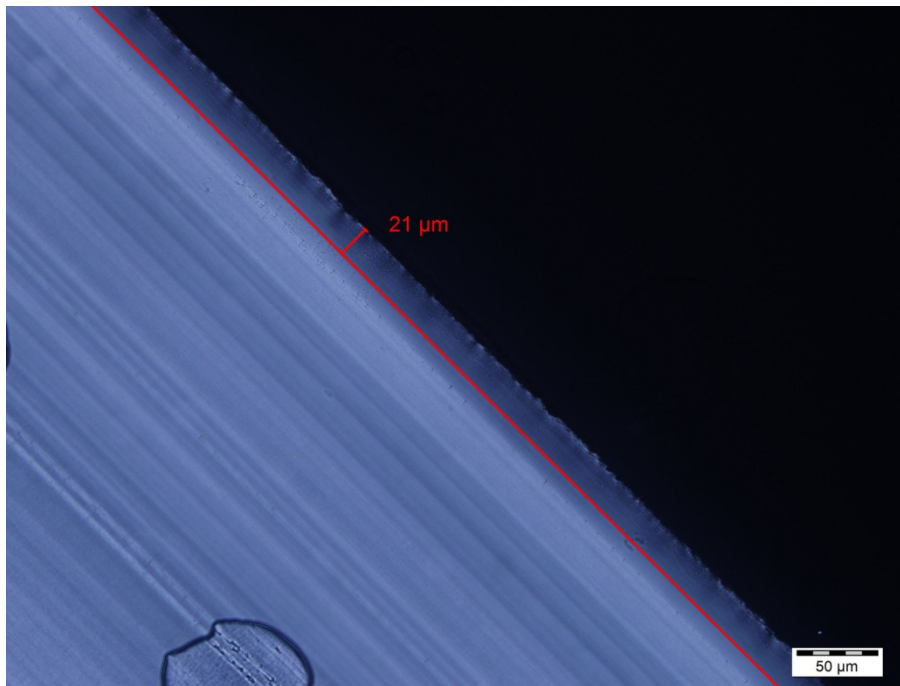
(a) Melt temperature 200°C , Surface roughness R_a $0.01\mu\text{m}$.



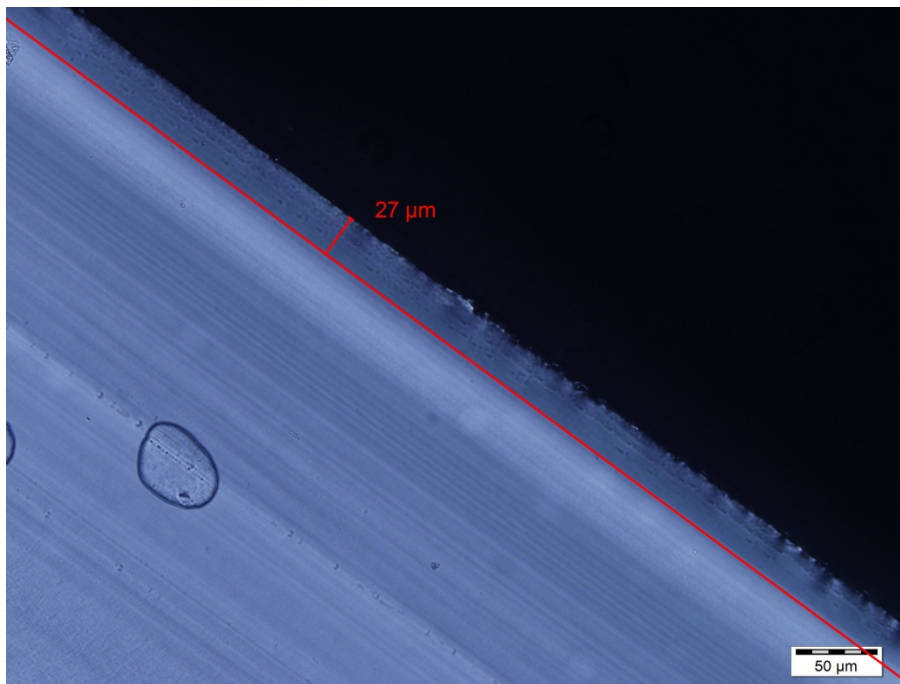
(b) Melt temperature 230°C, Surface roughness Ra 0.01μm.



(c) Melt temperature 260°C, Surface roughness Ra 0.01μm.



(d) Melt temperature 200°C, Surface roughness Ra 1.36μm.



(e) Melt temperature 200°C, Surface roughness Ra 5.81μm.

Fig. 5.2 Frozen layer morphology of plastic component under different surface roughness and melt temperature in vision field of microscope.

Without the statistical result based on a large number of experiments, accurate numerical relationship among wall layer thickness, surface roughness and melt temperature cannot be found out. However the tendency can be derived that wall layer thickness decreases with increasing melt temperature and increases with increasing value of surface roughness. Therefore the simulation result is conformance to the result observed by microscope.

5.2 Influence of HTC on part crystallinity

5.2.1 Crystallinity of part under different HTC

Before measuring the melting heat, the plastic component under different melt temperature and surface roughness of cavity wall were cut into thin slices by a microtome. The thickness of plastic component is 2mm, and the thin slices at the positions of 0, 0.5 and 1mm in thickness direction, shown as black lines in Fig.5.3, were selected for measuring, which means the positions of the surface, the core and the middle between them. The thickness of thin slices is 10 μ m and the other dimension is the same as that of studied object which is 15mm*15mm.

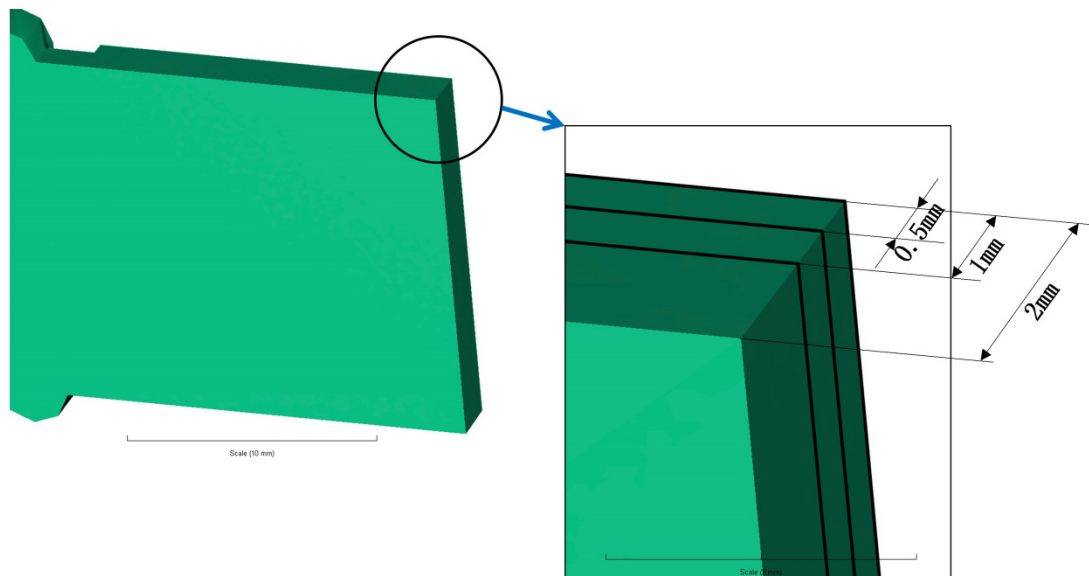


Fig. 5.3 Schematic of thin slice positions used for DSC measurement. The positions of thin slices are shown as black lines with dimension of 15mm*15mm*0.01mm.

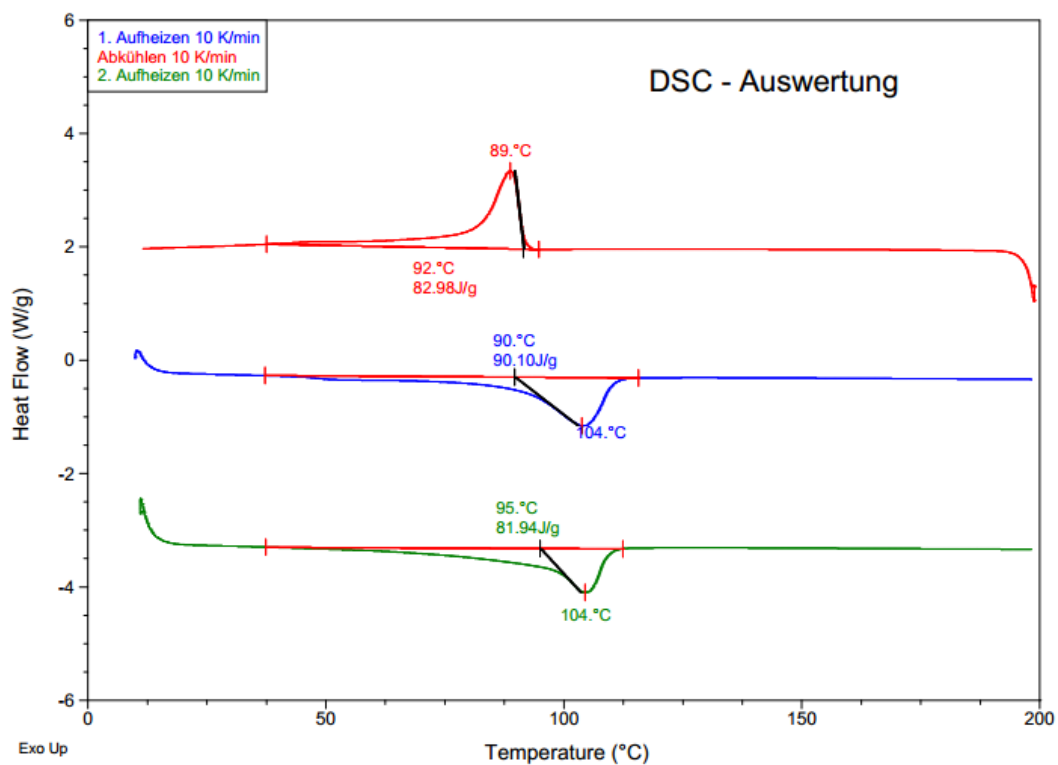
Differential scanning calorimetry (DSC) is a technique which measures heat flow into or out of a material as a function of time or temperature. Polymer crystallinity can be determined with DSC by measuring the heat associated with melting of the polymer. Crystallinity can be calculated by the ratio between this heat and the heat of melting for a 100% crystalline sample of the same material, shown as Eq. 5.1.

$$\%Crystallinity = \frac{\Delta Hm^{obs}}{\Delta Hm^{\circ}} \times 100\% \quad (5.1)$$

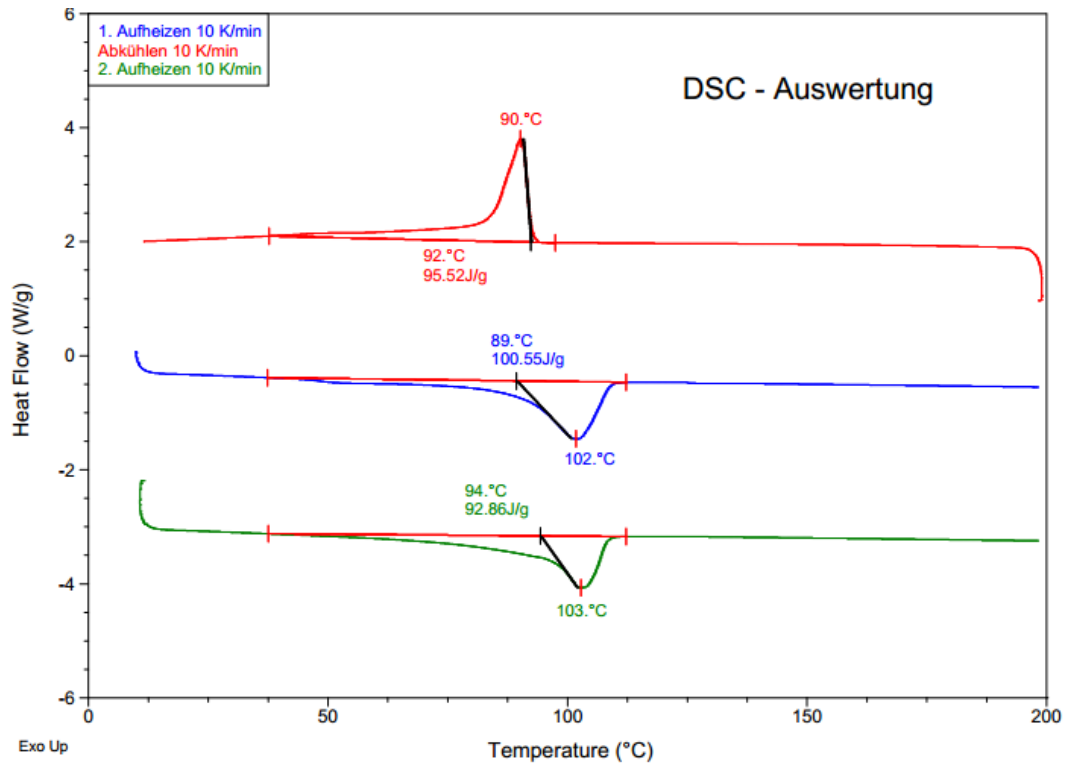
where ΔHm^{obs} is observed heat of melting and ΔHm° is a reference value and represents the heat of melting if the polymer is 100% crystalline.

DSC Q2000, from TA Instruments, was used for acquiring crystallinity ratio of components under various processing conditions. The measuring temperature range of Q2000 is from ambient to 998K, temperature accuracy is $\pm 0.1K$, temperature precision is $\pm 0.01K$, calorimetric precision is $\pm 0.05\%$ and sensitivity is $0.2\mu W$.

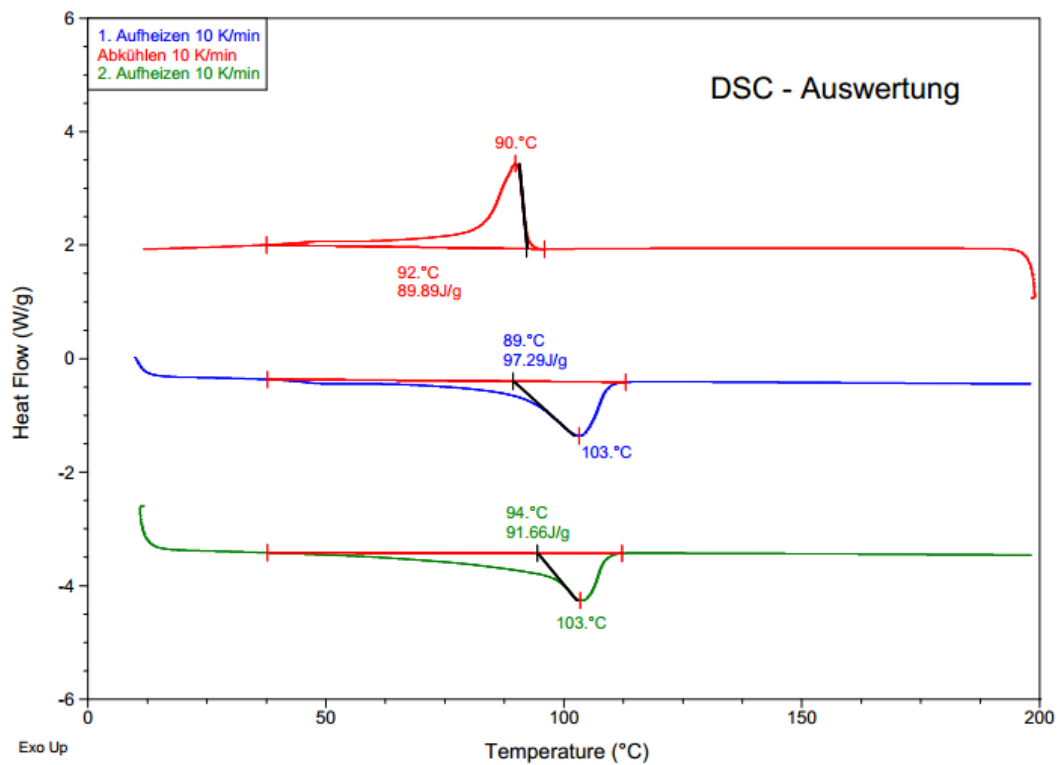
Partial DSC measurement results are shown in Fig.5.4 and 5.5.



(a) Surface roughness Ra 0.01 μm

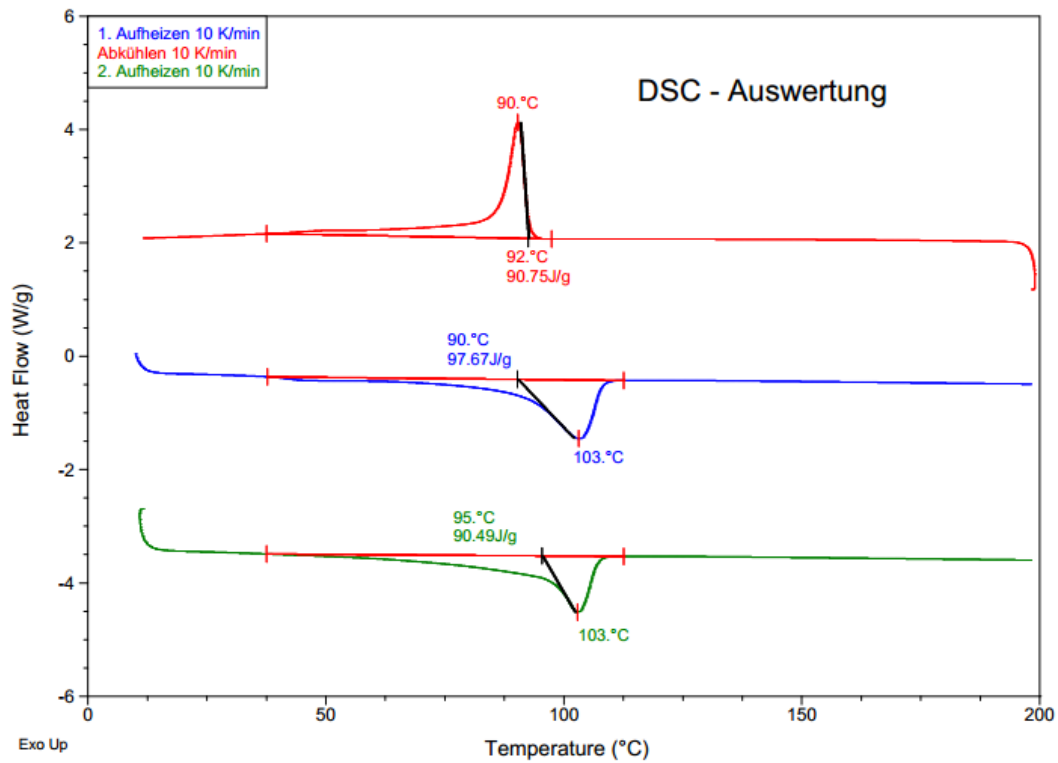


(b) Surface roughness Ra 1.36 μm

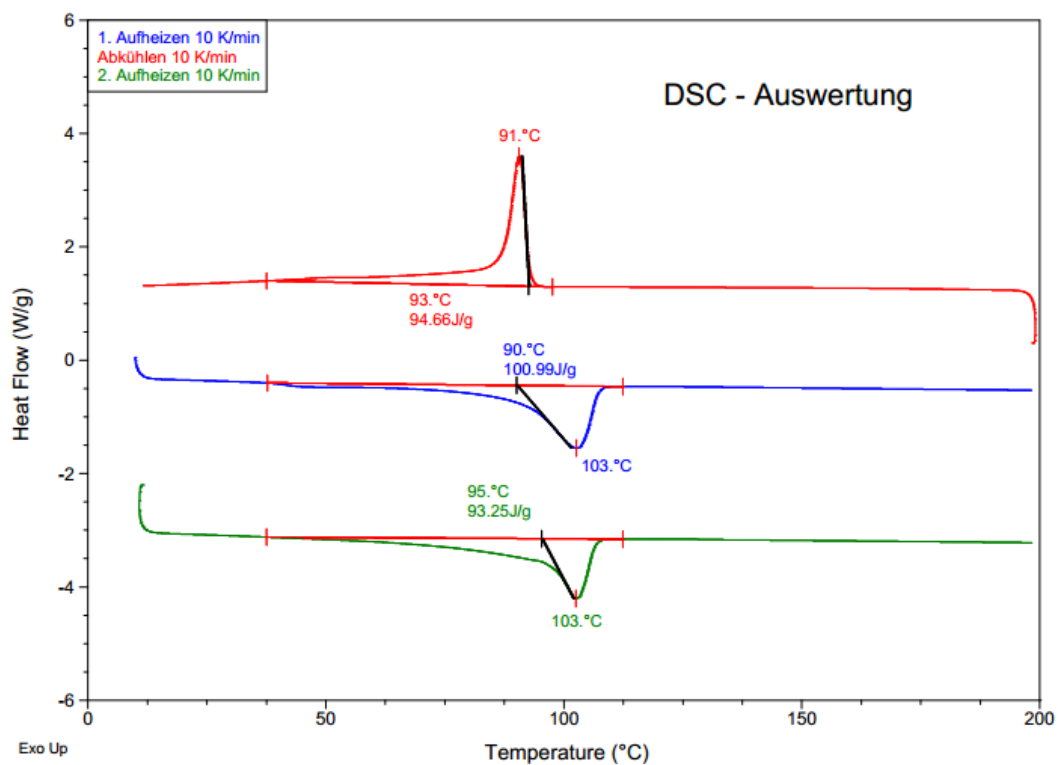


(c) Surface roughness Ra 5.81 μm

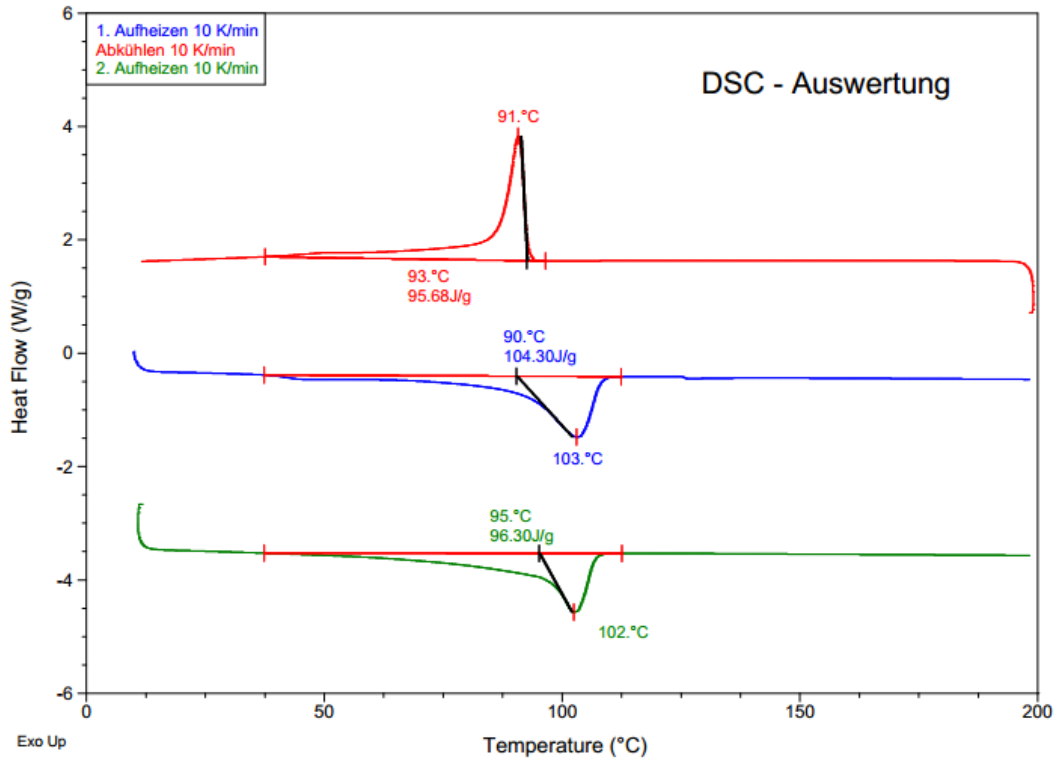
Fig.5.4 DSC measurement result under different surface roughness, melt temperature 260°C, sample layer 0mm



(a) Melt temperature 200°C



(b) Melt temperature 230°C



(c) Melt temperature 260°C

Fig.5.5 DSC measurement result under different melt temperature, surface roughness Ra 5.81μm, sample layer 0.5mm

After acquiring the part crystallinity, the value was turned into the form of relative crystallinity using Eq. 4.14, for the convenience to compare with simulated result.

Due to the relative crystallinity on different depth is scattering and the variation rule on different depth is not clear enough, the average value of relative crystallinity among different depth was calculated and the result under various melt temperature and surface roughness was shown in Fig. 5.6.

It can be seen from Fig. 5.6 that when the melt temperature is 200°C and surface roughness is 5.81μm, relative crystallinity reaches the lowest value of 55.79%. When the melt temperature is 260°C and surface roughness is 0.01μm, relative crystallinity reaches the highest value of 58.27%. And no matter what melt temperature is, relative crystallinity decreases with increasing value of surface roughness. And when the surface roughnesses are 1.36 and 5.81μm, the relative crystallinity rises with increasing melt temperature. However when the surface roughness are 0.01μm the value of relative crystallinity has a fluctuation with increasing melt temperature.

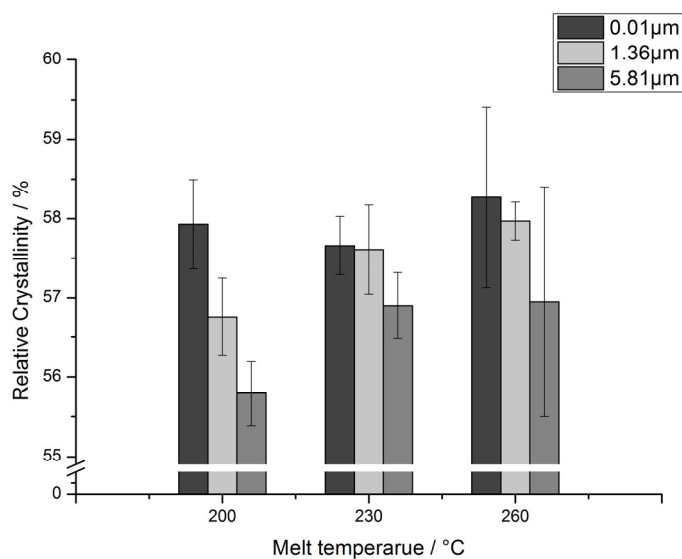


Fig. 5.6 Average value of measured relative crystallinity at different layers, under different melt temperature and surface roughness.

For showing more explicit variation trend of measured relative crystallinity with increasing melt temperature or increasing value of surface roughness, the average value of relative crystallinities at a certain melt temperature or a certain value of surface roughness were calculated based on the result in Fig. 5.6 and shown in Fig. 5.7 and 5.8.

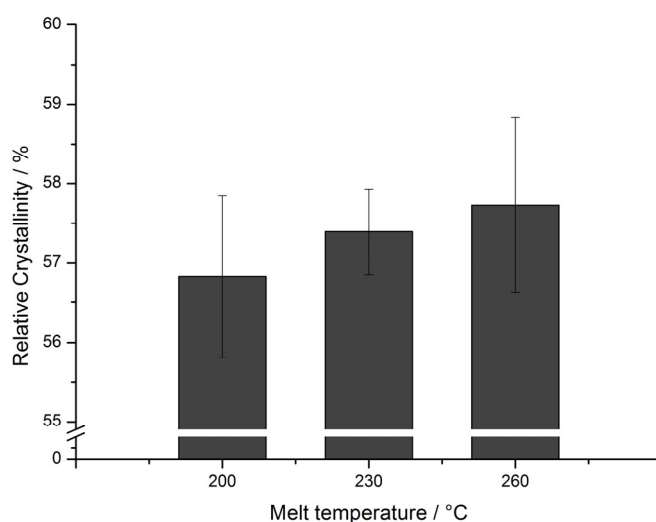


Fig. 5.7 Relation between melt temperature and average value of measured relative crystallinity at different surface roughness.

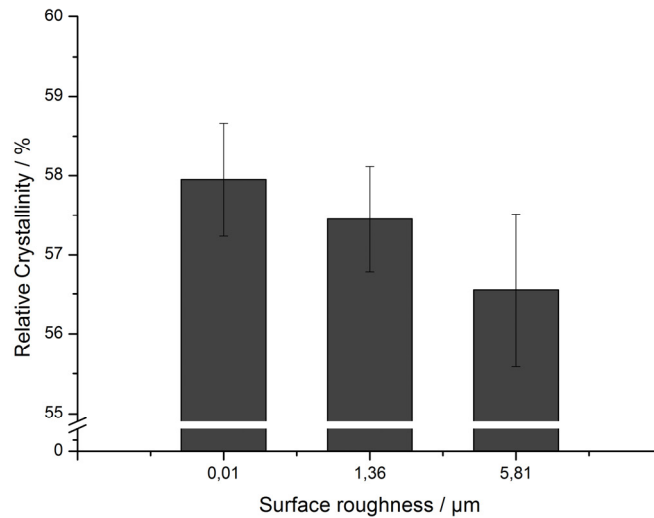


Fig. 5.8 Relation between surface roughness and average value of measured relative crystallinity at different melt temperature.

The variation tendency of relative crystallinity was quite clear which can be seen in Fig. 5.7 and 5.8. It rises with increasing melt temperature and falls with increasing value of surface roughness.

The reason is that although higher melt temperature causes a higher value of HTC and corresponding smaller thermal resistance, but mold temperature was raised when achieving thermal equilibrium. Therefore when the polymer temperature drops through the scope around crystalline temperature, the cooling rate is lower than that under other situation. So it acquires higher relative crystallinity. Moreover higher value of surface roughness provides a better contact situation between polymer and cavity wall which means a faster cooling rate, which can be seen in Fig. 3.12. So the relative crystallinity decreases correspondingly.

5.2.2 Comparison with crystallinity simulation

Under the situation when the surface roughness of cavity wall is $1.36\mu\text{m}$, the relative crystallinities measured by DSC, calculated with observed HTC and calculated with preset HTC are compared with each other as shown in Fig. 5.9, in which they are represented by the bars named “Measured, DSC”, “Simulated, observed HTC” and “Simulated, preset HTC”.

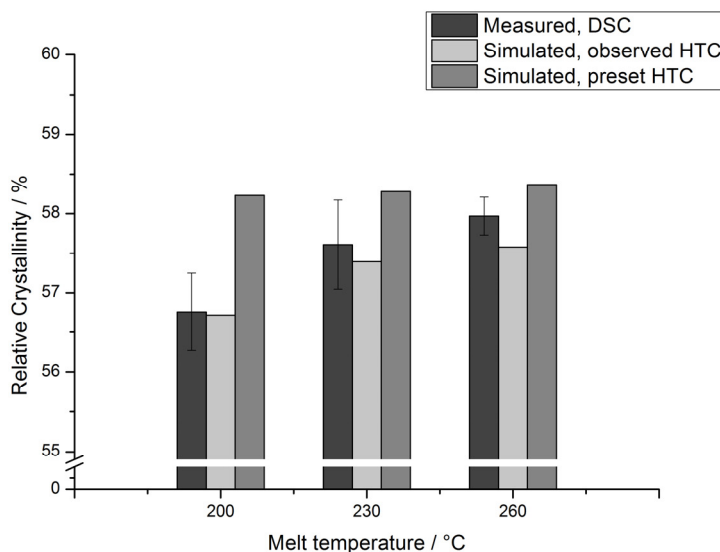


Fig. 5.9 Measured and simulated relative crystallinity calculated with HTC of preset value and observed value, under different melt temperature, surface roughness 1.36 μm .

It can be seen from Fig. 5.9 that no matter how the relative crystallinity acquires, it shows the same increasing tendency with increasing melt temperature. The value calculated with preset HTC is always higher than the others and has a less increasing variation for the observed value of HTC and also the value in reality are much higher than the default HTC in software. And the observed value of HTC instead of constant value can represent the actual heat transfer situation on the interface between polymer and cavity wall including the change which be brought by changing melt temperature.

The error between measured and simulated crystallinity under the situation when the surface roughness of cavity wall is 1.36 μm is shown in table 5.1, in which the measured crystallinity is regarded as the criteria. The error is positive means simulated value is bigger than measured value, and the negative error means the opposite condition.

From Table 5.1 it can be acquired that the error between simulated crystallinity calculated with observed HTC and measured crystallinity is always smaller than the error between simulated crystallinity calculated with preset HTC and measured crystallinity. In another word, the result of crystallinity simulation can be improved by using the value obtained in the process of HTC evaluation and it shows a preferable coincidence with the value measured practically.

Table 5.1 Error between simulated and measured crystallinity, surface roughness 1.36 μm .

| Calculating Errors / % | Melt temperature / °C | | |
|---|-----------------------|-------|-------|
| | 200 | 230 | 260 |
| Simulated, observed HTC – Measured, DSC | -0.07 | -0.38 | -0.67 |
| Simulated, preset HTC – Measured, DSC | 2.59 | 1.16 | 0.69 |

Under the situation when the melt temperature is 230°C, the relative crystallinities measured by DSC, calculated with observed HTC and calculated with preset HTC are compared with each other as shown in Fig. 5.10.

In Fig. 5.10 simulated crystallinity calculated with preset HTC is still higher than the others and it maintains at the same value in despite of varied surface roughness, due to no option can be altered for representing the different situation of surface roughness. But instead of that, simulated crystallinity calculated with observed HTC is highly dynamic changing with the value of surface roughness, which is the same to measured crystallinity.

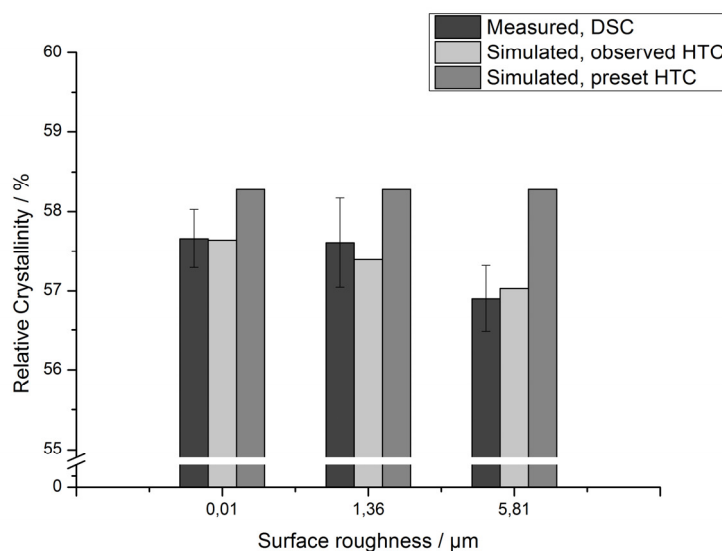


Fig. 5.10 Measured and simulated relative crystallinity calculated with HTC of preset value and observed value, under different surface roughness, melt temperature 230°C.

The error between measured and simulated crystallinity under the situation when the melt temperature is 230°C is shown in table 5.2 and in this table the measured crystallinity is also regarded as the criteria.

Table 5.2 Error between simulated and measured crystallinity, melt temperature 230°C.

| Calculating Errors / % | Surface roughness / μm | | |
|---|-----------------------------------|-------|------|
| | 0.01 | 1.36 | 5.81 |
| Simulated, observed HTC – Measured, DSC | -0.03 | -0.38 | 0.23 |
| Simulated, preset HTC – Measured, DSC | 1.08 | 1.16 | 2.43 |

From Table 5.2 it can be obtained a similar conclusion as the one from Table. 5.1. The simulated crystallinity calculated with observed HTC is closer to the result directly from DSC measurement. It is based on more accurate description of heat transfer situation during injection molding and cooling process of plastic component. Therefore it can receive a closer outcome to the reality comparing the simulated result calculated with preset HTC. At the same time, the creditability and accuracy of HTC evaluation and the improvement of corresponding injection molding were verified.

5.3 Influence of HTC on part density

5.3.1 Part density under different HTC

For measuring the density of plastic component, the density determination kit MC BA 100, Sartorius AG, was applied in the experiment, which is shown in Fig. 5.11.

The readability of measurement is 0.1mg, the repeatability is smaller than $\pm 0.1\text{mg}$ and the linearity is smaller than $\pm 0.2\text{mg}$. Ethanol was used as the referential fluid in this experiment.



Fig. 5.11 Sartorius MC BA 100

The density measurement of four samples under same processing parameter combination was carried out and average density value was calculated subsequently. The result is shown in Fig. 5.12.

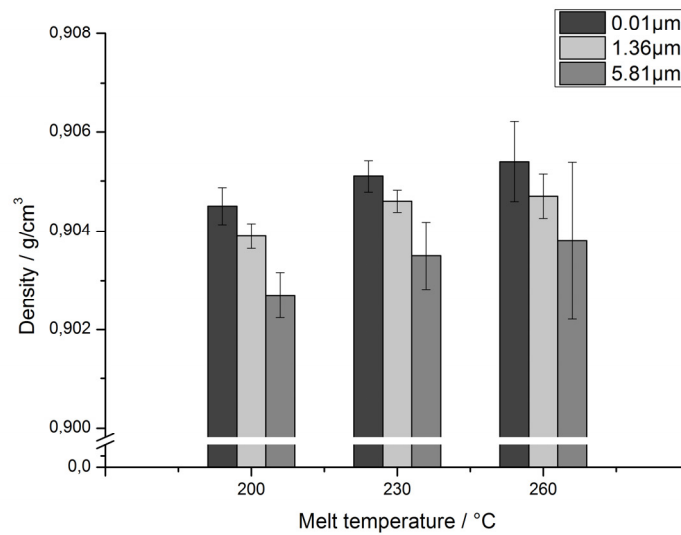


Fig. 5.12 Measured density value under different melt temperature and surface roughness.

It can be seen from Fig. 5.12 that no matter what the melt temperature is, the density decreases with increasing value of surface roughness. Moreover no matter what the surface roughness is, the density rises with increasing melt temperature. When the melt temperature is 200°C and

surface roughness is $5.81\mu\text{m}$, density reaches the lowest value 0.9027g/cm^3 . And when the melt temperature is 260°C and surface roughness is $0.01\mu\text{m}$, density reaches the highest value 0.9054g/cm^3 .

The average value of density was calculated under a certain melt temperature and a certain surface roughness and shown in Fig. 5.13 and 5.14.

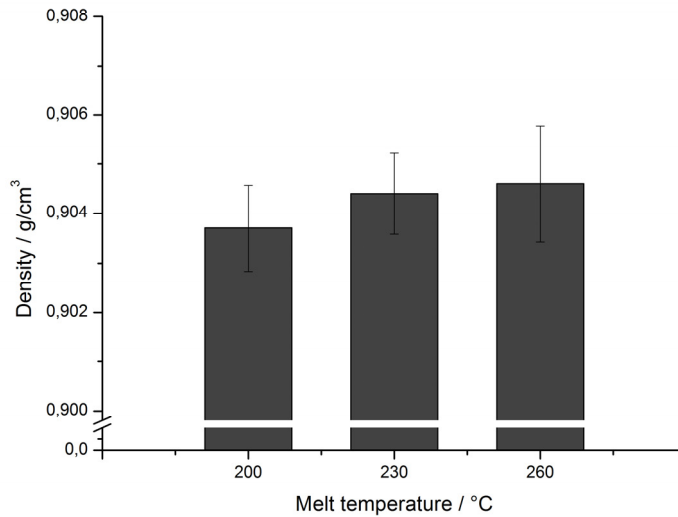


Fig. 5.13 Relation between average measured part density and melt temperature.

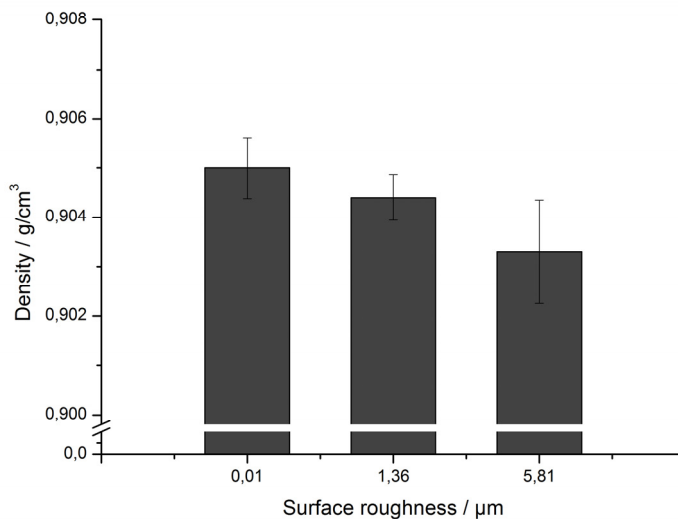


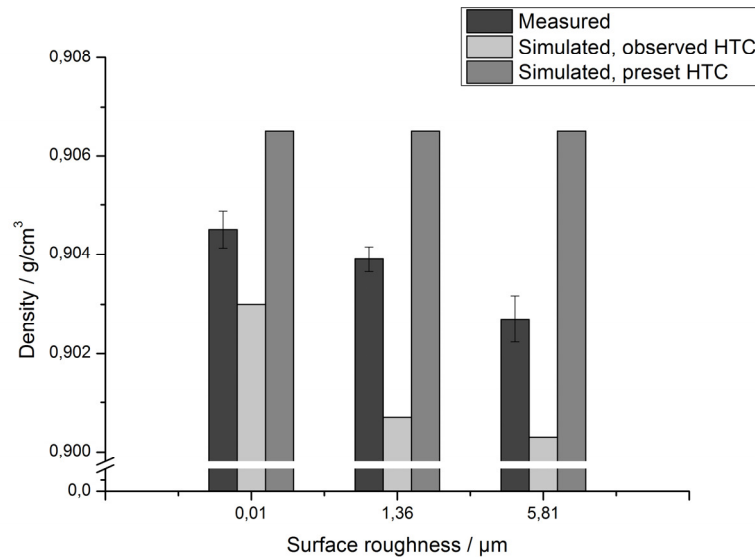
Fig. 5.14 Relation between average measured part density and surface roughness.

The variation trend is quite clear in Fig. 5.13 and 5.14 that density rises with increasing melt temperature and decreases with increasing value of surface roughness. The reason related to the density variation of plastic component from injection molding is complex. The melt temperature, mold temperature, polymer crystalline and packing pressure interact with each other and influence the final value of density. However polymer crystallization plays a relatively dominant role in density variation. Higher crystallinity leads to compact structure of polymer and higher value of density. Although melt temperature increases from 200 to 260°C and the shrinkage of polymer grows, it shows increasing tendency in density variation.

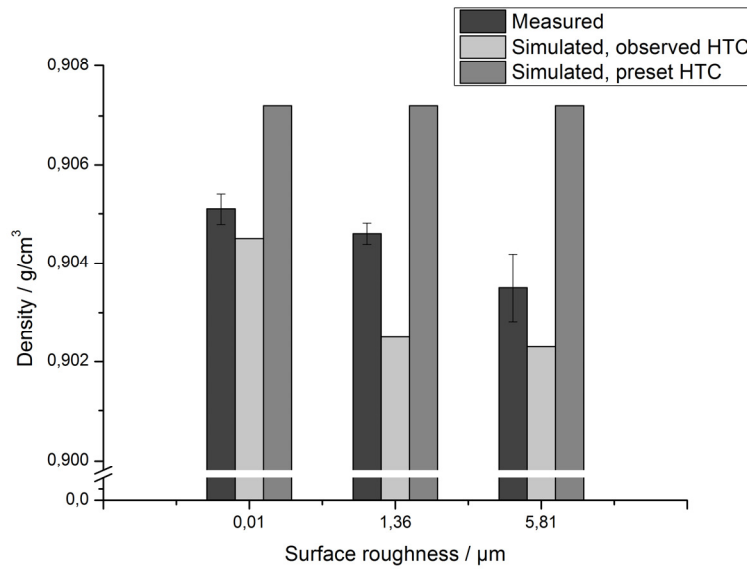
5.3.2 Comparison with the part density simulation

The part density measured by Sartorius MC BA 100, calculated with observed HTC and calculated with preset HTC are compared with each other at a certain melt temperature as shown in Fig. 5.15, in which they are represented by the bars named “Measured”, “Simulated, observed HTC” and “Simulated, preset HTC”.

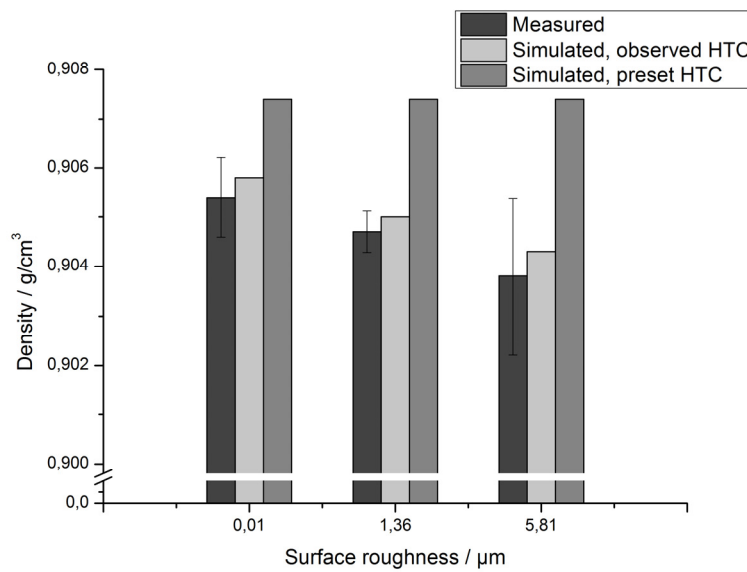
It can be seen from Fig. 5.15 that due to the constant value of preset HTC in software, which is a relatively low value, the part density calculated with preset HTC is kept on the same value at a certain melt temperature, even with changing value of surface roughness, and this value is always higher than the others.



(a) Melt temperature 200°C.



(b) Melt temperature 230°C.



(c) Melt temperature 260°C.

Fig. 5.15 Measured and simulated part density calculated with HTC of preset value and observed value, under different surface roughness and certain melt temperature.

The error between measured and simulated part density is shown in table 5.3, in which the measured density is regarded as the criteria. Positive error means simulated value is bigger than measured value, and the negative error means the opposite condition.

Table 5.3 Error between simulated and measured part density.

| Calculating Errors / % | | | Surface roughness / μm | | |
|---|-----|---|-----------------------------------|-------|-------|
| | | | 0.01 | 1.36 | 5.81 |
| Melt temperature / $^{\circ}\text{C}$ | 200 | Simulated, ob. ¹ – Measured | -0.18 | -0.35 | -0.27 |
| | | Simulated, pre. ² – Measured | 0.22 | 0.28 | 0.42 |
| | 230 | Simulated, ob. – Measured | -0.07 | -0.23 | -0.13 |
| | | Simulated, pre. – Measured | 0.23 | 0.28 | 0.41 |
| | 260 | Simulated, ob. – Measured | 0.04 | 0.03 | 0.06 |
| | | Simulated, pre. – Measured | 0.22 | 0.30 | 0.40 |

¹ ob. is short for observed HTC, ² pre. is short for preset HTC.

Table 5.3 shows that the error value of part density varies in a quite small range, from -0.35 to 0.42%, which means simulation with both of observed and preset HTC can predict the density accurately. And the optimization effect caused by introducing observed HTC into density simulation is relatively limited. However through result analysis, it is found that the error between simulated density calculated with observed HTC and measured density is a little smaller than the error between simulated density calculated with preset HTC and measured density in most cases. Therefore the comparison result shows that introducing observed HTC into density simulation can partly improve the accuracy of the result of that and normally has no practical application value. But in some occasions which require precise density prediction the method has its distinct importance.

5.4 Summary of Chapter

In this chapter, the microscopic photographs of frozen layer under different melt temperature and surface roughness were presented. The relative crystallinity and part density were measured and compared with the simulated value calculated with observed and preset HTC. The error between simulated result calculated with observed HTC and measured result and the

error between simulated result calculated with preset HTC and measured result were obtained subsequently.

The simulated results calculated with both observed and preset HTC have the same variation trend to that of measured value. The error between simulated result calculated with observed HTC and measured result is always smaller than the error between simulated result calculated with preset HTC and measured result, especially for the relative crystallinity.

Consequently the creditability and accuracy of the method by introducing observed HTC into injection molding were verified. And it was also validated that this method can make simulation result approaching to actual one and it can improve the accuracy of injection simulation. In addition, HTC value under different surface roughness can stand for the surface and corresponding heat transferring situation in reality and leads to individual and accurate simulation result instead of a certain HTC value used for all kinds of surface situation.

6. Summary

6.1 Conclusions

Injection molding plays a very important role in the manufacture field of automobile, household appliance, electronic product, industrial equipment etc. Nowadays it is expanding the application field to the ever-growing production of polymer-based composites. Heat transfer is one of critical physical processes during injection molding and the heat transfer between polymer and cavity wall has its own characteristic and complexity, which depends on various processing conditions and is time dependent.

This thesis focused on the heat transfer phenomenon between polymer and cavity wall and accomplished the following works.

- a. Based on injection molding condition heat transfer process, especially the process on the interface between polymer and cavity wall was theoretically studied. The influence factors of heat transfer process were located;
- b. According to the fundamental theory of heat transfer, the equation which can calculate actual heat transfer coefficient (HTC) was derived. Subsequently an injection mold, including temperature measurement system, was designed and prepared specially for acquisition of temperature and calculation of HTC. Meanwhile correspondingly experimental plan was formulated;
- c. The actual HTC value was obtained based on the real temperature of mold and melt under different conditions. The relationship among HTC, melt temperature and injection rate was figured out and above all the influence of surface roughness on HTC was investigated for the first time;
- d. The injection molding simulation by FEM was carried out, which utilized observed and preset HTC value. After that the frozen volume percentage, relative crystallinity and part density calculated with observed and preset HTC were obtained;
- e. The experiments for verifying simulation results were accomplished and the variation tendency and specific value of relative crystallinity and part density were obtained;
- f. The comparison among measured result, simulated result with observed HTC value and

simulated result with preset HTC value was performed.

Based on the accomplished work above, the research conclusions were shown as follows.

- a. HTC between polymer and cavity wall is only decided by the contact area between them. The value of HTC increases with increasing values of melt temperature and surface roughness dramatically. Injection rate has little influence on HTC value;
- b. A physical model which can describe the thermal contact condition, considering the air gap between polymer and cavity wall was presented. And the model can explain experimental phenomenon and fits experimental result perfectly;
- c. The simulation result calculated with observed HTC shows distinct difference from the result calculated with preset HTC. Normally it has higher cooling rate which leads to lower crystalline level and density correspondingly;
- d. Observed HTC can represent different surface roughness conditions instead of preset HTC in injection molding simulation and reach a more precise simulation result;
- e. The comparison among measured result, simulated result with observed HTC value and simulated result with preset HTC value can verify the reliability and precision of simulation with observed HTC. And it can also show the improvement of simulation result.

Through this work, it cannot only provide deep comprehending of heat transfer between polymer and cavity wall but also offer a variation regulation of HTC. It also shows the importance of utilizing observed HTC in injection molding, especially in the situation which requires result with high precision which must be beneficial for cooling and relevant analysis and improve the prediction various mechanical properties of plastic component, cycle time of injection molding and optimization of processing technology and parameters. In addition, it provides a substituting method for representing surface roughness of cavity wall in injection molding simulation.

6.2 Future works

Although a number of works were accomplished, there are some relevant fields needed to be explored and studied.

- a. Due to the complexity and highly dynamic characteristic of melt temperature measurement,

the temperature integral was used in this work instead of dynamic temperature. It is possible to acquire the average value of HTC in filling, packing and cooling stage respectively. However HTC is a kind of physical quantity dependent on time, so in next step accurate measurement of highly dynamic melt temperature is the first difficulty which should be overcome. Subsequently it is possible to cooperate with software company and achieve the secondary development for calculating with a function of time instead of a single value of HTC, which can improve the simulation result further;

- b. For some kinds of polymer whose flowability is relative poor, cooling rate plays an important role in cavity filling. Appropriate melt temperature and surface roughness of cavity wall can reduce the rate of flowability decreasing and be beneficial to receive plastic in high quality. So in next step, HTC evaluation and short-shot injection experiment with these kinds of polymer can be performed;
- c. Simulation parameter of Lupolen 1800S in Moldflow database is not very complete, which has only generic pVT data. That may cause inaccurate simulation result. Therefore, testing and fitting of pVT property should be considered and accomplished for reaching a more credible result from simulation;
- d. The simulation in micro scope was not carried out in this work due to the complexity of polymer properties and random surface condition. In future, it can be studied and accomplished with other software for comprehending the heat transfer process during injection molding more deeply.

7. Literature

- [Abe12] Abeykoon, C.; Martin, P. J.; Kelly, A. L.; etc.: *A review and evaluation of melt temperature sensors for polymer extrusion*. Sensors and Actuators A 182(2012), pp. 16–27.
- [Ame07] Amesöder, S.; Heinle, C.; Ehrenstein, G. W.: *Injection moulding of thermally conducting polymers for mechatronic applications*. The Polymer Processing Society 23rd Annual Meeting, Salvador, 2007.
- [And04] Andersen, B.: *Investigations on environmental stress cracking resistance of LDPE/EVA blends*. Doktorarbeit, Martin-Luther-Universität Halle-Wittenberg 2004.
- [Au07] Au, K. M.; Yu, K. M.: *A scaffolding architecture for conformal cooling design in rapid plastic injection moulding*. The International Journal of Advanced Manufacturing Technology 34(2007) 5-6, pp. 496–515.
- [Bai06] Bai, Y.; Yin, B.; Fu, X.; etc.: *Heat transfer in injection molding of crystalline plastics*. Journal of Applied Polymer Science 102(2006) 5, pp. 2249–2253.
- [Ban08] Bank, D.; Klafhen, D.; Smierciak, R.: *Why plastic flows better in aluminum injection molds*. Plastics Technology 54(2008) 9, pp. 41–47.
- [Bei07] Beilharz, F.; Kouba, K.; Blokland, H.; etc.: *Experimental investigation of friction, thermal conductivity and heat transfer and their mathematical description for the thermoforming process simulation*. Polymer Processing Society Regional Meeting, Gothenburg, 2007.
- [Ben98] Bentley, R. E.: *Handbook of temperature measurement: Volume 1, Temperature and Humidity*. Springer, Singapore 1998.
- [Ben04] Bendada, A.; Derdouri, A.; Lamontagne, M.; etc.: *Analysis of thermal contact resistance between polymer and mold in injection molding*. Applied Thermal Engineering 24(2004) 14-15, pp. 2029–2040.
- [Bru06] Brunotte, R.: *Die thermodynamischen und verfahrenstechnischen Abläufe der in-situ-Oberflächenmodifizierung beim Spritzgießen*. Doktorarbeit, Technische Universität Chemnitz 2006.
- [Bud10] Budzier, H.; Gerlach, G.: *Thermal Infrared Sensors: Theory, Optimisation and Practice*. Wiley, Weinheim 2010.
- [Bur04] Bur, A. J.; Roth, S. C.: *Temperature gradients in the channels of a single-screw extruder*. Polymer Engineering and Science 44(2004) 11, pp. 2148–2157.

- [Cha01] Chang, R. Y.; Yang, W. H.: A Numerical simulation of mold filling in injection molding using a three-dimensional finite volume approach. *Journal of Non-Newtonian Fluid Mechanics* 37(2001) 2, pp. 125–148.
- [Che07] Chen, S. C.; Wang, L. C.; Chiou, Y. C., etc.: *An investigation on the temperature behavior in mold embedded with heater*. ANTEC, Cincinnati, 2007.
- [Che10] Chen, S. C.; Li, H. M.; Huang, S. T.; etc.: *Effect of decoration film on mold surface temperature during in-mold decoration injection molding process*. *International Communications in Heat and Mass Transfer* 37(2010) 5, pp. 501–505.
- [Che11] Chen, S. C.; Minh, P. S.; Chang, J. A.: *Gas-assisted mold temperature control for improving the quality of injection molded parts with fiber additives*. *International Communications in Heat and Mass Transfer* 38(2011) 3, pp. 304–312.
- [Che12] Chen, S. C.; Liao, W. H.; Yeh, J. P.; etc.: *Rheological behavior of PS polymer melt under ultra-high speed injection molding*. *Polymer Testing* 31(2012) 7, pp. 864–869.
- [Cro04] Croce, G; Agaro, P. D.: *Numerical analysis of roughness effect on microtube heat transfer*. *Superlattices and Microstructures* 35(2004) 3-6. pp. 601–616.
- [Daw06] Dawson, A; Rides, M.; Nottay, J.: *The effect of pressure on the thermal conductivity of polymer melts*. *Polymer Testing* 25(2006) 2, pp. 268–275.
- [Daw08] Dawson, A.; Rides, M.; Allen, C. R. D.; etc.: *Polymer–mould interface heat transfer coefficient measurements for polymer processing*. *Polymer Testing* 27(2008) 5, pp. 555–565.
- [Dea13] Dealy, J. M.; Wang, J.: *Melt rheology and its applications in the plastics industry*. Springer, Dordrecht 2013.
- [Del00] Delaunay, D.; Bot, P. L.; Fulchiron, R.; etc.: *Nature of contact between polymer and mold in injection molding. Part I: Influence of a non-perfect thermal contact*. *Polymer Engineering & Science* 40(2000) 7, pp. 1682–1691.
- [Far05] Farouq, Y.; Nicolazo, C.; Sarda, A.; etc.: *Temperature measurements in the depth and at the surface of injected thermoplastic parts*. *Measurement* 38(2005) 1, pp. 1–14.
- [Ful01] Fuller, J. J.; Marotta, E. E.: *Thermal contact conductance of metal/polymer joints: an analytical and experimental investigation*. *Journal of Thermophysics and Heat Transfer* 15(2001) 2, pp. 228–238.
- [Gof05] Goff, R.; Poutot, G.; Delaunay, D.; etc.: *Study and modeling of heat transfer during the solidification of semi-crystalline polymers*. *International Journal of*

Heat and Mass Transfer 48(2005) 25-26, pp. 5417–5430.

- [Gof09] Goff, R. L.; Delaunay, D.; Boyard, N.; etc.: *On-line temperature measurements for polymer thermal conductivity estimation under injection molding conditions*. International Journal of Heat and Mass Transfer 52(2009) 5-6. pp. 1443–1450.
- [Gol08] Golebiewski, J.; Rozanski, A.; Dzwonkowski, J.; etc.: *Low density polyethylene-montmorillonite nanocomposites for film blowing*. Macromolecular Nanotechnology 44(2008) 2, pp. 270–286.
- [Gri06] Griffiths, C. A.; Dimov, S. S.; Pham, D. T.: *Micro injection moulding: the effects of tool surface finish on melt flow behavior*. 4M2006 Second International Conference on Multi-Material Micro Manufacture, Grenoble, 2006.
- [Gri07] Griffiths, C. A.; Dimov, S. S.; Brousseau, E. B.; etc.: *The effects of tool surface quality in micro-injection moulding*. Journal of Materials Processing Technology 189(2007) 1-3, pp. 418–427.
- [Hie80] Hieber, C. A.; Shen, S. F.: *A finite-element/finite-difference simulation of the injection-molding filling process*. Journal of Non-Newtonian Fluid Mechanics 7(1980) 1, pp. 1–32.
- [Hol10] Holman, J.: *Heat Transfer*. McGraw-Hill Press (10th Edition), Boston 2010.
- [Hu13] Hu, Wenbing.: *Polymer Physics: A Molecular Approach*. Springer, Vienna 2013.
- [Joh94] Johannaber, F.: *Injection molding machines: a user's guide*. Carl Hanser (4th Edition), Munich 1994.
- [Kam84] Kamal, M. R.; Lafleur, P. G.: *Heat transfer in injection molding of crystallizable polymers*. Polymer Engineering and Science 24(1984) 9, pp. 692–697.
- [Kan03] Kandlikar, S. G.; Joshi, S.; Tian, S. R.: *Effect of Surface Roughness on Heat Transfer and Fluid Flow Characteristics at Low Reynolds Numbers in Small Diameter Tubes*. Heat Transfer Engineering 24(2003) 3, pp. 4–16.
- [Kaz07] Kazmer, D.: *Injection molding design engineering*. Carl Hanser, Munich 2007.
- [Ken13] Kennedy, P.; Zheng, R.: *Flow Analysis of Injection Molds*. Carl Hanser, Munich 2013.
- [Kin73] Kinzie, P., A.: *Thermocouple temperature measurement*. John Wiley & Sons, New York 1973.
- [Kle04] Kleinstreuer, C.; Koo, J.: *Computational analysis of wall roughness effects for liquid flow in micro-conduits*. Journal of Fluids Engineering 126(2004) 1, pp. 1–9.
- [Kle09] Klein, Peter.: *Fundamentals of plastics thermoforming*. Morgan & Claypool, San

Rafael 2009.

- [Koo05] Koo, J.; Kleinstreuer, C.: *Analysis of surface roughness effects on heat transfer in micro-conduits*. International Journal of Heat and Mass Transfer 48(2005) 13, pp. 2625–2634.
- [Lau60] Lauritzen, J. I.; Hoffman, J. D.: *Theory of Formation of Polymer Crystals with Folded Chains in Dilute Solution*. Journal of Research of the National Bureau of Standards - A Physics and Chemistry 64(1960) 1, pp. 74–102.
- [Li94] Li, C.; Hung, C.; Shen Y.: *Computer Simulation and Analysis of Fountain Flow in Filling Process of Injection Molding*. Journal of Polymer Research 1(1994) 2, pp. 163–173.
- [Lin05] Lin, Y. W.; Li, H. M.; Chen, S. C.; etc.: *3D numerical simulation of transient temperature field for lens mold embedded with heaters*. International Communications in Heat and Mass Transfer 32(2005) 9, pp. 1221–1230.
- [Liu09] Liu, S. J.; Su, P. C.: *Novel three-dimensional in-cavity transient temperature measurements in injection molding and fluid-assisted injection molding*. Polymer Testing 28(2009) 1, pp. 66–74.
- [Liu13] Liu, Y.; Gehde, M.; Mennig, G.: *Heat Transfer during Injection Molding Process*. 23.Fachtagung TECHNOMER, Chemnitz, 2013.
- [Lös09] Löser, C.: *Thermo-rheologische Situation in einer Mikrokavität und deren Einfluss auf die Strukturbildung im Formteil*. Diplomarbeit, Technische Universität Chemnitz 2009.
- [Luc12] Lucchetta, M.; Fiorotto, M.; Bariani, P.F.: *Influence of rapid mold temperature variation on surface topography replication and appearance of injection-molded parts*. CIRP Annals – Manufacturing Technology 61(2012) 1, pp. 539–542.
- [Mad96] Madhusudana, C. V.: *Thermal Contact Conductance*. Springer, Berlin 1996.
- [Mal11] Malloy, R.: *Plastic part design for injection molding: an introduction*. Carl Hanser (2nd Edition), Munich 2011.
- [Mar07] Mark, J.: *Physical Properties of Polymers Handbook*. Springer (2nd Edition), New York 2007.
- [Mas04] Masse, H.; Arquís, E.; Delaunay, D.; etc.: *Heat transfer with mechanically driven thermal contact resistance at the polymer–mold interface in injection molding of polymers*. Applied Thermal Engineering 47(2004) 8-9, pp. 2015–2027.
- [Max10] Internet site <http://www.maximintegrated.com>, Maxim Integrated, 2010.
- [Men13] Mennig, G.; Stoeckhert, K.: *Mold-Making Handbook*. Carl Hanser (3rd Edition),

Munich 2013.

- [Mic91] Michalski, L.; Eckersdorf, K.; McGhee, J.: *Temperature measurement*. John Wiley & Sons, Chichester 1991.
- [Mic95] Michaeli, W.: *Plastic processing: an introduction*. Carl Hanser, Munich 1995.
- [Mo01] Mok, C. K.; Chin, K. S.; Ho, K. L.: *An interactive knowledge-based CAD system for mould design in injection moulding processes*. The International Journal of Advanced Manufacturing Technology 17(2001) 1, pp. 27–38.
- [Nag14] Nagel, J.; Pahner, F. A.; Zimmerer, C.; Härtig, T.; Gehde, M.; Heinrich, G. : *Electrostatic discharging behaviour of polycarbonate parts made by process-integrated surface modification*. Macromolecular Materials and Engineering doi: 10.1002/mame.201400114.
- [Nak03] Nakao, M.; Yoda, M.; Nagao, T.: *Locally controlling heat flux for preventing micrometer-order deformation with injection molding of miniature products*. CIRP Annals – Manufacturing Technology 52(2003) 1. pp. 451–454.
- [Nak08] Nakao, M.; Tsuchiya, K.; Sadamitsu, T.; etc.: *Heat transfer in injection molding for reproduction of sub-micron-sized features*. The International Journal of Advanced Manufacturing Technology 38(2008) 3-4, pp. 426–432.
- [Nar08] Naranjo, A.; Michaeli, W.; Lingk, O.: *Propagation of Crystallization Heat and other Observations during Injection Moulding of Semicrystalline Polymers*. Journal of Plastics Technology 2(2008), pp. 1–20.
- [Ngu08] Nguyen-Chung, T.; Jüttner, G.; Pham, T.; Mennig, G.; Gehde, M.: *Die Bedeutung präziser Randbedingungen für die Simulation des Mikrospritzgießens*. Zeitschrift Kunststofftechnik 4(2008) 6, pp.1–25.
- [Ngu10] Nguyen-Chung, T.; Jüttner, G.; Löser, C.; Pham, T.; Gehde, M.: *Determination of the heat transfer coefficient from short-shots studies and precise simulation of microinjection molding*. Polymer Engineering & Science 50(2010) 1, pp. 165–173.
- [Ngu11] Nguyen-Chung, T.; Löser, C.; Jüttner, G.; Obadal, M.; Pham, T.; Gehde, M.: *Analyse der Morphologie spritzgegossener Mikrobauteile*. Zeitschrift Kunststofftechnik 7(2011) 3, pp. 86–114.
- [Nic10] Nicolazo, C.; Sarda, A.; Vachot, P.; etc.: *Change on temperature at the surface of injection moulded parts*. Journal of Materials Processing Technology 210(2010) 2, pp. 233–237.
- [Ong09] Ong, N. S.; Zhang, H. L.; Lam, Y. C.: *Three-dimensional modeling of roughness effects on microthickness filling in injection mold cavity*. The International Journal

of Advanced Manufacturing Technology 45(2009) 5-6, pp. 481–489.

- [Oss06] Osswald, T.; Hernandez-Ortiz, J. P.: *Polymer Processing: modeling and simulation*. Carl Hanser, Munich 2006.
- [Otm11] Otmani, R. E.; Zinet, M.; Boutaous, M.; etc.: *Numerical simulation and thermal analysis of the filling stage in the injection molding process Role of the mold-polymer interface*. Journal of Applied Polymer Science 121(2011) 3, pp. 1579–1592.
- [Ots11] Otsuka, M.; Oyabe, A.; Ito, H.: *Effects of Mold Surface Conditions on Flow Length in Injection Molding Process*. Polymer Engineering & Science 51(2011) 7, pp.1383–1388.
- [Par97] Parihar, S. K.; Wright, N. T.: *Thermal contact resistance at elastomer to metal interfaces*. International Communications in Heat and Mass Transfer 24(1997) 8, pp. 1083–1092.
- [Pol91] Pollock, D. D.: *Thermocouples: theory and properties*. CRC Press, Boca Raton 1991.
- [Pol14] Internet site <http://polymers.lyondellbasell.com>, Lyondell Basell Polymers, 2014.
- [Pöt95] Pötsch, G.; Michaeli, W.: *Injection molding: an introduction*. Carl Hanser Verlag, Munich 1995.
- [Ree02] Rees, H.: *Mold engineering*. Carl Hanser (2nd Edition), Munich 2002.
- [Rog08] Rogelj, S.; Kranjc, M.: *Pressure and temperature behavior of thermoplastic polymer melts during high-pressure expansion injection molding*. Polymer Engineering and Science 48(2008) 9, pp. 1815–1823.
- [Rub73] Rubin, I.: *Injection Molding - theory and practice*. Wiley, New York 1973.
- [Sch98] Schmidt, G.; Michaeli, W.: *High pressure blow moulding, an innovative way for decreasing cooling time*. ANTEC, Atlanta, 1998.
- [Sch09] Schuck, M.: *Kompatibilitätsprinzipien beim Montagespritzgießen*. Doktorarbeit, Friedrich-Alexander-Universität Erlangen-Nürnberg 2009.
- [Sma99] Smallman, R.; Bishop, R.: *Modern physical metallurgy and materials engineering: Science, Process, Applications*. Butterworth-Heinemann, Oxford 1999.
- [Smi98] Smialek, C. D.; Simpson, C. L.: *Flow instabilities in thin-wall injection molding of thermoplastic polyurethane*. ANTEC, Atlanta, 1998.
- [Sri00] Sridhar, L.; Sedlak, B. M.; Narh, K. A.: *Parametric study of heat transfer in injection molding: Effect of thermal contact resistance*. Journal of Manufacturing

Science and Engineering 122(2000) 4, pp. 698–705.

- [Su04] Su, Y.; Shah, J.; Lin L.: *Implementation and analysis of polymeric microstructure replication by micro injection molding*. Journal of Micromechanics and Microengineering 14(2004) 3, pp. 415–422.
- [Sum06] Summers, J.; Zaikov, G.: *Basic research in polymer and monomer chemistry*. Nova Science Publishers, New York 2006.
- [The03] Theilade, U. R.; Kjær, E.; Hansen, H. N.: *The Effect of Mold Surface Topography on Plastic Part In-Process Shrinkage in Injection Molding*. ANTEC, Nashville, 2003.
- [Tur56] Turner, M. J.; Clough, R. W.; Martin, H. C.; etc.: *Stiffness and deflection analysis of complex structures*. Journal of Aeronautical Sciences 23(1956) 9, pp. 805–823.
- [Wil55] Williams, M. L.; Landel, R. F.; Ferry, J. D.: *The temperature dependence of relaxation mechanisms in amorphous polymers and other glass-forming liquids*. Journal of the American Chemical Society 77(1955) 14, pp. 3701–3707.
- [Yan00] Yang, Y.; Gao, F. R.: *Adaptive control of the filling velocity of thermoplastics injection molding*. Control Engineering Practice 8(2000) 11, pp. 1285–1296.
- [Yan12] Yang, C.; Yin, X. H.; Castro, J. M.: *Experimental Investigation of the Mold Surface Roughness Effect in Microinjection Molding*. Applied Mechanics and Materials 138-139(2012), pp. 1258–1262.
- [Yos93] Yoshii, M; Kuramoto, H.; Kato, K.: Experimental study of transcription of smooth surfaces in injection molding. Polymer Engineering & Science 30(1993) 19, pp. 1251–1260.
- [You07] Young, W. B.: *Analysis of filling distance in cylindrical microfeatures for microinjection molding*. Applied Mathematical Modelling 31(2007) 9, pp. 1798–1806.
- [Yu90] Yu, C. J.; Sunderland, J. E.; Poli, C.: *Thermal contact resistance in injection molding*. Polymer Engineering & Science 30(1990) 24, pp. 1599–1606.
- [Yu04] Yu, L. Y.; Lee, L. J.; Koelling, K. W.: *Flow and Heat Transfer Simulation of Injection Molding With Microstructures*. Polymer Engineering & Science 44(2004) 10, pp. 1866–1876.
- [Zha07] Zhang, H. L.; Ong, N. S.; Lam, Y. C.: *Effects of Surface Roughness on Microinjection Molding*. Polymer Engineering & Science 47(2007) 12, pp. 2012–2019.
- [Zha08] Zhang, H. L.; Ong, N. S.; Lam, Y. C.: *Experimental Investigation of Key*

Parameters on the Effects of Cavity Surface Roughness in Microinjection Molding. Polymer Engineering & Science 48(2008) 3, pp. 490–495.

- [Zha08] Zhang, H. L.; Ong, N. S.; Lam, Y. C.: *Mold surface roughness effects on cavity filling of polymer melt in micro injection molding.* The International Journal of Advanced Manufacturing Technology 37(2008) 11-12, pp. 1105–1112.
- [Zhe11] Zheng, R.; Tanner, R.; Fan, X. J.: *Injection molding: Integration of theory and modeling methods.* Springer, Berlin 2011.
- [Zho06] Zhou, J.; Turng, L. S.: *Three-dimensional numerical simulation of injection mold filling with a finite-volume method and parallel computing.* Journal of Non-Newtonian Fluid Mechanics 25(2001) 4, pp. 248–258.

8. List of symbols and abbreviations

Symbols

| | | |
|-------------|----------------------|-------------------------------|
| T_R | [°C] | Room temperature |
| T_O | [°C] | Operating temperature |
| T_E | [°C] | Ejection temperature |
| \vec{q} | [W/m ²] | Heat flux |
| $-\nabla T$ | [K/m] | Temperature gradient |
| k | [W/m·K] | Thermal conductivity |
| t | [s] | Time |
| A | [m ²] | Area |
| Q | [J] | Heat amount |
| ΔT | [K] | Temperature difference |
| d | [m] | Distance of heat transfer |
| c | [J/(kg·K)] | Specific heat |
| m | [kg] | Mass |
| $\Delta T'$ | [K] | Temperature increment |
| α | [m ² /s] | Thermal diffusivity |
| ρ | [kg/m ³] | Density |
| TR_p | [m·K/W] | Thermal resistance of polymer |

| | | |
|-----------------|-----------------------------|--|
| TCR_I | $[m^2 \cdot K/W]$ | Thermal contact resistance of the interface between polymer and mold |
| TR_m | $[m \cdot K/W]$ | Thermal resistance of mold |
| T_{poly} | $[^{\circ}C]$ | Polymer temperature |
| T_{mold} | $[^{\circ}C]$ | Mold temperature |
| h | $[W/m^2 \cdot K]$ | Heat transfer coefficient |
| T_{undist} | $[^{\circ}C]$ | Actual temperature of object |
| T_{rep} | $[^{\circ}C]$ | Final temperature of measurement |
| $M(T)$ | $[J/s \cdot m^2]$ | Total energy radiated per unit surface area of a black body across all wavelengths per unit time |
| σ | $[J/s \cdot m^2 \cdot K^4]$ | Stefan–Boltzmann constant |
| T | $[K]$ | Object temperature |
| t_0 | $[s]$ | Cycle time |
| ΔT_{12} | $[K]$ | Temperature difference between Sensor 1 and Sensor 2 |
| ΔT_{23} | $[K]$ | Temperature difference between Sensor 2 and Sensor 3 |
| Ra | $[\mu m]$ | Surface roughness, arithmetic average of absolute values |
| Rz | $[\mu m]$ | Surface roughness, average distance between the highest peak and lowest valley in each sampling length |
| T_{ref} | $[^{\circ}C]$ | Reference temperature |
| $\log(a_T)$ | | Horizontal shift ratio in WLF equation |

| | | |
|--|----------------------|---|
| C_1, C_2 | | Material dependent constants in WLF equation |
| $A_1, A_3, D_1, D_2, D_3, b_1, b_2, b_3, b_4, b_5, b_6, b_7, b_8, b_9$ | | Data-fitted coefficients for Cross-WLF equation |
| T_{trans} | [°C] | Transition temperature of polymer |
| p | [Pa] | Pressure |
| ρ_0 | [kg/m ³] | Density at reference temperature |
| \vec{v} | | Velocity vector |
| $\underline{\tau}$ | | Stress tensor |
| β | [1/K] | Thermal expansivity |
| $\frac{Df}{Dt}$ | | Material derivative of f |
| g | [m/s ²] | Gravitational acceleration |
| η | [Pa/s] | Melt viscosity |
| $\dot{\gamma}$ | [s ⁻¹] | Shear rate |
| $\tilde{u}(x_i)$ | | Approximations of the exact solution at the points $x_i, i \in \{1, \dots, 6\}$ |
| η_0 | [Pa/s] | Zero shear viscosity |
| τ^* | [Pa] | Critical stress level at the transition to shear thinning |
| G_0, K_g | | Grade-specific constant of crystallization |
| T_g | [°C] | Glass transition temperature |
| U^* | | Activation energy of motion |

| | | |
|-------------------|-------|---|
| R_g | | Gas constant of crystallization |
| T_m^0 | [°C] | Pressure-dependent equilibrium melting temperature |
| T_{eq} | [°C] | Equilibrium melting temperature |
| N | | Nucleus generation |
| N_0 | | Number of activated nuclei in the quiescent condition |
| N_f | | Number of activated nuclei induced by the flow |
| a_N, b_N | | Grade-specific constant of activated nuclei in the quiescent condition |
| α | [%] | Ultimate crystallinity |
| α_R | [%] | Relative crystallinity |
| ΔHm^{obs} | [J/g] | Observed heat of melting |
| ΔHm° | [J/g] | Reference value and represents the heat of melting if the polymer is 100% crystalline |

Abbreviations

| | |
|-------|-----------------------------------|
| HTC | Heat transfer coefficient |
| FEM | Finite element method |
| FVM | Finite volume method |
| GHS | Generalized Hele-Shaw |
| YAG | Yttrium aluminium garnet |
| IR | Infrared |
| LDPE | Low density polyethylene |
| pVT | Pressure-volume-temperature |
| WLF | Williams-Landel-Ferry |
| 2D | 2 dimensional |
| 2.5D | 2.5 dimensional |
| 3D | 3 dimensional |
| DSC | Differential scanning calorimetry |

Appendix

Table A.1: Experimental schedule of injection molding

| Sequence number | Time | Melt temperature / °C, injection rate / cm ³ /s | | |
|-----------------|-----------------------|--|-----------|-----------|
| | | Day 1 | Day 2 | Day 3 |
| | | Ra 0.01μm | Ra 1.36μm | Ra 5.81μm |
| 1 | 9:00 – 10:00 – 10:20 | 200, 5 | 200, 5 | 200, 5 |
| 2 | 10:20 – 10:30 – 10:50 | 200, 25 | 200, 25 | 200, 25 |
| 3 | 10:50 – 11:00 – 11:20 | 200, 45 | 200, 45 | 200, 45 |
| 4 | 11:20 – 12:20 – 12:40 | 230, 5 | 230, 5 | 230, 5 |
| 5 | 12:40 – 12:50 – 13:10 | 230, 25 | 230, 25 | 230, 25 |
| 6 | 13:10 – 13:20 – 13:40 | 230, 45 | 230, 45 | 230, 45 |
| 7 | 13:40 – 14:40 – 15:00 | 260, 5 | 260, 5 | 260, 5 |
| 8 | 15:00 – 15:10 – 15:30 | 260, 25 | 260, 25 | 260, 25 |
| 9 | 15:30 – 15:40 – 16:00 | 260, 45 | 260, 45 | 260, 45 |

